

# **Mechanical and Microscopic Investigation of Concrete Incorporating Ceramic Waste Powder as Partial Replacement of Binding Material**

**By**

**Md. Hamidul Islam**

A thesis report submitted to the Department of Civil Engineering, Khulna University of Engineering & Technology (KUET), Khulna, Bangladesh in partial fulfillment of the requirements for the degree of

**Master of Science in Civil Engineering**



Khulna University of Engineering & Technology

Khulna-9203, Bangladesh

October 2018

## Declaration

This is to certify that the thesis work entitled "Mechanical and Microscopic Investigation of Concrete Incorporating Ceramic Waste Powder as Partial Replacement of Binding Material" has been carried out by Md. Hamidul Islam in the Department of Civil Engineering, Khulna University of Engineering & Technology, Khulna, Bangladesh. The above thesis work or any part of this work has not been submitted anywhere for the award of any degree or diploma.



---

Dr. Ismail Saifullah

Assistant Professor



---

Md. Hamidul Islam

Roll: 1501510

## **Dedication**

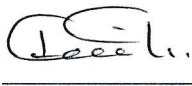


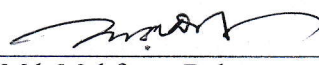

To My Parents (Md. Daud Ali and Mst. Johura Khatun),  
My Beloved Better Half (Mst. Miftahul Zannat),  
My Elder Brother (Md. Hafizur Rahman) and Freedom Fighters of Bangladesh



## Approval

This is to certify that the thesis work submitted by Md. Hamidul Islam entitled "Mechanical and Microscopic Investigation of Concrete Incorporating Ceramic Waste Powder as Partial Replacement of Binding Material" has been approved by the board of examiners for the partial fulfillment of the requirements for the degree of Master of Science in Civil Engineering in the Department of Civil Engineering, Khulna University of Engineering & Technology, Khulna, Bangladesh in October 2018.

### BOARD OF EXAMINERS

1.  30.10.18  
Dr. Ismail Saifullah  
Assistant Professor  
Department of Civil Engineering, KUET  
Khulna-9203, Bangladesh  
Chairman  
(Supervisor)
2.   
Dr. Md. Shahjahan Ali  
Professor and Head  
Department of Civil Engineering, KUET  
Khulna-9203, Bangladesh  
Member
3.   
Dr. Abu Zakir Morshed  
Professor  
Department of Civil Engineering, KUET  
Khulna-9203, Bangladesh  
Member
4.   
Dr. Md. Mahfuzur Rahman  
Assistant Professor  
Department of Civil Engineering, KUET  
Khulna-9203, Bangladesh  
Member
5.   
Dr. Md. Nazrul Islam  
Professor  
Department of Civil Engineering, DUET  
Gazipur-1700, Bangladesh  
Member  
(External)

## **Acknowledgement**

All praises belongs to Almighty Allah for immense blessing for the successful completion of this research work.

I would like to express sincere gratitude to my supervisor Dr. Ismail Saifullah, Assistant Professor, Department of Civil Engineering, Khulna University of Engineering & Technology (KUET), Khulna, Bangladesh for his valuable advice, guidance, suggestion, patient and encouragement throughout the execution of this research. His unfailing optimism and constant encouragement always prompted me to overcome the difficulties in completing this research.

I would like to express my sincerely thanks to the Department of Civil Engineering, Khulna University of Engineering & Technology, Khulna, Bangladesh. Also, I express grateful thank to the laboratory technicians in the Engineering Materials Laboratory, Department of Civil Engineering, KUET, Khulna, Bangladesh.

I gratefully express my acknowledgement to Prof. Dr. Abu Zakir Morshed and Dr. Md. Mahfuzur Rahman, Department of Civil Engineering, KUET, Khulna, Bangladesh for their valuable time and suggestions to review this research work.

I am grateful and expresses special thanks to Department of Glass and Ceramic Engineering, Rajshahi University of Engineering & Technology, Rajshahi, Bangladesh for their X-ray Diffraction (XRD) and Scanning Electron Microscopy (SEM) Laboratory support. Also, hearty acknowledged Seven Rings Cement Factory, Khulna, Bangladesh for their X-ray Fluorescence (XRF) laboratory assistance.

Finally, I solemnly acknowledge my parents and brothers for the unceasing encouragement, support and attention. Also place on record, our sense of gratitude to one and all, who directly or indirectly, have lent their hands in this research.

October 2018

Author  
KUET, Khulna, Bangladesh

## ABSTRACT

Concrete is the most important construction material in construction industry. The ceramic industry generates large amounts of pozzolanic clay wastes every year in Bangladesh and worldwide. So far massive parts of ceramic wastes (CW) are directly dumped into the landfills. Reusing the ceramic wastes in concrete would be the sustainable solution. Also, it leads to avoid the environmental problems related to landfill wastes. Generally, two types of ceramic wastes are found in the ceramic industry such as white and red ceramic waste. This study investigates the mechanical properties and microscopy of concrete incorporating the ceramic waste powder as partial replacement of cement. In this research work, chemical composition by X-ray fluorescence (XRF) analysis, compressive strength test, splitting tensile strength test, X-ray diffraction (XRD) analysis and scanning electron microscopy (SEM) analysis were conducted on cement and partially replaced ceramic waste powder (CWP) concrete. The partial replacement proportions of cement by CWP were 0%, 5%, 10%, 15%, 20%, 25% and 30%. Ceramic wastes powders have been made by ball machine to conduct XRF analysis, mechanical and microscopic investigation. Total 195 cylinders have been made to perform mechanical properties in this research, where 117 cylinders were used for compressive strength test and 78 cylinders were used for splitting tensile strength test. Specific samples have been prepared to conduct microscopic investigation i.e. XRD and SEM analysis. The XRF analysis illustrated that the  $\text{SiO}_2$  and  $\text{Al}_2\text{O}_3$  exist in ceramic powder (both red and white) which is almost twice that of cement. The XRF analysis of red and white ceramic powder provided satisfactory results compared to ASTM specification of Portland cement, fly ash, slags and control cement. Analyzing and illustrating the compressive strength test and splitting tensile strength test results, the CWP concrete provides satisfactory mechanical properties. The most favourable proportion in concrete for red and white ceramic waste powder were found 20% and 15% of partial replacement of cement respectively. The partially replaced CWP concrete presented satisfactory results up to most favourable mix proportions considering modulus of elasticity, stress-strain diagram and Poisson's ratio of cement concrete, although, the modulus of elasticity calculated by ACI and ASTM methods have minor variations. The alite and tobermorite is the most dominating compound found in the XRD analysis of CWP concrete samples. Based on the XRD investigation, it was revealed that the intensity

of alite and tobermorite of CWP concrete is greater than control specimen. From the SEM analysis, it was observed that with the increase of curing ages the alite was hydrated, tobermorite developed and jointly formed a continuous matrix. The density of the surface morphology was very denser of red and white CWP concrete than cement concrete samples. The red CWP concrete specimens were denser and compact having lesser micro-cracks than cement and white CWP concrete. Therefore, this study revealed that the ceramic waste powder (CWP) provides better performance and hence, it can be used in concrete as partial replacement of binder (cement) up to certain proportion. Also, reusing the ceramic wastes in concrete industry would be the win-win solution considering the costs of cement production and environmental related problems.

# CONTENTS

	<b>Page</b>
Declaration	i
Dedication	ii
Approval	iii
Acknowledgement	iv
Abstract	v
Contents	vii
List of Figures	x
List of Tables	xiii
List of Abbreviations / Notations / Symbols	xiv

## **CHAPTER I: INTRODUCTION**

1.1 Background	1
1.2 Objectives	3
1.3 Methodology	3
1.4 Scope and Limitations of this Study	4
1.5 Organization of the Thesis	5

## **CHAPTER II: LITERATURE REVIEW**

2.1 General	6
2.2 Cement	6
2.2.1 Functions of Various Ingredients of Cement	7
2.2.2 Hydration Process of Cement and Ceramic Waste Powder	8
2.3 Ceramic Waste	9
2.4 Ceramic Waste as Pozzolanic Material	13
2.5 Recent Developments of Reusing Ceramic Waste	15
2.6 Strength Properties of Concrete	18
2.7 Durability Performance of Ceramic Waste Based Concrete	22
2.8 Microscopic Investigation of Concrete	26
2.8.1 X-ray Fluorescence (XRF) Analysis	26



2.8.2 X-ray Diffraction (XRD) Analysis	29
2.8.3 Scanning Electron Microscopy (SEM) Analysis	34

### **CHAPTER III: MATERIALS AND RESEARCH METHODOLOGY**

3.1 General	40
3.2 Description of Materials	40
3.2.1 Ordinary Portland Cement (OPC)	40
3.2.2 Ceramic Waste Powder (CWP)	41
3.2.3 Coarse Aggregate	43
3.2.4 Fine Aggregate	44
3.3 Sample Preparation and Testing	44
3.3.1 Preparation of Cylindrical Concrete Specimens	44
3.3.1.1 Capping of Cylindrical Concrete Specimens	47
3.3.2 Testing of Compressive Strength of Cylindrical Concrete Specimens	48
3.3.3 Testing of Splitting Tensile Strength of Cylindrical Specimens	49
3.3.4 X-ray Fluorescence (XRF) Analysis	50
3.3.5 X-ray Diffraction (XRD) Analysis	52
3.3.5.1 Sample Collection and Preparation of XRD Analysis	54
3.3.5.2 Test Procedure of XRD Analysis	55
3.3.5.3 Data Collection and Results Presentation of XRD Analysis	57
3.3.6 Scanning Electron Microscopy (SEM) Analysis	59
3.3.6.1 Test Procedure of SEM Analysis	60

### **CHAPTER IV: RESULTS AND DISCUSSION**

4.1 General	63
4.2 X-ray Fluorescence (XRF) Analysis of Cement and Ceramic Waste Powder	63
4.3 Sieve Analysis	66
4.4 Test Results for Material Properties	69
4.5 Workability of Concrete	70
4.6 Strength Tests of Concrete	72
4.6.1 Compressive Strength of Cylindrical Concrete Specimens	72
4.6.2 Splitting Tensile Strength of Concrete	76

4.7 Failure Types of Control and Ceramic Waste Powder Concrete	79
4.8 Stress-Strain Diagram of Concrete	80
4.9 Modulus of Elasticity of Concrete	84
4.10 Poisson's Ratio of Concrete	86
4.11 Test Results of X-ray Diffraction (XRD) Analysis	88
4.12 Test Results of Scanning Electron Microscopy (SEM) Analysis	91

## **CHAPTER V: CONCLUSIONS AND RECOMMENDATIONS**

5.1 Conclusions	108
5.2 Recommendations for Future Study	110

<b>REFERENCES</b>	<b>111</b>
-------------------	------------

## LIST FIGURES

Figure 2.1	Classification of ceramic wastes by type and production process	12
Figure 2.2	Stress and strain diagram of concrete containing ceramic waste coarse aggregate with different w/c ratio	21
Figure 2.3	Compressive strength of cement replaced by ceramic brick wastes concrete	22
Figure 2.4	Water absorption for ceramic brick powder based concrete	23
Figure 2.5	Permeability test for concrete containing ceramic aggregate	24
Figure 2.6	Vacuum water absorption for concrete containing ceramic	25
Figure 2.7	The X-ray fluorescence (XRF) process	27
Figure 2.8	Principles of X-ray Diffraction (XRD) analysis	30
Figure 2.9	View of XRD instrument (a) Full view and (b) Inside view: (i) X-ray tube, (ii) Sample holder and (iii) X-ray detector	32
Figure 2.10	View of SEM instrument (a) Full view and (b) Inside view of sample holder	35
Figure 2.11	Schematic drawing of the electron and X-ray optics of a combined SEM-EPMA	36
Figure 2.12	SEM image of cement clinker	38
Figure 3.1	A glimpse of ordinary Portland cement in pan	41
Figure 3.2	Field photo of waste ceramic tiles (white and red mixed)	42
Figure 3.3	Steps of CW powder preparation: (a) Field CW after grinding by hammer (b) Ball machine grinding and (c) Sieving by IS #200 sieve (d) White CW powder and (e) Red CW powder after sieving	42
Figure 3.4	Coarse aggregate i.e. crushed stone used in the study	43
Figure 3.5	Sieve analysis technique	43
Figure 3.6	Preparation of cylindrical concrete specimens for compressive strength test	46
Figure 3.7	Gypsum capping of cylindrical concrete specimens	47
Figure 3.8	Compressive strength test setup of cylindrical concrete specimens	48
Figure 3.9	Splitting tensile strength test setup of cylindrical concrete specimens	49
Figure 3.10	Process flow diagram of XRF analysis	52

Figure 3.11	The basic layout of an X-ray diffractometer	53
Figure 3.12	X-ray diffractometer (Bruker D8 Advance, Germany)	53
Figure 3.13	Packing of fine powder into a sample holder	55
Figure 3.14	Typical X-ray diffractogram	58
Figure 3.15	The scanning electron microscope SEM of type EVO 18 Research	59
Figure 4.1	XRF analysis results of cement and ceramic waste powder	66
Figure 4.2	Gradation curve of fine aggregate	69
Figure 4.3	Gradation curve of coarse aggregate	69
Figure 4.4	Slump value measurement	70
Figure 4.5	Variation of w/c ratio with ceramic content due to constant slump value	71
Figure 4.6	Compressive strength of concrete specimens at 7 days	73
Figure 4.7	Compressive strength of concrete specimens at 28 days	74
Figure 4.8	Compressive strength of concrete specimens at 90 days	74
Figure 4.9	Splitting tensile strength of cylindrical concrete specimens at 7 days	77
Figure 4.10	Splitting tensile strength of cylindrical concrete specimens at 28 days	77
Figure 4.11	Sketches of types of cylinders fracture	79
Figure 4.12	Different failure patterns of cylindrical concrete specimens	79
Figure 4.13	Stress-strain diagram of control and white CWP concrete at 28 days	80
Figure 4.14	Stress-strain diagram of control and red CWP concrete at 28 days	81
Figure 4.15	Stress-strain diagram of control and white CWP concrete at 7 days	82
Figure 4.16	Stress-strain diagram of control and red CWP concrete at 7 days	82
Figure 4.17	Stress-strain diagram of control and white CWP concrete at 90 days	83
Figure 4.18	Stress-strain diagram of control and red CWP concrete at 90 days	83
Figure 4.19	XRD Results of control (cement) concrete specimens (cs-alite; csh-hydrated calcium silicate (tobermorite); p-portlandite; e-ettringite, b-belite; c-celite; bw-browmillerit)	88
Figure 4.20	XRD Results of white CWP concrete specimens	89
Figure 4.21	XRD Results of red CWP concrete specimens	89
Figure 4.22	SEM analysis results of cement concrete samples at 7 days	94
Figure 4.23	SEM analysis results of white CWP concrete samples at 7 days	97
Figure 4.24	SEM analysis results of red CWP concrete samples at 7 days	100

Figure 4.25	SEM analysis results of cement concrete samples at 28 days	102
Figure 4.26	SEM analysis results of white CWP concrete samples at 28 days	104
Figure 4.27	SEM analysis results of red CWP concrete samples at 28 days	107

## LIST OF TABLES

Table 2.1	Composition of construction and demolition wastes	11
Table 2.2	Properties of ceramic wastes coarse aggregate	19
Table 2.3	Strength properties of the ceramic waste coarse aggregate concrete and conventional concrete mixes at 28 days	20
Table 2.4	ASTM specification of the chemical composition of Portland cement	28
Table 2.5	ASTM standard mineralogical composition of Portland cement	28
Table 3.1	Properties of coarse aggregates	44
Table 3.2	Properties of fine aggregates	44
Table 3.3	Mix proportions of cylindrical concrete specimens	45
Table 4.1	Chemical composition of cement through XRF analysis	64
Table 4.2	Chemical composition of ceramic waste powder through XRF analysis	65
Table 4.3	Sieve analysis of fine aggregate	67
Table 4.4	Sieve analysis of coarse aggregate	67
Table 4.5	Material properties for mix design	70
Table 4.6	Variations of compressive strength of concrete specimens at 7, 28 and 90 days	75
Table 4.7	Variations of splitting tensile strength of concrete at 7 and 28 days	78
Table 4.8	Comparison of modulus of elasticity of cement and CWP concrete	85
Table 4.9	Poisson's ratio of concrete mixes at 7, 28 and 90 days	86

# CHAPTER I

## INTRODUCTION

### 1.1 Background

Concrete is one of the most significant construction material used at all phases of the infrastructure development. Construction and demolition (C&D) wastes afford the maximal percentage (approximately 75%) of wastes worldwide (Zimbili et al., 2014). However, ceramic materials i.e. ceramic tiles, brick walls and all other ceramic products, contribute approximately 54% of wastes within the C&D wastes (Juan et al., 2010).

The ceramic industry is increasing day by day in Bangladesh. The use of ceramic products is expanding day by day in different form like tiles, sanitary fittings, brick walls, and electrical insulators etc. Nevertheless, due to its brittle behavior huge amounts of ceramic materials turn into wastage during processing, transporting and fixing. C&D wastes and ceramic industry produce tremendous amount of ceramic wastes. Ceramic waste in Dhaka City of Bangladesh reaches 1.13% out of total municipal solid wastes (Islam and Rashid, 2015). Most of these wastes are directly dumped into the landfill, increasing the burden on landfill loading. There is no effective use of ceramic wastes in construction sector because of inaccessibility of standards, avoidance of threat, lack of knowledge and experience. The ceramic wastes can be used in construction industry, exclusively in the concrete industry, in such a way that safely with no essential for vivid change in production and application phase. The cost of dumping of ceramic waste in landfill will not only be saved but also raw materials and natural resources will be replaced. Therefore, resulting saving energy and shielding the environment. The finest approach in the construction sector, especially the concrete sector, in a sustainable tactic is by using wastes from other industries as building materials (Mehta, 2001; Meyer, 2009).

Gartner (2004) reported that the cement production needs maximal energy input (850 kcal per kg of clinker) and indicates the mining of huge amounts of raw materials from the earth (1.7 tons of rock to produce 1 tons of clinker). Furthermore, the complete production of one ton of cement required a total of 0.94 tons of CO<sub>2</sub>, whereas 0.55 tons of chemical

CO<sub>2</sub> induces during production process and required an extra 0.39 tons of CO<sub>2</sub> in fuel emissions (Gartner, 2004). The replacements of cement in concrete by ceramic wastes powder have a key effect on reducing concrete costs. Puertas et al. (2008) showed that the cement cost exemplifies more than 45% of the concrete cost. Several researchers have investigated and confirmed that ceramic waste powder possesses the pozzolanic reactivity which is an essential in binding material (Puertas et al., 2008; Lavat et al., 2009). Pacheco-Torgal and Jalali (2010) stated that the temperature used in the manufacturing of these ceramic tiles is approximately 900 °C. The temperatures are enough to stimulate pozzolanic properties of clay. Every ceramic waste powder mineral reacts at a diverse rate and tends to form divergent solid phases when it hydrates (Jennings, 2014). Gartner (2004) investigated that the partial replacement of cement by ceramic wastes in concrete exemplifies a huge saving of energy. Thus, it has vital environmental merits.

The best tactical ways should be taking remedial measures during the investigation and probable pilot application of an industrial waste altercation initiative. The practical mechanism of waste reduction will be the replacement of waste through reuse, reducing and recycling. Key points to be concluded that the ceramic wastes have active use in the construction industry especially in the concrete production (Juan et al., 2010). In essence, concrete is one of the most consumed materials in Bangladesh as well as over the world. Most of construction project consume concrete as the key material for the structural members. The most plentiful area of the concrete such that it covers about 75% (by volume) of aggregates (Tay and Tam, 1996). Moreover, in most of the cases where there is a necessity for huge demand of concrete, the natural environment trimmings up being surrendered for economic reasons. Considering the economy and most vital the environmental consciousness, there has been significant amount of investigation in reusing and recycling wastes, particularly C&D wastes, into the production of concrete (Boyle, 1997).

Generally, ceramic wastes directly dumped into landfill might not be the best solution indeed, because the landfill wastes leach the chemicals that can be harmful to the environment. This approach also denies the idea of sustainable development, and for this reason it is essential to examine alternative positive use of ceramic wastes, to save energy that has been used to manufacture these ceramics by some means, in an optimistic way.



Therefore, the necessity for its effective use in other industry mostly concrete industry is becoming truly vibrant.

The substitution of cement in concrete by ceramic wastes powder signifies a remarkable saving of energy. Moreover, it has significant environmental benefits. Hence using these wastes in concrete industry could be a win-win solution for maintaining the environment and at the same time the properties of concrete. Although, several researches have been carried out to confirm the pozzolanic reactivity of ceramic waste (CW) powder, nevertheless, research conducted so are scare. Surprisingly most of the researchers did not evaluate chemical composition and microscopic pattern of the CW powder. Therefore, this research investigates the feasibility of partial replacement of cement in concrete using CW powder towards sustainable construction. Accordingly, the aim of this research is to investigate the mechanical and microscopic properties of concrete incorporating CW powder as partial replacement of cement.

## **1.2 Objectives**

The specific objectives of this research are as follows:

1. To investigate the chemical composition of cement and ceramic waste powder by X-ray Fluorescence (XRF) analysis.
2. To investigate the mechanical properties of concrete incorporating waste ceramic powder (white and red) as partial replacement of binding materials (cement).
3. To investigate the most favourable proportions of partial replacement of cement by waste ceramic (white and red) powder in the production of concrete through experiments.
4. To investigate the microscopic pattern through X-ray Diffraction (XRD) and Scanning Electron Microscopy (SEM) analyses of cement and ceramic waste powder concrete for the most favourable mix.

## **1.3 Methodology**

To achieve the objectives of this research, the following steps were completed:

- ✓ Review of literature
- ✓ Measurement of material properties
- ✓ Specimens preparation

- ✓ X-ray Fluorescence (XRF) analysis
- ✓ Cylindrical compressive strength test
- ✓ Splitting tensile strength test
- ✓ X-ray Diffraction (XRD) analysis
- ✓ Scanning Electron Microscopy (SEM) analysis
- ✓ Analyses and observation of these test results

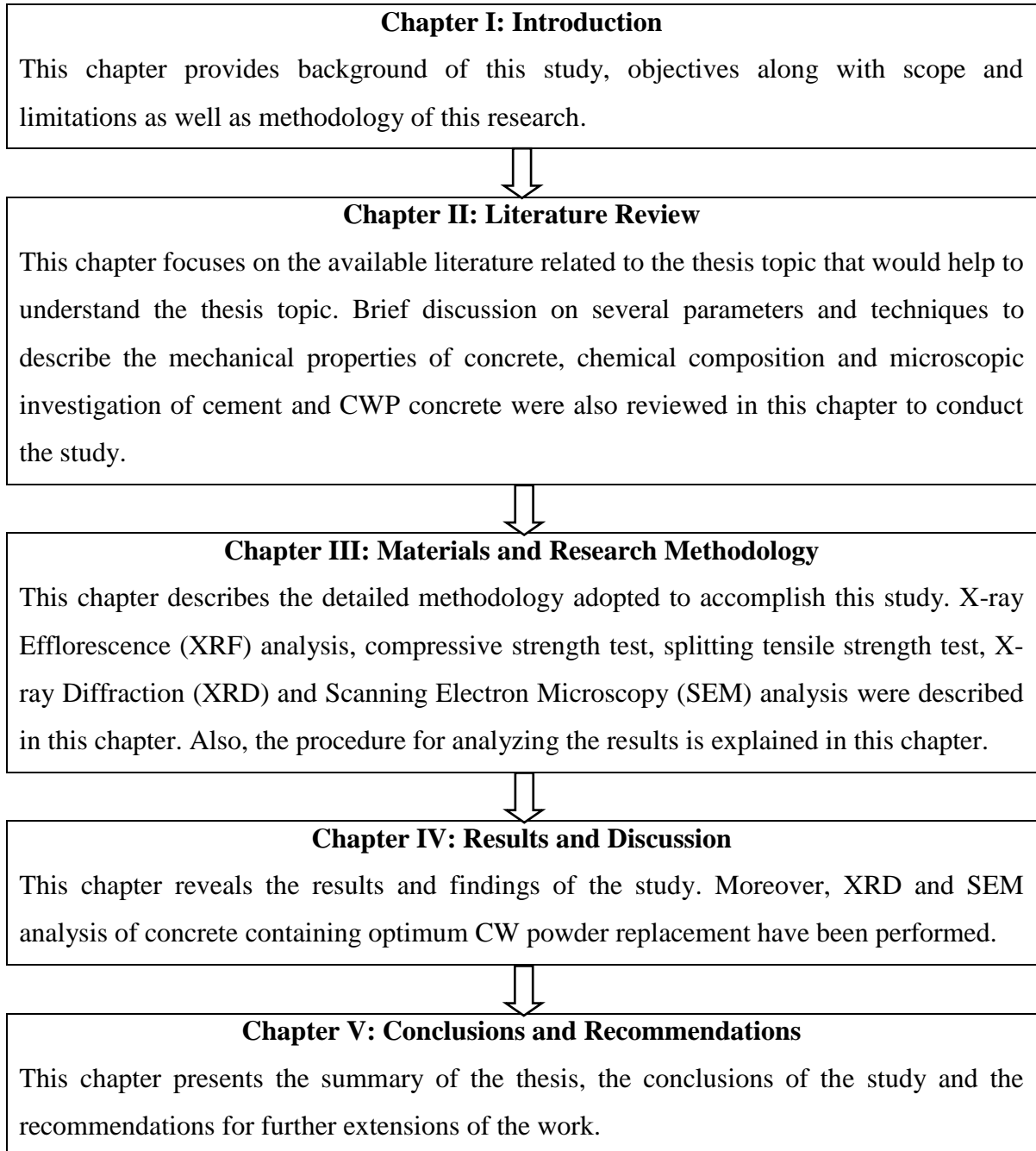
#### **1.4 Scope and Limitations of this Study**

The research work has been carried on cement and CWP concrete. The concrete were made by cement and cement partially replaced by CW powder up to 5% to 30%. Ceramic wastes powders have been made by ball machine to conduct XRF analysis. Total 195 specific cylinders have been made to perform this work, where 117 cylinders were used for compressive strength of cylindrical concrete specimen and 78 cylinders were used for splitting tensile strength test. Specific samples have been prepared to conduct microscopic investigation i.e. XRD and SEM analysis. Reusing the ceramic wastes in concrete could be a win-win solution. The outcomes obtained through this research work can be used for solving the waste management problem in ceramic industry and at the same stage it's forwarding to produce a more sustainable concrete by decreasing the usage of non-renewable resources like cement. The chemical composition and reactions will help to decide the uses of ceramic powder as binding materials. The mechanical properties of the ceramic waste concrete will lead to find the optimum concrete mix. Finally, microscopic analysis of ceramic waste concrete will help to hydrated mineralogical compositions and morphology of CWP concrete. Also, this research will assists to reduce environmental problems related to landfill wastes by using waste ceramic. The outcomes of this research work can also be used as a guideline for the practicing engineers as well as in the construction industry.

Limitation of this work is to measure the surface morphology of the CWP concrete by SEM, because this analysis performed only on 1 cm<sup>2</sup> sample. For this reason, more samples have to perform by SEM to find out the actual surface morphology that was time consuming and costly job.

## 1.5 Organization of the Thesis

This thesis paper contains the following chapters.



## CHAPTER II

### LITERATURE REVIEW

#### 2.1 General

Before presenting the details of testing program, it is important to review the state of the art regarding topics that would help to understand the thesis topic. Brief discussion on several parameters and techniques to describe the mechanical properties of concrete, chemical composition and microscopic investigation of cement and CWP concrete were also reviewed in this chapter.

#### 2.2 Cement

Khajuria et al. (2013) reported that all the materials required i.e. cement, sand, water and coarse aggregate to produce concrete mix are vital. Among them cement is incredibly usually the foremost vital due to its property to link within the chain as a binding material. Firstly, the cement binds the sand and stone together. Secondly, it fills up the voids spaces amongst sand and coarser stone particles to make a compacted mass. It constitutes solely concerning 20% of the total volume of concrete mix. It's the vigorous side of binding medium and is the merely technically controlled element of concrete. Any variance in its amount impacts the compressive strength of the concrete mix (Khajuria et al., 2013). Portland cement denoted as ordinary Portland cement is that the furthestmost significant kind of cement and could be a fine powder manufactured by grinding Portland cement clinker. Generally, the ordinary Portland cement (OPC) is categorized into three grades, specifically 33 Grade, 43 Grade, and 53 Grade relying upon the strength of 28 days. It is possible to manufacture best quality of cement by using best quality limestone, up-to-date equipment's, maintaining better particle size distribution, finer grinding and better packing. Normally use of best quality grade cement compromises several merits for producing resilient concrete. Though they're very little pricier than low quality grade cement, but they provide 10-20% saving in cement feeding. Also, they provide several concealed profits. Faster rate of development of strength is one of the most vital benefits among them (Neville, 1995).

Neville (1995) stated that the aggregates represent the majority of a concrete mixture and provide dimensional firmness to concrete. The aggregates are often used in two or more sizes to extend the density of resulting mix. Fine aggregate helps in making of workability and uniformity in mixture, which is the most vital function of this aggregate. The fine aggregate contribute the cement paste to carry the coarse aggregate particles in holdup. This approach increases the plasticity in the mixture and also avoids the probable segregation of paste and coarse aggregate, mainly when it is essential to move the concrete far from the mixing plant to placement site (Khajuria et al., 2013).

### **2.2.1 Functions of Various Ingredients of Cement**

Several researchers (Mayfield, 1988; Popovics, 1992; Neville, 1995) described the functions of various ingredients of cement. These are including:

- ❖ Lime (CaO)
  - Lime is the principal constituents of cement. The proportion of lime in cement is properly regulated.
  - Excess of lime reduces the strength of cement. It makes the cement Unsound, expand and disintegrate.
  - Less of lime reduces the strength of cement and makes it set quickly
- ❖ Silica (SiO<sub>2</sub>)
  - It contributes strength of cement by forming the comoups of dicalcium and tricalcium silicates.
  - Silica in additional offers better strength to the cement but at the same time extends its setting time.
- ❖ Alumina (Al<sub>2</sub>O<sub>3</sub>)
  - This makes the cement set quickly. Excess of alumina weakens the cement.
- ❖ Magnesia (Magnesium oxides, MgO)
  - This imparts hardness and color to cement when present in small quantity.
  - Excess is harmful and reduces the strength of cement.
- ❖ Iron Oxide (Fe<sub>2</sub>O<sub>3</sub>)
  - This gives cement color, hardness and strength.
  - It conveys quick setting quality to the cement.
  - It acts as a flux and drops the temperature of clinkering process.

- Excess of iron oxide decreases the strength of cement.
- ❖ Sulphur Trioxide (SO<sub>3</sub>)
  - Small portion of sulphur and sulphur compounds imparts soundness to cement.
  - Excess of it reduces the soundness of cement.
- ❖ Alkalies
  - Additional amount of alkalies helps the cement efflorescent.
- ❖ Calcium Sulphate (CaSO<sub>4</sub>)
  - This helps to delay the setting action of cement.
  - It increases the initial setting time of cement.

### 2.2.2 Hydration Process of Cement and Ceramic Waste Powder

Ordinary Portland cement and every ceramic powder mineral reacts at completely diverse rate and have tendency to form diverse solid phases at what time it hydrates. Several researchers (Ahmaruzzaman, 2010; Li, 2011; Gartner et al., 2002; Lilkov et al., 1997) mentioned the performance of every of cementing minerals has been investigated by synthesizing it in its clean form and hydrating it under standard circumstances, and these reactions are explained below.

- ❖ Hydration of the calcium silicate minerals (C<sub>3</sub>S and C<sub>2</sub>S):

Tricalcium silicate (C<sub>3</sub>S) is the most abundant and vital cement mineral in cement and ceramic powder, providing foremost of the early curing ages strength development. The hydration of C<sub>3</sub>S can be written as:



where C<sub>1.7</sub>-S-H<sub>x</sub> is the calcium silicate hydrate (C-S-H) gel phase and CH is calcium hydroxide, which has the mineral known as hydrated lime. The variable x in equation (2.1) signifies the volume of water related with the C-S-H gel, which varies from about 1.4 to 4 based on the comparative humidity inside the paste and amount of the water associated with the C-S-H is measured to be part of its authentic composition.

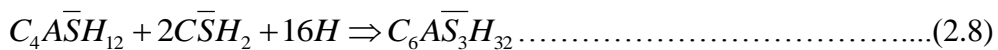
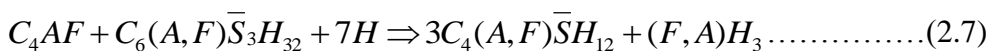
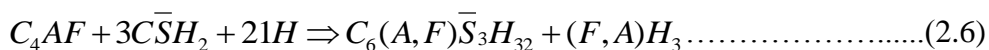
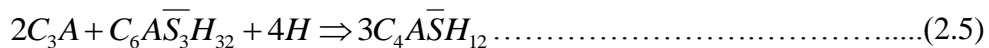
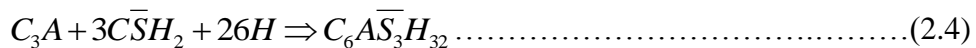
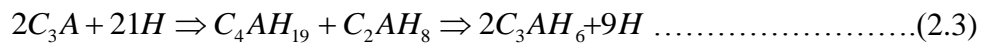
- ❖ The dicalcium silicate phase (C<sub>2</sub>S) reacts according to:



The hydration products are the equivalent as those of C<sub>3</sub>S, but the comparative quantity of CH made is less. C<sub>2</sub>S is less soluble than C<sub>3</sub>S, so the rate of hydration is much slower. C<sub>2</sub>S hydration provides little to the early curing age's strength of ceramic powder, but makes considerable assistances to the strength of mature ceramic paste.

❖ Hydration of the calcium aluminate/ferrite minerals (C<sub>3</sub>A and C<sub>4</sub>AF):

The hydration of the aluminate and ferrite minerals is slightly a lot of complicated than that of the calcium silicate minerals. Also, the reactions that manifest it rely on whether or not sulfate ions are present in the pore solution. C<sub>3</sub>A is very soluble, even a lot of therefore than C<sub>3</sub>S. If C<sub>3</sub>A is hydrated in pure water, calcium aluminate hydrates form. The reaction sequence is:



However, using ceramic wastes as partial replacement of cement will be the best solution in construction industry especially concrete industry. Dumping ceramic waste directly to the landfill possibly not be the best decision, depending on whether there may be leakage of chemicals that can be harmful to the environment. This approach also denies the perception of sustainable development. Hence it is crying essential to examine the alternative helpful use of these ceramic wastes, to recuperate energy that is been used to produce these ceramics somehow, in an optimistic manner. Hence, the need for its use in other industries is becoming absolutely vigorous. Therefore, using these ceramic wastes in concrete production could be a win-win solution considering the environment as well as the durability and strength properties of concrete.

### 2.3 Ceramic Waste

According to the Bangladesh Environmental Conservation Act (ECA, 1995) “waste means any solid, liquid, gaseous, radioactive substance, the discharge, disposal and dumping of

which may cause harmful change to the environment”. The C&D wastes contribute the significant percentage of wastes at construction industry in many countries. Apparently ceramic industry and clay bricks have the maximum percentage of wastes produced under the classification of stony fraction (Zimbili et al., 2014).

In general, ceramic is formed by ionic and covalent bond mainly inorganic, non-metallic, solid material involving metal, non-metal or metalloid atoms. According to Johnson (2009) “ceramics are generally made by taking mixtures of clay, earthen elements, powders, and water and shaping them into preferred forms. Once the ceramic has been molded, it is fired in a high temperature oven a kiln. Regularly, ceramics are covered in decorative, waterproof, paint-like materials known as glazes”.

Ceramic waste can initiate from the production or demolition of a multitude of products such as wall and floor tiles, bricks and roof tiles, household ceramics, sanitary ware, refractory products, technical ceramics, vitrified clay pipes, prolonged clay aggregates and inorganic bonded abrasives. Consequently the chemical composition and physical properties vary considerably. A large quantity of waste is generated in the production stage. Researchers such as Senthamarai and Manoharan (2005) assessed that approximately 30% of the daily manufacturing volume in the ceramic industry converts to waste. Juan et al. (2010) reported that the C&D wastes afford the maximal percentage of wastes in all over the world. Moreover, ceramic materials i.e. ceramic tiles, brick walls and all other ceramic products, contribute the maximal percentage of wastes in the arena of C&D wastes as shown in Table 2.1.



Table 2.1: Composition of construction and demolition wastes (Juan et al., 2010).

Materials		Composition (%)
Stony Fraction (75%)	Wall tiles, bricks and other ceramics materials	54.0
	Concrete	12.0
	Stone	5.0
	Sand, gravel and other aggregates	4.0
Non Stony Fraction (25%)	Rubbish	7.0
	Asphalt	5.0
	Wood	4.0
	Metals	2.5
	Plastic	1.5
	Glass	0.5
	Paper	0.3
	Plaster	0.2
	Others	4.0

A classification is presented in Figure 2.1, where ceramic waste can be divided into two categories in accordance with the source of its raw materials. In every category, the fired ceramic waste is classified in accordance with the production process, separating them by the use of red or white ceramic pastes.

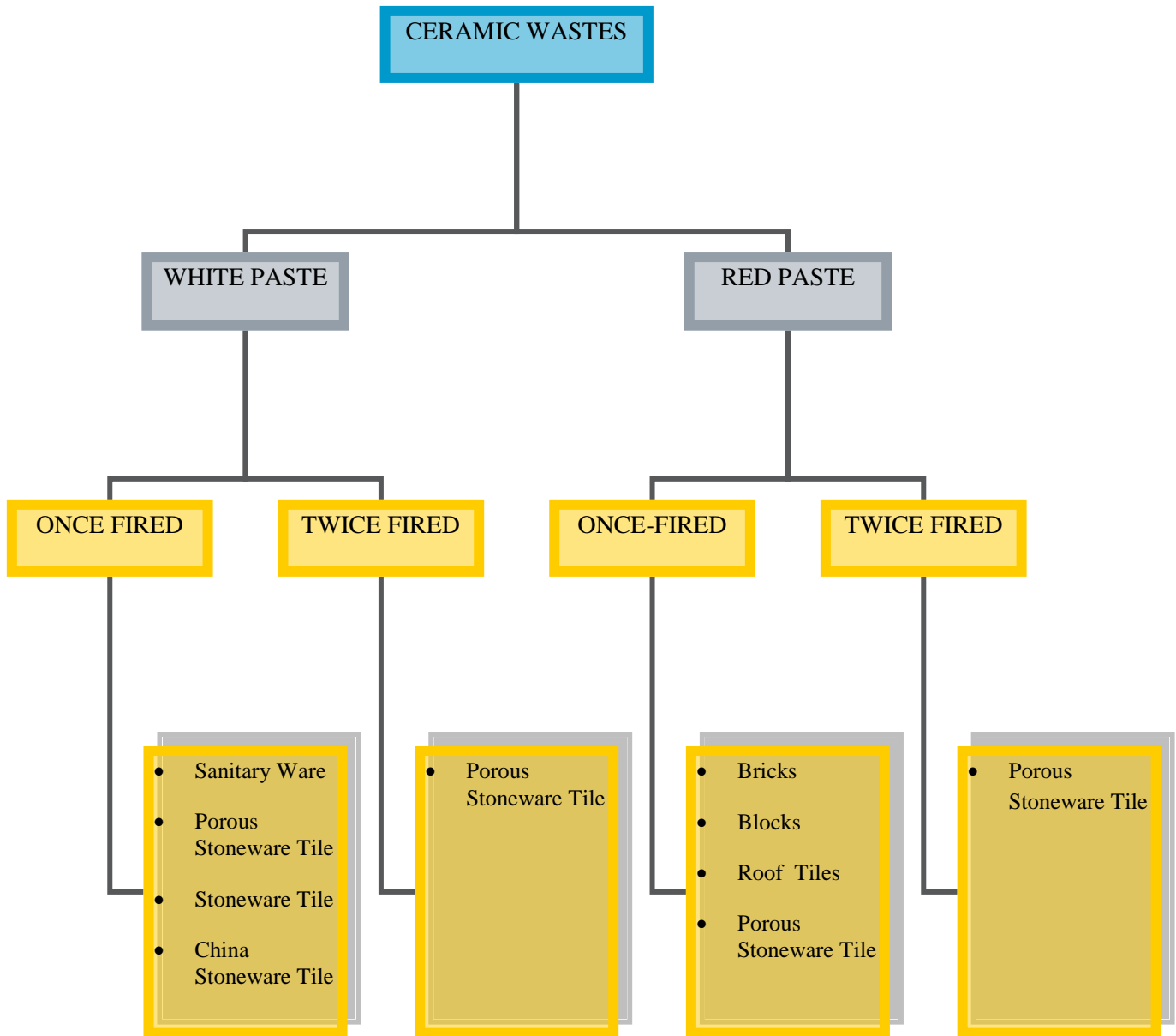


Figure 2.1: Classification of ceramic wastes by type and production process (Pacheco-Torgal and Jalali, 2010).

The ceramic industry is increasing day by day in Bangladesh. Ceramic waste in Dhaka City reaches 1.13% out of total municipal solid wastes (Islam and Rashid, 2015). C&D wastes and ceramic industry produce tremendous amount of ceramic wastes. Most of these wastes are directly dumped into the landfill, increasing the burden on landfill loading. There are no potential uses of ceramic wastes in the construction industry due to inaccessibility of standards, escaping of threat, lack of awareness and experience. Ceramics wastes can be used in construction industry, especially the concrete industry, without major changing it's in manufacture and application methods. Firstly, the price of

directly dumping of ceramic waste into landfill will be optimized. Secondly, raw materials and natural resources will be exchanged, consequently effectively optimizing the energy and shielding the ecosystem. Several researchers (Mehta, 2001; Meyer, 2009) informed that the most effective technique for the construction industry especially concrete industry to convert wastes as a more sustainable materials is that it is used as a raw materials in other industry.

The cost of preparation of ceramic wastes into powder by grinding is depending on the amount of material grounded. Due to this approach the cost varies approximately 10% and 20% of the cost of Portland cement. This is meaning that the approach saving of approximately 17% in the cost of Portland cement in concrete. So generally price of concrete will be decreased by more than 7.5%. To saving materials cost it can be noted that this is a significant achievement. Considering the solid ceramic waste management i.e. dumping price and at the same the land occupied by landfill will be an extra achievement in effectiveness and savings (Pacheco-Torgal and Jalali, 2010).

#### **2.4 Ceramic Waste as Pozzolanic Material**

The term ceramics is used to specify the ceramic products or materials. Depending on the manufactured products ceramics are generally wall tiles, floor tiles, sanitary ware, household ceramics and technical ceramics. Sometimes ceramic is described as to designate inorganic materials (with perhaps some organic elements), made up of non-metallic composites and completed permanent by a firing method (Ibáñez-Forés et al., 2013). Juan et al. (2010) stated that the clay, generally which is not a pozzolanic material, used to prepare most of the ceramics. For this reason, this clay does not contain silicate properties. This silica formed by calcium hydroxide reacting with water in the manufacture of concrete. Several authors conducted researches on the possibility of uses of waste materials as pozzolanic. Most of the study demonstrated that the stimulation of clay converted to pozzolanic starts at the time of dehydration process. The pozzolanic properties induces in the clay when heating clay from around 500 °C, and the breakdown of amorphous and very dynamic aluminum oxide. The kinds of materials presents in the clay minerals demonstrate the temperature requirement to reach the maximal intensity of the Al<sub>2</sub>O<sub>3</sub>. Juan et al. (2010) also reported that at time of manufacturing of ceramics, clay is fired at comparatively huge temperatures, the actual temperature relying on the category of

ceramic being manufactured. By the key points, this study focuses on ceramic tile wastes mainly reject tiles, which found by the full heating processes at high temperature. Several researchers said that the ceramic wall tiles are heated at approximately 1150 °C. Apparently, it is rationale to introduce the wastes from the ceramic industry (ceramic wastes) have characteristics similar to pozzolanic materials. Consequently, ceramic wastes are appropriate for use in the production of concrete.

Ceramic wastes have distinctive properties regarding pozzolanic activity, for this reason they might contribute certainly in areas of recycling and reusing in construction. Devanathan et al. (2011) steered investigation on the characteristics of ceramic waste forms to find out whether it was appropriate to afford a unchanging geological formation, which might act as obstacle to specific nuclear wastes (radionuclides) for long duration. They found that the toxic radioisotopes have very long half-lives. Exemplifies such as plutonium 239 ( $^{239}\text{Pu}$ ), which has half-life of around 24200. It will take to decay half of the material is called half-life that means it will take double the time to deterioration the entire material. For example, 1 kg of plutonium will be 0.5 kg plutonium and 0.5 kg uranium, since plutonium decays to uranium after half-life (Devanathan et al., 2011). Material such as  $^{239}\text{Pu}$  needs to be disposed in a protected environment, such that the radioisotopes (radionuclides) are not likely to be leaked into the groundwater over long time. Devanathan et al. (2011) settled that the ceramic waste had degradation capacity potential to offer such stability. Also the ceramic waste has potential degradation ability to implementation in nuclear waste management.

Authors such as Sánchez et al. (2006) conducted widespread studies on ceramic wastes usage in construction industry. Their emphasis was examining the opportunity of using general ceramic wastes (often ceramic tiles and bricks) as a stabilizer of cement and on the producing of concrete-made roofing tiles as well as the morphology of the mixed cement. The researchers not thoroughly checked out the pozzolanic properties of the ceramic wastes, but additionally compared their effects with ones of other regarded cement stabilizers along with fly ash and silica fume. Sánchez et al. (2006) revealed that most of the ceramic tiles and bricks are heated at approximately 900 °C or greater, that is enough to stimulate clay minerals to gain pozzolanic properties.

## 2.5 Recent Developments of Reusing Ceramic Waste

There have been several researches in all over the world relating to use of ceramics wastes in construction industry especially concrete production, as a partial replacement of cement or aggregates. Although the researchers conducted the study regarding the incorporating of ceramic wastes powder partially into the concrete are scarce. Researchers (Ay and Ünal, 2000; Lavat et al., 2009) steered investigation on partial replacement of cement by ceramic roofing waste powder. They investigated the most important properties of concrete i.e. pozzolanic properties of ceramic waste powder as well as setting time, volume stability, particle size, density, and specific surface area (Ay and Ünal, 2000). Their results showed that waste roofing tiles have pozzolanic characteristics. Moreover, they possess physical and chemical properties parallel to cement, thus compatible to cement properties. Researchers such as Lavat et al. (2009) was more concerned in the mineralogical structure of ceramic wastes. They concluded that waste tiles provide satisfactory results concerning the pozzolanic properties and the compressive strength with partial replacement of cement up to certain proportions. The mixtures showed parallel to the compressive strength of Portland cement concrete. Pozzolanic compounds react with  $\text{Ca(OH)}_2$  combined or free in the hydration of Portland Cement. After starting hydration steps it quite similar to the PC silicates hydration compounds (Sabir et al., 2001). Since the ancient era the calcined clays have been recycled as pozzolans (Malhotra, 1987). In case of raw form the clays don't demonstrate pozzolanic property, but when the calcined and ground to an suitable fineness clays could be recycled as pozzolanic reactive materials for cement (Benezet and Benhassaine, 1999). Several researchers (Bahoria et al., 2013; Jiménez et al., 2013; Feng et al., 2013) conducted research on partial replacement of aggregate by ceramic wastes aggregate. Researches directed concerning the additional uses of ceramic wastes in concretes and mortars (Asensio et al., 2016; Sadek et al., 2016). They revealed that the partial replacement of ceramic aggregate concrete gave satisfactory outcomes.

Ceramic waste tiles manufactured in a confined plant and heated at 950 - 1000 °c. This waste tiles were combined into a mix in cement manufacture. To reuse of the ceramic floor tiles in the cement mortar would be a win-win solution. This waste recycling approach reduce harmful environmental effects and cost of concrete production (Lavat et al., 2009). Several applications for handling these ceramic wastes by means of most of structural components as cement concrete based, as number one binder (Batchelor, 2006;

Gaucher and Blanc, 2006; Botta et al., 2004). The usage of waste generated from construction sites as an alternative for most of the concrete industry as raw materials used in Ordinary Portland Cement (OPC) concrete has been stated (Batayneh et al., 2007). Researchers (De Brito et al., 2005; Koyuncu et al., 2004) investigated and showed the opportunity of utilization of well-known recycled ceramic waste aggregates in case of making of non-structural concrete. Moreover, they acquired satisfactory outcomes, with growth in abrasion resistance and tensile strength, appropriate for utilization in the construction of paving slabs.

Authors such as Naceri and Hamina (2009) steered an investigation on the feasibility of usage of ceramic clay blocks wastes as partial alternative of cement in the manufacture of mortars. They found that partial replacement of cement by ceramic clay blocks waste powder enhanced the mechanical and durability properties of the mortar. Gomes and de Brito (2009) investigated the use of wastes in the shape of ceramic bricks wastes powder and mortar, and recycled concrete and a combination of the two as partial replacement for coarse aggregates and observed that the uses of ceramic aggregates in cement concrete provide in acceptable durability. Although, the ceramic bricks wastes aggregates showed a higher value of water absorption, the better-quality concrete mix thereof, ascertained to be reasonable. However, little bit terrible effects were attained when totally replacing the fraction of 4.32 mm of natural stone aggregates with ceramic waste aggregates (Gomes and de Brito, 2009).

Researchers such as Medina et al. (2012) performed experimental study on partial replacement of coarse aggregates in concrete (15 to 25%) by sanitary ceramics wastes and observed that with the increase of the partial replacement resulted in decrease the density of concrete, and better compressive and tensile strength. The concrete manufactured turned into appropriate for structural usage. Lopez et al. (2007) conducted a research on the opportunity of exploiting the partial replacement for both coarse and fine aggregates by ceramic sanitary ware wastes. The investigation conducted on the physical properties of concretes in which natural coarse aggregate were partially replaced by coarse ceramic aggregate found by crushing ceramic sanitary ware wastes. At the same time, the natural fine aggregate were partially replaced by ceramic waste powder. Satisfactory outcomes were achieved in this each case. Electrical insulation porcelain ceramic wastes were examined directly to determine their future for partial replacement into concrete (Portella

et al., 2006). Regardless positive outcomes on the probable use in the production of concrete, the usage of sulphate resistant cements shows to be the pleasant option, to escape adverse impacts, which generate alkali-aggregate reaction with the usage of Portland cement (Portella et al., 2006). Higashiyama et al. (2012) performed an investigation on fine aggregate partially replaced by ceramic wastes and examined the compressive strength and chloride penetration of mortars. They used ceramic electric wastes as partial replacement of fine aggregate. They revealed that ceramic wastes based mortars showed higher compressive strength than control (cement mortar) sample produced from natural river sand. Additionally, they made concrete incorporating ceramic wastes as partial replacement of cement, and found better compressive strength for partial replacement up to certain proportions. They observed that the chloride penetration of mortar specimen fabricated from ceramic wastes was decreased significantly. Additionally, Higashiyama et al. (2012) determined that the ceramic wastes sample showed less value of pore volume and pore diameter than control cement concrete. Consequently, the decrement of the chloride diffusion, greater compressive strength and compact pore volume was meaning to give greater durability of the using ceramic wastes mortars (Higashiyama et al., 2012).

High performance concrete (HPC) principally develop early cracks due to very low water: cement (w/c) ratio, except safety measures were taken. One of the safety measures inspected is chance of internal curing of concrete (Lindquist, 2008). Suzuki et al. (2009) conducted test to reduce shrinkage on recycled waste porous ceramic coarse aggregates (PCCA) incorporating into the conventional coarse aggregates. This concept was built from the partial replacement of natural aggregate by waste lightweight aggregate, as investigated by several authors. The study gave satisfactory results, with the increase of PCCA amount there was slight decrease in the tensile strength. The opportunity to use the PCCA might be helpful pleasantly at dropping or abolishing shrinkage on high performance concrete (Suzuki et al., 2009).

Puertas et al. (2008) did an extraordinary study on ceramic waste as a raw compound in manufacturing clinkers and cements. Several properties like the hydration, physical-chemical properties and leaching behavior in numerous acid media were inspected and located to be morphologically and compositionally parallel in hydration behavior, when related to natural cement. Optimistic outcomes were found whereby the new cement

providing all the practical conditions to be made and used as cement. This observed the efforts were realistic.

## **2.6 Strength Properties of Concrete**

In United State, the cylinder specimen of concrete (150 mm diameter and 300 mm height) is a standard specimen that is generally used to test the compressive strength. Whereas in Britain and Europe, a cube (150 x 150 x 150 mm) is generally used as the standard specimen for testing the compressive strength (Kim and Yi, 2002). The cubes specimens have very smaller relation with the cylinder specimen of concrete. Therefore, the merits of cylinders do not rely on the excellence and condition of the molds and that their density can be more eagerly and precisely recognized by weighing and measuring (Bhattacharjee, 2015). The cylinder specimens are cast and tested in the same situation, but the cube specimens are casts in one plane and tested at right angles to the position cast. For this reason, there is no necessity of capping or grinding. In real structures in the construction site, the casting and loading is equivalent to that of the cylinder and not just like the cube (Shetty, 2009). The correlation between the compressive strength of cube specimens and compressive strength of cylindrical specimens is considered by a factor of 0.8 to the cube strength is frequently applied for normal strength concrete (Al-Sahawneh, 2013). The most common testing method used by the engineers and professionals is the compressive strength of concrete in designing buildings and other structures. The compressive strength of concrete is determined by crushing cylindrical concrete specimens in a compression testing machine.

Senthamarai and Manoharan (2005) investigated the properties of ceramic wastes coarse aggregate as shown in Table 2.2. The surface texture of the ceramic waste coarse aggregate was obtained to be flatter than that of crushed stone aggregate. From Table 2.2 it has been assumed that after 30 cycles of the soundness test the ceramic waste coarse aggregate lost its weight that was about 51% less than that of traditional crushed stone aggregate, although the ceramics wastes aggregate has greater resistance against all chemicals. Generally, ceramic wastes coarse aggregate showed properties very close to those of conventional crushed stone aggregate.



Table 2.2: Properties of ceramic wastes coarse aggregate (Senthamarai and Manoharan, 2005).

Properties		Ceramic Waste	Crushed Stone
Specific Gravity		2.45	2.68
Maximum Size (mm)		20	20
Fineness modulus		6.88	6.95
Water Absorption 24 h (%)		0.72	1.20
Bulk density (kg/m <sup>3</sup> )	Loose	1200	1350
	Compacted	1325	1566
Voids (%)	Loose	50	48
	Compacted	45	44
Crushing Value (%)		27	24
Impact Value (%)		21	17
Abrasion Value (%)		28	20
Soundness Test: Weight loss after 30 cycles (%)		3.3	6.8

Nehdi and Khan (2001) investigated the compressive and tensile strengths of the ceramic wastes coarse aggregate concrete as presented in Table 2.3. The outcomes shown in the Table 2.3 are the average of six samples tests results. The study showed that the fresh ceramic waste coarse aggregate concrete gave satisfactory results. It showed greater value of cohesiveness and workability than conventional cement concrete. This is due to that the ceramic wastes coarse aggregate have the lower water bsorption and smooth surface texture. The compressive strength was found range from 51 to 30 MPa. Considering the main outcomes of the compressive strength, the key behavior of ceramic waste coarse aggregate shown in Table 2.3 is not major different from that of natural crushed stone aggregate concrete. The splitting tensile strength found in between 4.5 to 3.2 MPa. The splitting tensile strength of traditional cement concrete was greater than that of ceramic waste coarse aggregate concrete. Although the tensile to compressive strength ratio was lower for ceramic waste concrete than that of the conventional cement concrete. The flexural strength ranged in between 6.9 to 4.7 MPa. Conclusion can be drawn that the

differences in flexural strength between traditional crushed stone aggregate and ceramic waste coarse aggregate concrete are very minor.

Table 2.3: Strength properties of the ceramic waste coarse aggregate concrete and conventional concrete mixes at 28 days (Nehdi and Khan, 2001).

Mix	w/c	Cement content (kg/m <sup>3</sup> )	Ceramic waste coarse aggregate concrete								Conventional concrete											
			Slump (mm)		Compressive strength		Splitting tensile strength		Flexural strength		Modulus of elasticity		Slump (mm)		Compressive strength		Splitting tensile strength		Flexural strength		Modulus of elasticity	
			Mean (MPa)	C.V	Mean (MPa)	C.V	Mean (MPa)	C.V	Mean (GPa)		Mean (MPa)	C.V	Mean (MPa)	C.V	Mean (MPa)	C.V	Mean (GPa)		Mean (MPa)	C.V	Mean (GPa)	
1	0.35	531	13	51.0	3.28	4.5	6.00	6.9	4.35	22.2	10	53.0	2.79	5.5	4.36	7.0	4.57	25.1				
2	0.40	465	24	45.8	4.17	4.3	6.51	6.1	3.93	20.3	18	46.0	2.35	5.0	4.00	6.4	3.44	23.5				
3	0.45	413	45	40.0	4.05	3.8	6.87	5.6	2.86	19.0	35	40.0	3.18	4.5	4.06	5.8	3.10	21.3				
4	0.50	372	64	37.0	2.46	3.6	4.72	5.3	2.45	17.9	48	38.0	2.29	4.4	3.18	5.5	2.91	20.5				
5	0.55	338	99	34.0	2.44	3.5	3.71	5.0	3.00	17.5	80	35.0	2.03	4.1	3.42	5.3	2.64	18.3				
6	0.60	310	155	30.0	2.73	3.2	5.63	4.7	2.55	16.1	148	31.0	1.77	3.9	3.59	5.0	3.40	16.5				

Note: C.V is Coefficient of variation.

The stress-strain diagram of concrete containing ceramic waste coarse aggregates with different w/c ratio were investigated by Senthamarai and Manoharan (2005) and presented in Figure 2.2. From the Figure 2.2 it has been observed that the modulus of concrete containing ceramic waste coarse aggregate varied from 22.2 to 16.1 GPa. The outcome is 13.6% to 2.4% lower than that of traditional cement concrete (Senthamarai and Manoharan, 2005).

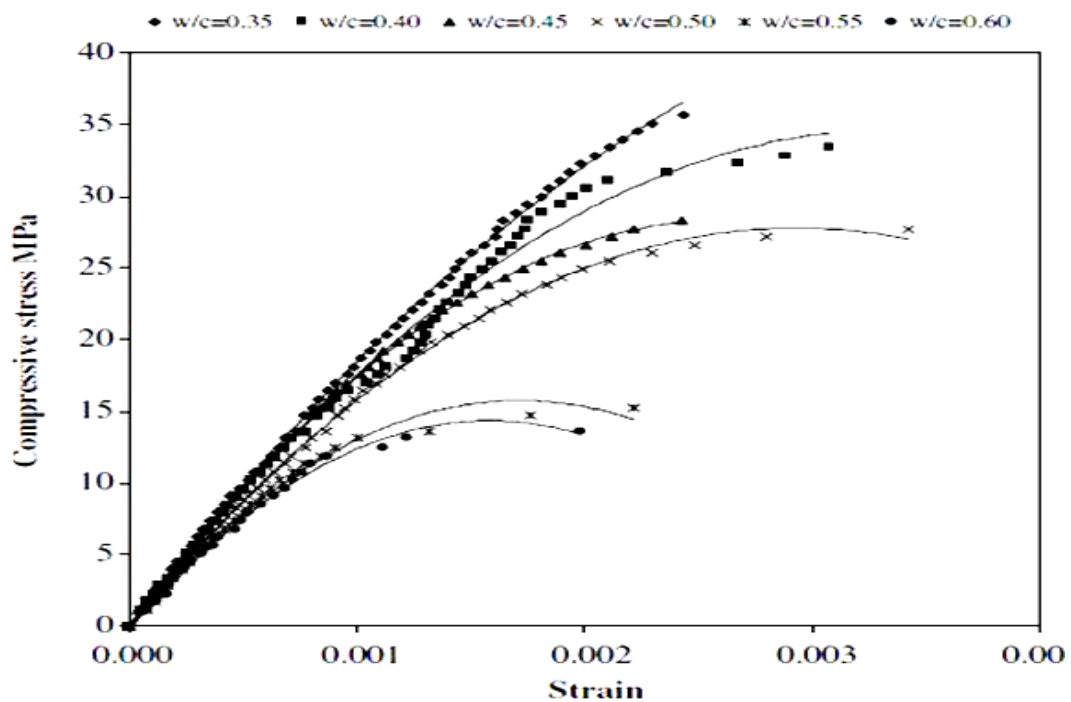


Figure 2.2: Stress and strain diagram of concrete containing ceramic waste coarse aggregate with different w/c ratio (Senthamarai and Manoharan, 2005).

Pacheco-Torgal and Jalali (2010) conducted compressive strength tests by replacing cement with ceramic brick wastes in concrete. The compressive strength test results are shown in Figure 2.3. The outcomes of their research specified that the huge variation in initial curing ages and lesser differences at extended curing ages. The ceramic brick wastes gave satisfactory outcomes up to certain proportion compared to the control cements concrete. Moreover, the ceramic brick waste concrete has improved pozzolanic reactivity. Each one is named after the source of the ceramic waste: ceramic bricks (CB); white stoneware twice-fired (WSTF); sanitary ware (SW); white stoneware once-fired (WSOF). The WSOF wastes concrete has the poorest mechanical behavior at initial ages, signifying 74.8% of control strength for 7 days curing test as shown in Figure 2.3. The concrete combination has nearly 80% of the control strength index at 28 days. Nevertheless, the compressive strength activity index of the WSOF combination extents 90.4% for 90 days. Since advanced curing temperatures growth the trend of pozzolanic action pre-fabrication industry might be a perfect method to their engagement. This is due to advanced curing temperatures are usage in concrete pre-fabrication for faster demolding (Pacheco-Torgal and Jalali, 2010).

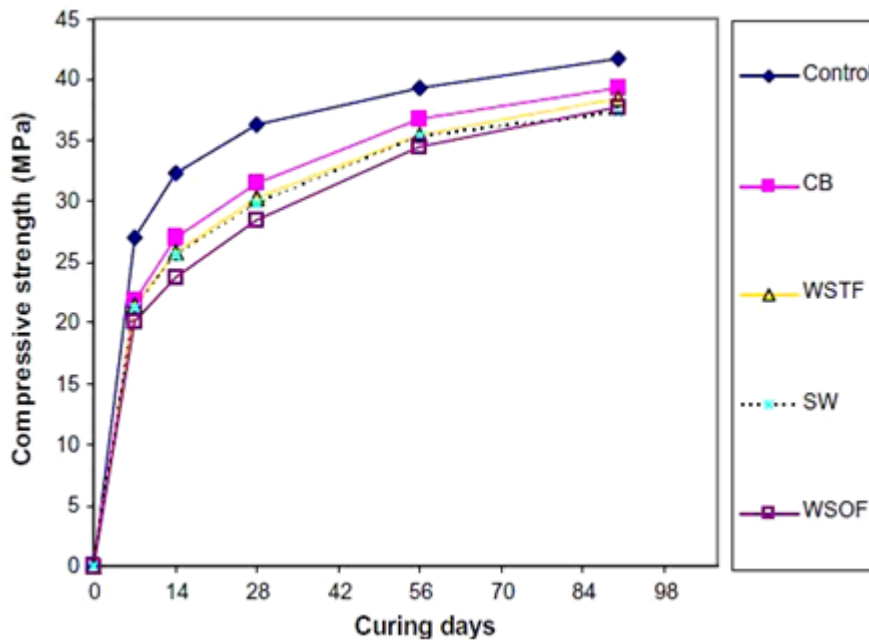


Figure 2.3: Compressive strength of cement replaced by ceramic brick wastes concrete (Pacheco-Torgal and Jalali, 2010).

## 2.7 Durability Performance of Ceramic Waste Based Concrete

Pacheco-Torgal and Jalali (2010) performed water absorption test in ceramic waste concrete. Every sample one is named after the source of the ceramic waste: ceramic bricks (CB); white stoneware twice-fired (WSTF); sanitary ware (SW); white stoneware once-fired (WSOF). The water absorption of control and ceramic brick powder are shown in Figure 2.4. From Figure 2.4 it can be seen that the ceramic brick specimen which has greater value of vacuum water absorption than the control cement concrete specimen, rest of others have lesser vacuum water absorption than the control cement mixture. The oxygen permeability of ceramic brick and control specimen investigated by Pacheco-Torgal and Jalali (2010) as shown in Figure 2.5. It can appear that two mixes (WSTF and WSOF) showed lesser value and others two mixes (CB and SB) showed values slightly greater than the control specimen. The differences, though, are between 6% and 12% in contrast with control mix. The oxygen permeability values of these specimens showed that there are no related differences. Although the water permeability is the main outcomes of the study regarding cement was partially replaced by ceramic waste powder. The water permeability found for ceramic waste concrete was better than control specimens. Several ceramic wastes concrete showed different values of water permeability. There was inferior

water permeability in case of WSOF wastes based concrete. Consequently the wastes obligate the inferior strength value that could be accordance to the hydration of unreacted elements.

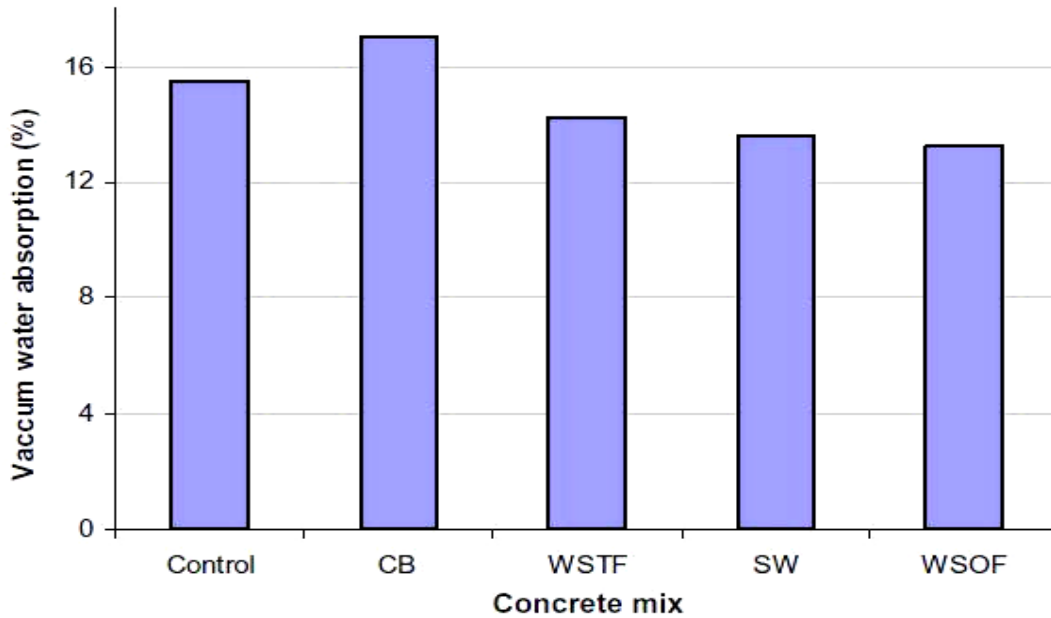


Figure 2.4: Water absorption for ceramic brick powder based concrete (Pacheco-Torgal and Jalali, 2010).

Pacheco-Torgal and Jalali (2010) also specified that the ceramic wastes accomplished better compared to the control specimen, although the SW mixture showed the parallel value of chloride ion diffusion coefficient to the control specimen. There was an exception in case of ceramic sanitary ware powder wastes specimens. It can be observed that the cement partially replaced by ceramic wastes concrete gave very small chloride diffusion index. According to the classification suggested by Gjrv (1996), these types of ceramic wastes concrete mixtures own a very greater resistance against chloride penetration. This behavior must be connected to the compact microstructure given by the pozzolanic reaction in between ceramic waste powder and calcium hydroxide producing secondary C-S-H. Pacheco-Torgal and Jalali (2010) also performed accelerated aging test and provided acceptable results. The benefits of using quicker tests is that the whole life of the concrete specimen can be replicated (Monteny et al., 2001). Although, the ceramic wastes powder concrete gave only 6% lesser strength than control cement concrete, due to changing between 2% (CB) and 5% (WSOF). These outcomes stated that all ceramic wastes based

concrete showed better durability performance assessed with the aging test which settles the optimistic effects of the ceramic incorporation as cement partial replacement.

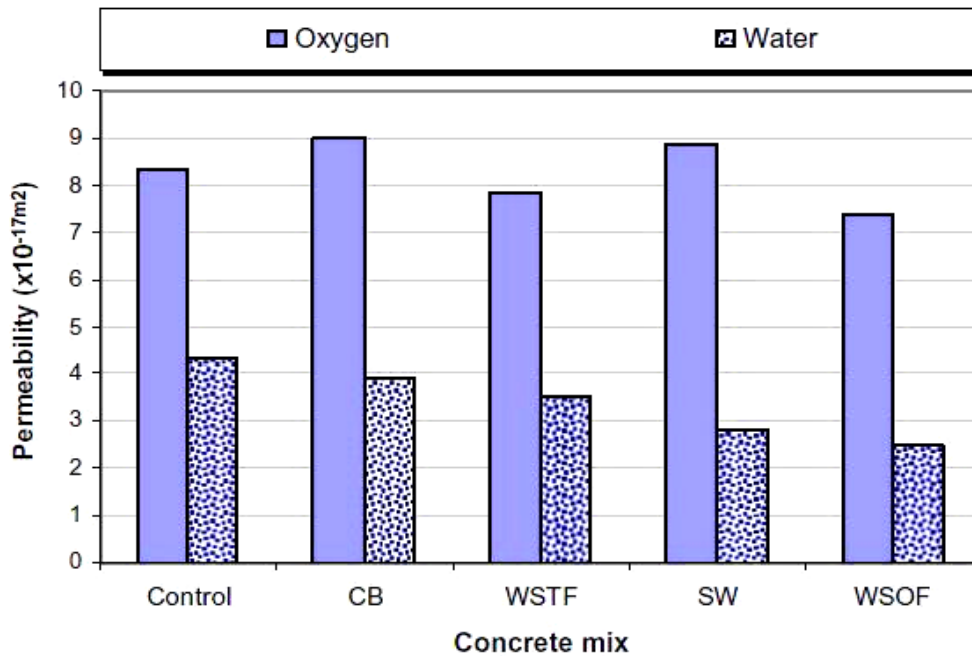


Figure 2.5: Permeability test for concrete containing ceramic aggregate (oxygen and water) (Pacheco-Torgal and Jalali, 2010).

The permeability test of concrete containing aggregate replaced partially by ceramic aggregate concrete has been investigated by Pacheco-Torgal and Jalali (2010) and presented in Figure 2.5. When relating the permeability outcomes with the ones obtained by other authors such as (Cabrera et al., 1989; Torgal and Castro-Gomes, 2006), that indicates to the finalization that ceramic waste aggregates centered concrete achieves better quality. Regarding the water permeability index the three combinations does not give appropriate variances.

The vacuum water absorption test of concrete containing aggregate replaced partially by ceramic aggregate concrete has been investigated by Pacheco-Torgal and Jalali (2010) and presented in Figure 2.6. From Figure 2.6 it can be stated that the ceramic sand and aggregate concrete provide better water absorption rather than conventional aggregate concrete under the vacuum condition (Pacheco-Torgal and Jalali, 2010), however there is very minor difference. Also Pacheco-Torgal and Jalali (2010) stated that the capillarity water absorption index the variances are most significant since capillary water absorption

for control conventional aggregate concrete. It almost doubles the capillarity water absorption index of ceramic waste aggregates concrete. For this reason it may defines that using ceramic waste aggregates conclude to greater durability services considering the resistance of concrete to stop the entrance of water into concrete. The moral performance of the concrete mixtures with ceramic waste aggregates has been settled by the oxygen permeability results.

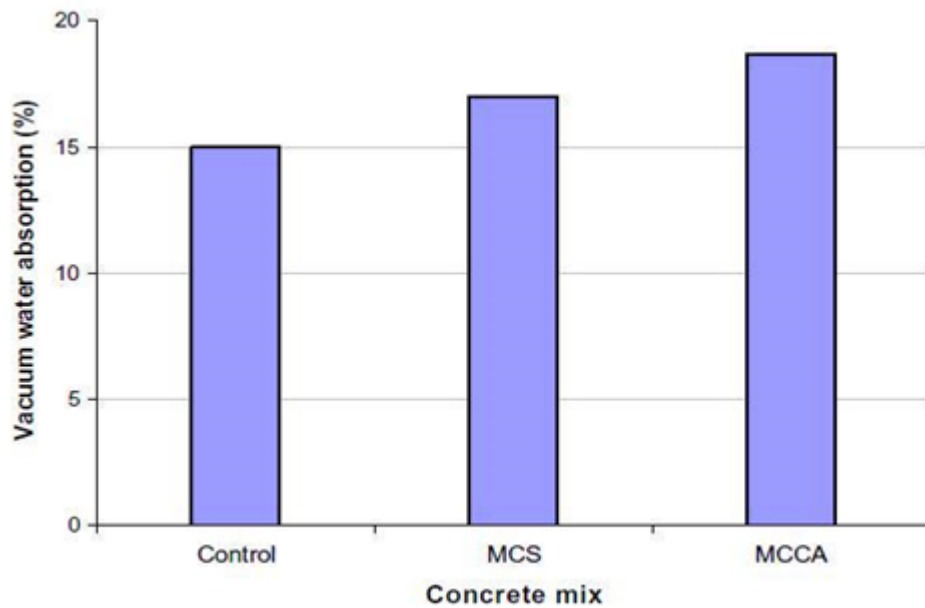


Figure 2.6: Vacuum water absorption for concrete containing ceramic (Pacheco-Torgal and Jalali, 2010).

However, the compressive strength after the aging test is still greater in ceramic waste aggregates based concrete, being greater for the ceramic sand manufactured from ceramic wastes. It is well-known that the water absorption, penetration of oxygen, chloride and other impurities ions into the concrete is the most significant index in the physical and chemical procedure of concrete corrosion (Oh et al., 2002; Glasser et al., 2008), ceramic waste sand concrete does not negotiation durability necessities allowing structures with extended service life and minor environmental influence (Mora, 2007). The partial replacement of conventional sand in concrete by ceramics wastes sand may direct to related environmental paybacks. This ceramic waste recycled approach helps to avoid the withdrawal of huge amounts of raw materials from the earth, decreases energy prices and also stops landfill related difficulties.

## **2.8 Microscopic Investigation of Concrete**

### **2.8.1 X-ray Fluorescence (XRF) Analysis**

X-ray Fluorescence (XRF) analysis is a non-destructive investigative method used to analyze the elementary composition mainly chemical composition of any materials (Hatsopoulos, 2006). XRF analyzers decide the chemical composition of a particular sample by calculating the fluorescent (or secondary) X-ray released from a sample when it is excited by a primary X-ray source. Every of the elements exists in a sample creates a set of characteristic fluorescent X-rays ("a fingerprint") that is excellent for that particular element, for this reason XRF spectroscopy is an outstanding technique for qualitative and quantitative investigation of material composition (Hatsopoulos, 2006).

The X-ray fluorescence process (shown in Figure 2.7) has been described below (Hatsopoulos, 2006):

- ❖ A powder or solid or a liquid sample is illuminated with huge energy X-rays from an organized X-ray tube.
- ❖ When the sample is being hit by an atom with an X-ray of adequate energy (bigger than the atom's K or L shell binding energy), an electron is dislodged from one of the atom's inner orbital shells.



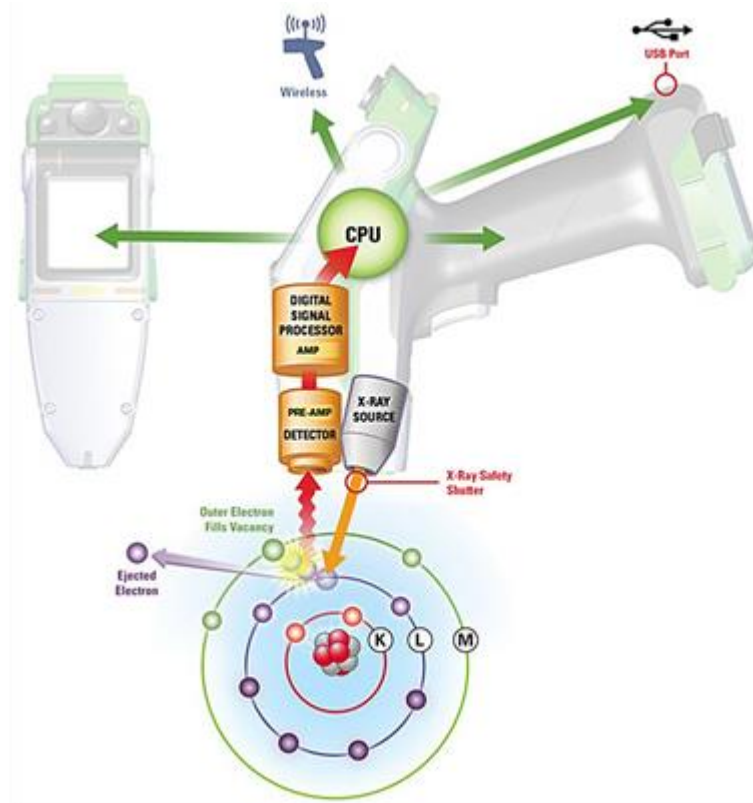


Figure 2.7: The X-ray fluorescence (XRF) process (Hatsopoulos, 2006).

- ❖ The atom regains steadiness, satisfying the position left within the inner orbital shell with an electron from one among the atom's greater energy orbital shells.
- ❖ The electron emits to the inferior energy by cathartic a fluorescent X-ray. The energy of this X-ray is up to the precise distinction in energy between two quantum states of the electron. The activity of this energy is the base of XRF investigation techniques.

Abdunnabi (2012) conducted a study on XRF analysis of Portland cement for major and trace elements on several cement factories in Libya. The mineral content shows that the Libyan cement meets the requirements of the international specifications of the Portland cement. The various standard specifications showed different requirements of chemical and physical properties for Portland cement;  $\text{SO}_3$ ,  $\text{MgO}$ , alkalis as  $\text{Na}_2\text{O}$ , loss on ignition, unsolvable deposit, fineness (Blaine), soundness, autoclave expansion, compressive strength and initial and final setting time (Abdunnabi, 2012). Table 2.4 depicts the requirements of the chemical composition of Portland cement in accordance with ASTM

specification, whereas, the mineralogical composition of Portland cement has been represented in Table 2.5.

Table 2.4: ASTM specification of the chemical composition of Portland cement (ASTM, 2015).

Chemical Name	Common Name	Chemical Notation	Abbreviated Notation	Mass Contents (%)
Calcium Oxide	Lime	CaO	C	58-66
Silicon Dioxide	Silica	SiO <sub>2</sub>	S	18-26
Aluminium Oxide	Alumina	Al <sub>2</sub> O <sub>3</sub>	A	4-12
Ferric Oxide	Iron	Fe <sub>2</sub> O <sub>3</sub>	F	1-6
Magnesium Oxide	Magnesia	MgO	M	1-3
Sulphur Trioxide	Sulphurican Hyrite	SO <sub>3</sub>	St	0.5-2.5
Alkaline Oxides	Alkalis	K <sub>2</sub> O and Na <sub>2</sub> O	K+N	<1

Table 2.5: ASTM standard mineralogical composition of Portland cement (ASTM, 2015).

Chemical Name	Common Name	Chemical Notation	Abbreviated Notation	Mass Contents (%)
Tricalcium Silicate	Alite	3CaO.SiO <sub>2</sub>	C <sub>3</sub> S	38-60
Dicalcium Silicate	Belite	2CaO.SiO <sub>2</sub>	C <sub>2</sub> S	15-38
Tricalcium Aluminate	Aluminate	3CaO.Al <sub>2</sub> O <sub>3</sub>	C <sub>3</sub> A	4-12
Tetracalcium Aluminoferrite	Celite	4CaO.Al <sub>2</sub> O <sub>3</sub> .Fe <sub>2</sub> O <sub>3</sub>	C <sub>4</sub> AF	10-18
Pentacalcium Trialuminate	Celite	5CaO.Al <sub>2</sub> O <sub>3</sub>	C <sub>5</sub> AF	1-3
Calcium Sulphate Dihydrate	Gypsum	CaSO <sub>4</sub> .H <sub>2</sub> O	CSH <sub>2</sub>	2-5

Several researchers such as Scrivener and Kirkpatrick (2008) reported that the regular chemical compositional analysis is a very important part in observing the production process of cement, from the complete investigation of raw materials to testing every phase of the manufacture process. In a conventional process, natural minerals like limestone and

clay form the raw mix that drives into the kiln for firing by coal, oil, or natural gas to make clinker. Management of the fundamentals reaction needs correct analysis for maintain the optimum proportions of calcium, silicon, aluminum, and iron within the raw mixes. Estimations using these four components (sometimes including sulfur) provide the essential manufacture management factors such as lime saturation factor (SLF) and silica ratio (SR). Analysis of the clinker involves the similar elements as for the raw meal, but management of the extra gypsum during the final milling phase solely needs to quantify of sulfur content (Scrivener and Kirkpatrick, 2008).

Waste materials are gradually being used in the cement manufacturing process, conveying in several changes. Once they cover the most cement manufacturing elements, waste materials can substitute a number of the natural raw materials and flammable wastes can facilitate from the kiln. This suggests a lot of testing of the received raw materials, each throughout the procedure and in the final product. Consequently, for a cement plant to contest in today's cost conscious market, its investigative competences should be in depth, cost-effective, and versatile. Finally, if someone decide to replace cement by others waste materials, it is concluded from the above discussion that XRF analysis is crucially needed to check the chemical composition similarity or dissimilarity of the waste material with cement. To control the quality of cement manufacturing and final product of cement XRF analysis is mandatory.

### **2.8.2 X-ray Diffraction (XRD) Analysis**

X-ray diffraction (XRD) is a faster investigative method mainly used for phase detection of a crystalline material and can deliver data on unit cell dimensions. The analyzed material should be finely powdered, standardized, and average bulk composition is determined (Dutrow and Clark, 2017). Several researchers (Brady and Boardman, 1995; Cullity, 1978; Hovis, 1997; Klug and Alexander, 1974; Moore and Reynolds, 1989) conducted XRD related study presented below.

The crystalline substances act as three-dimensional diffraction gratings for X-ray wavelengths parallel to the spacing of planes in a crystal lattice was invented by Max von Laue in 1912. Now a days, X-ray diffraction (XRD) is very common and popular method

for the analysis of crystal structures and atomic spacing. Figure 2.8 depicts the fundamental principles of X-ray diffraction (XRD) analysis.

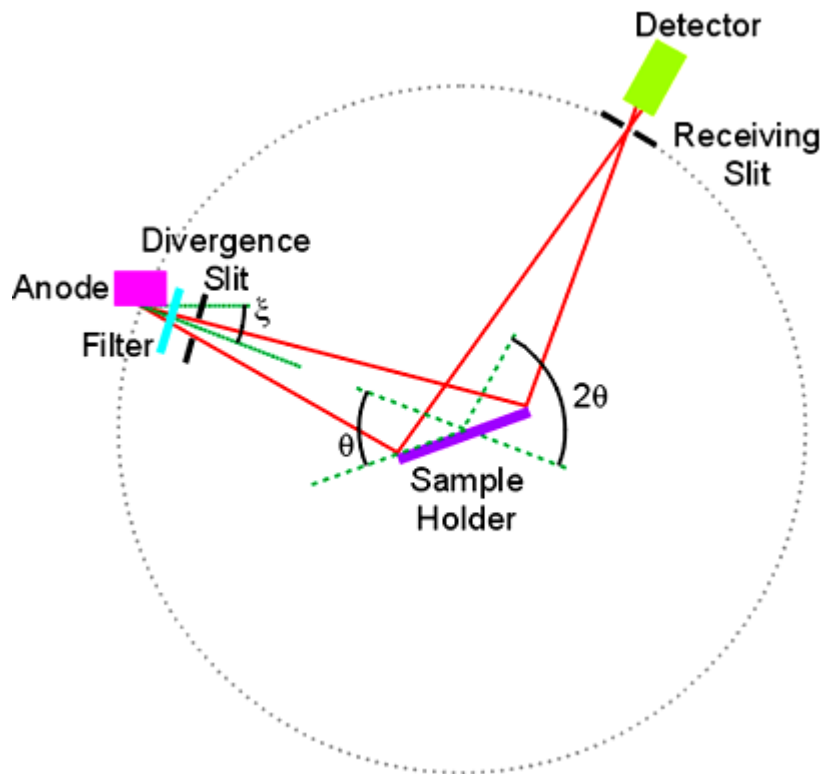


Figure 2.8: Principles of X-ray Diffraction (XRD) analysis (Dutrow and Clark, 2017).

Several researchers (Brady and Boardman, 1995; Cullity, 1978; Hovis, 1997; Klug and Alexander, 1974; Moore and Reynolds, 1989) explained that the X-ray diffraction is built on constructive interloping of monochromatic X-rays and a crystalline sample. These X-rays emitted a cathode ray tube, sieved to produce monochromatic radiation, collimated to concentrate, and focused toward the sample. The interaction of the incident rays with the sample creates constructive interference (and a diffracted ray) when assumptions satisfy Bragg's Law ( $n\lambda = 2d\sin\theta$ ). This law narrates the wavelength of electromagnetic radiation to the diffraction angle and the lattice spacing in a crystalline sample. These diffracted X-rays are then perceived, treated and calculated. By scanning the sample through a spread of  $2\theta$  angles, all attainable optical phenomenon directions of the lattice ought to be achieved because of the arbitrary positioning of the fine material. Alteration of the diffraction peaks to d-spacings permits identification of the mineral as a result of every mineral includes a set of distinctive d-spacings. Naturally, this is often attained by contrast

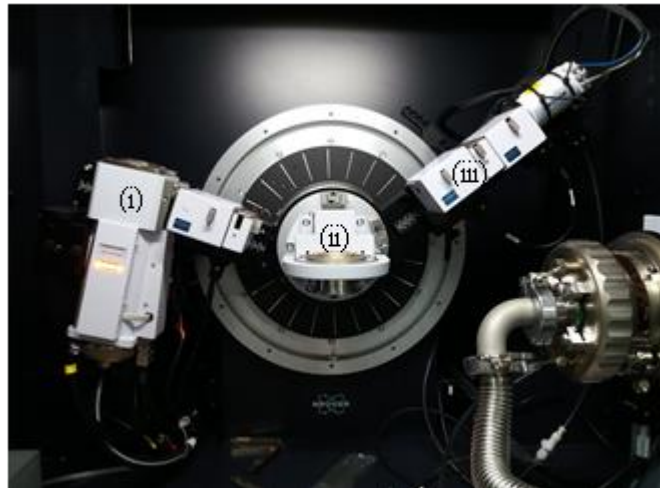
of d-spacings with regular orientation patterns (Brady and Boardman, 1995; Cullity, 1978; Hovis, 1997; Klug and Alexander, 1974; Moore and Reynolds, 1989).

All diffraction approaches are supported generation of X-rays in an X-ray tube. These X-rays are focused at the sample, and also the diffracted rays are together. A main part of all diffraction is that the angle between the incident and diffracted rays. Powder and single crystal diffraction differ in arrangement on the far side (Brady and Boardman, 1995; Hovis, 1997).

X-ray diffractometers should be made of three basic elements i.e. a sample holder, an X-ray tube, and an X-ray detector as shown in Figure 2.9. X-rays are produced in a cathode ray tube by heating a filament to produce electrons, rushing the electrons near a marked by smearing a voltage, and bombing the marked sample by the electrons (Brady and Boardman, 1995; Cullity, 1978; Hovis, 1997; Klug and Alexander, 1974; Moore and Reynolds, 1989). Brady and Boardman (1995) and Cullity (1978) stated that once electrons have adequate energy to dislodge inner shell electrons of the marked sample, characteristic X-ray spectra are formed. This spectrum accommodates of many elements, the foremost common being  $K_{\alpha}$  and  $K_{\beta}$ .  $K_{\alpha}$  consists, in quantity, of  $K_{\alpha 1}$  and  $K_{\alpha 2}$ .  $K_{\alpha 1}$  has a marginally smaller wavelength and twice the concentration as  $K_{\alpha 2}$ . The definite wavelengths are characteristic of the marked material (Cu, Fe, Mo, Cr). Sieving, by foils or crystal monochrometers, is obligatory to create monochromatic X-rays required for diffraction.  $K_{\alpha 1}$  and  $K_{\alpha 2}$  are adequately adjacent in wavelength such that a weighted average of the two is employed. Copper is the commonest marked material for one side crystal diffraction, with  $CuK_{\alpha}$  radiation = 1.5418 Å. These X-rays are collimated and focused onto the sample materials (Brady and Boardman, 1995; Hovis, 1997; Moore and Reynolds, 1989). The full and inside view of XRD instruments has been presented in Figure 2.9.



(a)



(b)

Figure 2.9: View of XRD instrument (a) Full view and (b) Inside view: (i) X-ray tube, (ii) Sample holder and (iii) X-ray detector (Photo taken by author).

As the sample and detector are alternated, the concentration of the imitated X-rays is verified. Once the geometry of the incident X-rays imposing the sample fulfills the Bragg Equation, beneficial intrusion happens and a peak in concentration happens. A detector counts and procedures this X-ray signal and transforms the signal to a predefined frequency which is then display by a computer monitor or output by a printer (Brady and Boardman, 1995; Cullity, 1978; Hovis, 1997).

The geometry of an X-ray diffractometer is specified the sample exchanges within route of the collimated X-ray beam at an angle  $\theta$ , whereas the X-ray detector is straddling on an arm to collect the diffracted X-rays and rotates at an angle of  $2\theta$ . The instrument accustomed to sustain the angle and exchange the sample is named a goniometer. For classic powder forms, information is gathered at  $2\theta$  from  $\sim 5^\circ$  to  $70^\circ$  angles that are found in the X-ray scan (Hovis, 1997; Klug and Alexander, 1974; Moore and Reynolds, 1989).

X-ray diffraction (XRD) is a broadly used investigation technique for the analysis of indefinite crystalline materials (e.g. minerals, inorganic compounds) (Moore and Reynolds, 1989). Determination of indefinite solids is complex to research in geology, environmental science, material science, engineering and biology. The widespread ranges of applications are described below (Brady and Boardman, 1995; Cullity, 1978; Hovis, 1997; Klug and Alexander, 1974; Moore and Reynolds, 1989):

- ❖ Classification of crystalline materials
- ❖ Documentation of fine-grained minerals i.e. clays and mixed layer clays which are problematic to define visually
- ❖ Calculation of unit cell sizes
- ❖ Determination of sample pureness.

With specified techniques, XRD could be used to (Brady and Boardman, 1995; Cullity, 1978; Hovis, 1997; Moore and Reynolds, 1989):

- ❖ Measurement of crystal structures by Rietveld refinement
- ❖ Calculation of modal quantities of minerals, also known as quantitative analysis
- ❖ Characterize skinny films samples by:
  - Defining lattice mismatch between film and substrate and to inferring stress and strain
  - Formative dislocation compactness and superiority of the film by rocking curve measurements
  - Measuring super lattices in compound epitaxial structures
  - Determining the roughness and thickness of the film exhausting glancing incidence X-ray reflectivity measurements
- ❖ Investigate textural quantities, such as the alignment of grains, in a polycrystalline section.

Several researchers (Brady and Boardman, 1995; Cullity, 1978; Hovis, 1997; Klug and Alexander, 1974; Moore and Reynolds, 1989) stated that there are some strengths of XRD that are designated below:

- Powerful and fast (< 20 min) technique for investigation of an indefinite mineral
- In maximum cases, it delivers an clear-cut mineral patterns
- Minimal sample preparation is mandatory
- XRD units are extensively available
- Data explanation is comparatively easy.

Few other authors (Brady and Boardman, 1995; Hovis, 1997; Moore and Reynolds, 1989) also reported some limitations of XRD and stated below:

- Standardized and single phase material is top suited for the investigation of an unidentified mineral
- Must have right to use to a typical standard file location of inorganic compounds (d-spacings, hkl's)
- Needs tenths of a gram of material in the powder form
- For diverse materials, detection limit is ~ 2% of the material sample
- For unit cell analysis, classification of patterns for non-isometric crystal systems is complex
- Peak overlap might happen and degrades for prime angle 'reflections'.

### **2.8.3 Scanning Electron Microscopy (SEM) Analysis**

The scanning electron microscope (SEM) uses a centered beam of high-energy electrons to come with a wide range of signals at the solid surface of the specimens (Beane, 2004; Clarke and Eberhardt, 2002). The signals that originate from electron-sample exchanges expose data regarding the sample as well as external surface morphology (texture), chemical compositional elements, and crystalline structure and positioning of materials production up the sample. In most circumstances, data are gathered over a specific area of the surface of the sample, and a 2-dimensional image is generated that shows three-dimensional differences in these properties (Beane, 2004; Egerton, 2005; Reimer, 2013). Areas reaching from nearly 1 cm to 5 microns in breadth could be imaged in a scanning mode using traditional SEM techniques (magnification ranging from 20X to approximately 50,000X, three-dimensional resolution of 50 to 100 nm). The SEM analysis is additionally accomplished of execution examines of selected point locations on the sample; this tactic is particularly supportive in qualitatively or semi-quantitatively determining chemical compositions (using EDS), crystalline structure, and crystal alignments (using EBSD). The design and function of the SEM is incredibly almost like the EPMA and sizable overlap in capabilities occurs between the two instruments (Swapp, 2017). Several researchers (Beane, 2004; Clarke and Eberhardt, 2002; Egerton, 2005; Reimer, 2013) also described the detailed scanning electron microscopy (SEM) process. The full and inside view of sample holder of SEM instrument has been described in Figure 2.10.





(a)



(b)

Figure 2.10: View of SEM instrument (a) Full view and (b) Inside view of sample holder  
(Photo taken by author).

Beane (2004) reported that the augmented electrons in an SEM investigation carry considerable volumes of mechanical energy, and this energy is dissolute as a spread of signals induced by electron-sample connections once the incident electrons are drop down within the solid sample surface. These signals contain secondary electrons (that create SEM images), backscattered electrons (BSE), diffracted backscattered electrons (EBSD that are used to analyze crystal structures and orientations of minerals), photons (characteristic X-rays that are used for fundamental analysis and continuum X-rays), visible light (cathodoluminescence--CL), and heat. Several researchers (Beane, 2004; Egerton, 2005; Reimer, 2013) described for the imaging samples secondary electrons and backscattered electrons are normally used: secondary electrons are most significant for presenting surface morphology and topography on samples and backscattered electrons are most vital for demonstrating contrasts in structure in multiphase samples (i.e. for rapid phase discrimination). X-ray generation is formed by rigid impacts of the incident electrons with electrons in discrete orbitals (shells) of atoms in the sample. As the excited electrons back to inferior energy positions, they yield X-rays that are of a static wavelength (that is related to the variance in energy levels of electrons in altered shells for a given element). Thus, characteristic X-rays are created for every element in a mineral that is "excited" by the electron beam. It is generally well known that the SEM analysis is a "non-destructive" test method; that is, x-rays produced by electron connections do not direct to volume loss of the sample, so it is probable to investigate the same materials

frequently (Beane, 2004; Clarke and Eberhardt, 2002; Egerton, 2005; Reimer, 2013). The schematic diagram of the electron and X-ray optics of a combined SEM-EPMA has been mentioned in Figure 2.11.

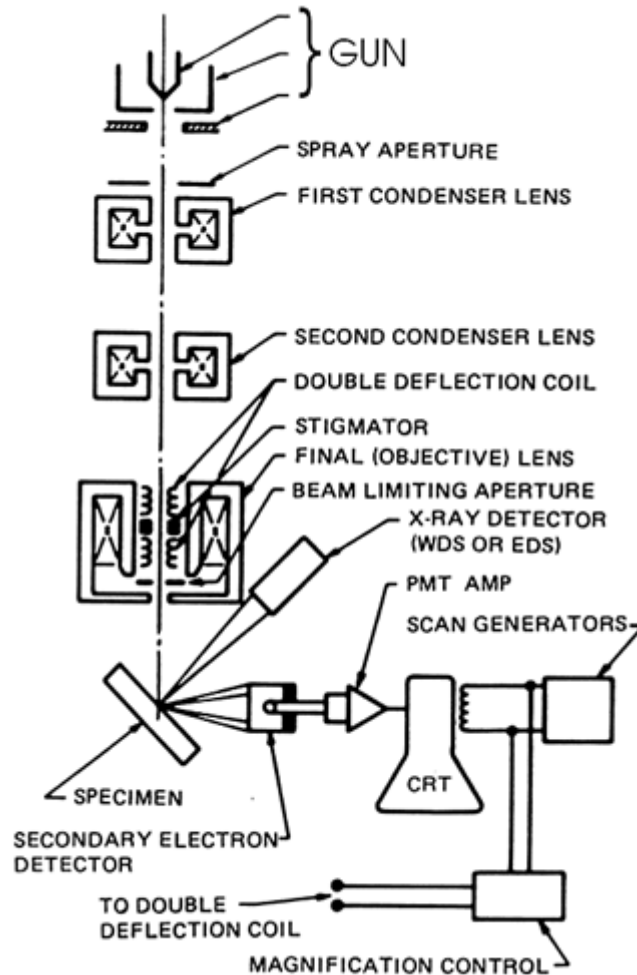


Figure 2.11: Schematic drawing of the electron and X-ray optics of a combined SEM-EPMA (Egerton, 2005).

Several researchers (Beane, 2004; Clarke and Eberhardt, 2002; Egerton, 2005; Reimer, 2013) stated that there are some necessary components of all SEMs including:

- ❖ Electron Source ("Gun")
- ❖ Electron Lenses
- ❖ Sample Stage
- ❖ Detectors for all noticed signals
- ❖ Display / Data output devices
- ❖ Infrastructure Requirements:

- Power Supply
- Vacuum System
- Cooling system
- Vibration-free floor
- Room free of ambient magnetic and electric fields.

Scanning electron microscopy (SEM) continually have a minimum of one detector (usually a secondary electron detector), and maximum have extra detectors. The precise abilities of a specific instrument are censoriously reliant on which detectors it accommodates (Beane, 2004; Clarke and Eberhardt, 2002; Egerton, 2005; Reimer, 2013).

The SEM is regularly used to produce high-resolution photos of forms of objects (SEI) and to point out three-dimensional differences in chemical compositions (Beane, 2004; Clarke and Eberhardt, 2002; Egerton, 2005; Reimer, 2013):

- ❖ Obtaining elemental maps and / or spot chemical examines using EDS. A typical cement clinker image by SEM has been showed in Figure 2.12.
- ❖ Judgment of phases supported by mean atomic number (commonly associated with comparative density) using BSE.
- ❖ Compositional maps are made on differences in trace element "activators" using CL.
- ❖ The SEM is additionally broadly used to determine stages based on qualitative chemical analysis and/or crystalline arrangement. Detailed measurement of very tiny features and objects all the way down to 50 nm in size is additionally accomplished using the SEM. Backscattered electron pictures (BSE) are often used for fast discrimination of phases in poly-phase samples.
- ❖ SEMs prepared with deflected backscattered electron detectors (EBSD) are often accustomed to inspect micro-fabric and crystallographic location in several materials.

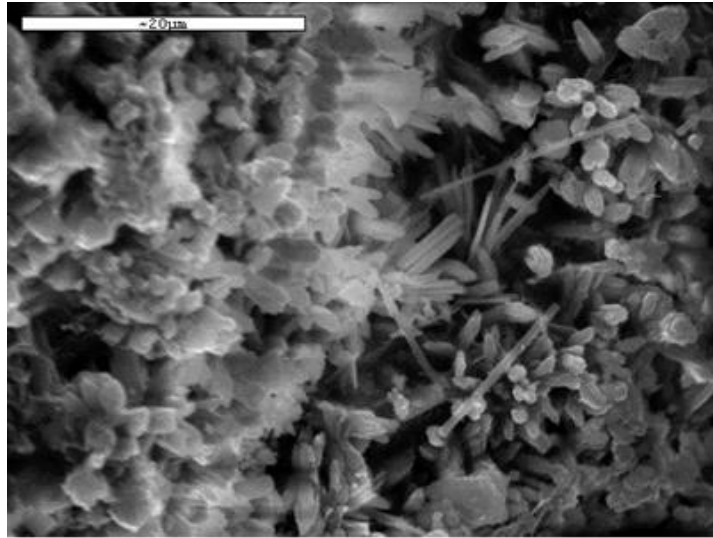


Figure 2.12: SEM image of cement clinker (Imaggeo, 2012).

Several researcher (Beane, 2004; Clarke and Eberhardt, 2002; Egerton, 2005; Reimer, 2013) reported there are various strengths of SEM analysis including:

- ❖ There is questionably no new tool or technique with the extent of applications in the study of solid elements that equals to the SEM analysis.
- ❖ The SEM is most important in all fields that need characterization of solid materials. Whereas this input is mostly involved with geological properties, it is vital to notice that these uses are an awfully tiny set of the technical and industrialized applications that exist for this instrumentation.
- ❖ Most SEM's analyses are relatively straightforward to control, with very friendly usage interfaces.
- ❖ For several applications, data acquisition is speedy (not greater than 5 minutes / image for SEI, BSE, spot EDS analyses).
- ❖ Recent SEMs produce data in numerical formats, which are extremely transportable.

Some limitations of SEM analysis are described below as reported by (Egerton, 2005; Reimer, 2013):

- ❖ Samples should be solid and they should appropriate in size into the microscope chamber. Maximum size in horizontal directions is generally 10 cm; vertical directions are typically far more inadequate and barely exceed 40 mm. For many instruments samples should be stable in a vacuum on the order of  $10^{-5}$  -  $10^{-6}$  torr.

- ❖ Samples need to outgas at little pressures are inappropriate for investigation in traditional SEM's.
- ❖ EDS detectors on SEM's cannot detect very light elements (H, He, and Li).
- ❖ An electrically conductive covering should be used to electrically conductive the samples in traditional SEM's, except the instrument is skilled of process in a low vacuum approach.

## **CHAPTER III**

### **MATERIALS AND RESEARCH METHODOLOGY**

#### **3.1 General**

This chapter is to elaborate the description of materials properties, specimen's details and test setup. This chapter describes the detailed methodology adopted to accomplish this study. X-ray Fluorescence (XRF) Analysis, compressive strength test, splitting tensile strength test, X-ray Diffraction (XRD) and Scanning Electron Microscopy (SEM) analysis have been described in this chapter. Also, the procedure for analyzing the results is explained in this chapter.

#### **3.2 Description of Materials**

This study covers the mechanical and microscopic investigation of concrete, where the cement is replaced by waste ceramic powder up to certain proportions. As the concrete analysis is the main target of this study; so the ordinary Portland cement, coarse aggregate, fine aggregate, water and ceramic waste are the key materials of this study.

##### **3.2.1 Ordinary Portland Cement (OPC)**

Neville (1995) stated that approximately 75% of the body of the concrete may be given by the aggregates. Thus, its impact is tremendously significant. The concrete quality meets up to the required if the concrete is to be workable, better strength, durable and cost-effective. The aggregates should be proper shape and size, neat and clean, hard, strong and well graded (Khajuria et al., 2013).



Figure 3.1: A glimpse of ordinary Portland cement in pan.

Cement is a binding material within the concrete and mortar. It binds all the concreting materials together. Concrete mixtures were prepared using Ordinary Portland Cement (OPC) as the main binder and cement was partially replaced by ceramic waste powder. The OPC conforms to the ASTM C150, Type-I, CEM-I, 53.5 N. Composition of this cement is 95-100% clinker, and 0-5% gypsum as indicated by manufacturer. The specific surface area of cement was  $388 \text{ m}^2/\text{kg}$ . Cement was replaced partially by ceramic waste (CW) powder by 0%, 5%, 10%, 15%, 20%, 25% and 30% respectively.

### **3.2.2 Ceramic Waste Powder (CWP)**

According to the source of raw materials, ceramic wastes are divided into two categories. The pictorial view of ceramic waste in dumping points has shown in Figure 3.2. Firstly, structural ceramic industry manufactured all fired wastes that are generally red pastes products. These ceramic wastes include ceramic brick, blocks and roof tiles. Secondly, other categories of ceramic produced that is stoneware ceramic such as wall, floor tiles and sanitary ware. Depending on the manufacturer, there are usually two types of ceramic paste available. These are red and white pastes. Although, the white paste are used in more common and much larger in volume. The chemical compositions of ceramic pastes were examined and outcomes are reported in results and discussion chapter.





Figure 3.2: Field photo of waste ceramic tiles (white and red mixed).

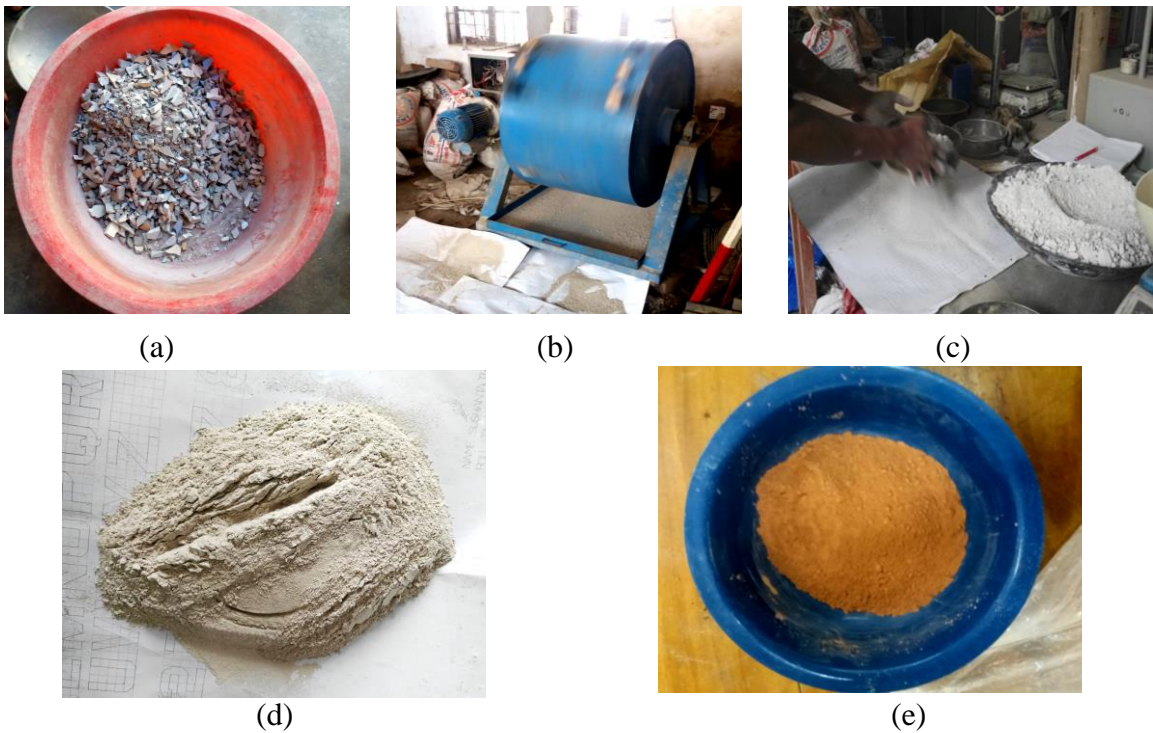


Figure 3.3: Steps of CW powder preparation: (a) Field CW after grinding by hammer (b) Ball machine grinding and (c) Sieving by #200 sieve (d) White CW powder after sieving and (e) Red CW powder after sieving.

The ceramic powders are prepared by ball mill machine with metal balls at the laboratory. The complete steps of ceramic waste (CW) powder preparation have been described in Figure 3.3. This research conducted on the partial replacement of cement by ceramic powder as a binder. The ceramic powders with a particle size less than  $75 \mu\text{m}$  were selected for the partial replacement of cement. The concrete were mixed and tested using the ASTM standard method.



### 3.2.3 Coarse Aggregate

Crushed stone chips were used in all mixes as coarse aggregate with the nominal size of 19 mm. Properties of the selected coarse aggregate are shown in Table 3.1. The selected crushed stone chips (shown in Figure 3.4) were used as coarse aggregate to prepare cylinders for compressive strength test, splitting tensile strength test according to ASTM C127 and ASTM C29 respectively; and the microscopic analysis i.e. X-ray diffraction (XRD) and Scanning Electron Microscopy (SEM) analysis. The grain size distribution of coarse and fine aggregates has been conducted by sieve analysis. This was done by sieving the aggregate as per ASTM C136. The sieve analysis strategy has been illustrated in Figure 3.5.



Figure 3.4: Coarse aggregate i.e. crushed stone used in the study.

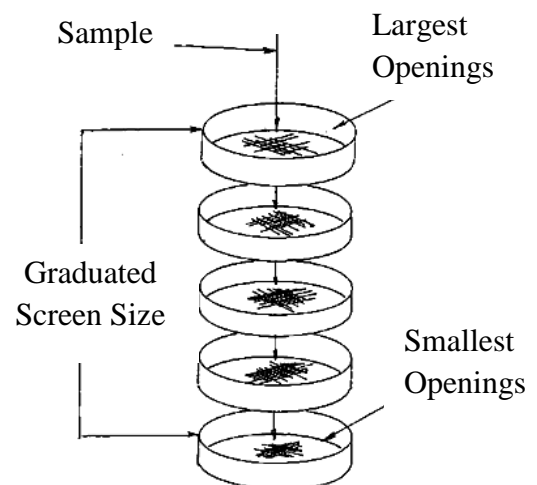


Figure 3.5: Sieve analysis technique.

Table 3.1: Properties of coarse aggregates.

Characteristics	Value
Specific Gravity	2.84
Unit Weight	1570 kg/m <sup>3</sup>
Fineness Modulus	7.06
Water Absorption	1.1%

### 3.2.4 Fine Aggregate

The aggregates most of which pass through 4.75 mm sieve are defined as fine aggregates. Processed Ottawa sand was used to prepare cube specimen for mortar test. A sand is called Ottawa sand, if it passed sieve #30 (96% to 100%), #40 (65% to 75%), # 50 (20% to 30%) and #100 (0% to 4%) (Baldi et al., 1985). Sylhet sand was used as fine aggregate to prepare cylinders for compressive strength test, splitting tensile strength test and XRD & SEM analysis. Different properties as specific gravity, water absorption, fineness modulus, unit weight was determined according to ASTM C128, ASTM C136 and ASTM C29 standards respectively. Properties of selected sand are shown in Table 3.2.

Table 3.2: Properties of fine aggregates.

Characteristics	Value
Specific Gravity	2.65
Unit Weight	1452 kg/m <sup>3</sup>
Fineness Modulus	2.55
Water Absorption	2.12%

## 3.3 Sample Preparation and Testing

### 3.3.1 Preparation of Cylindrical Concrete Specimens

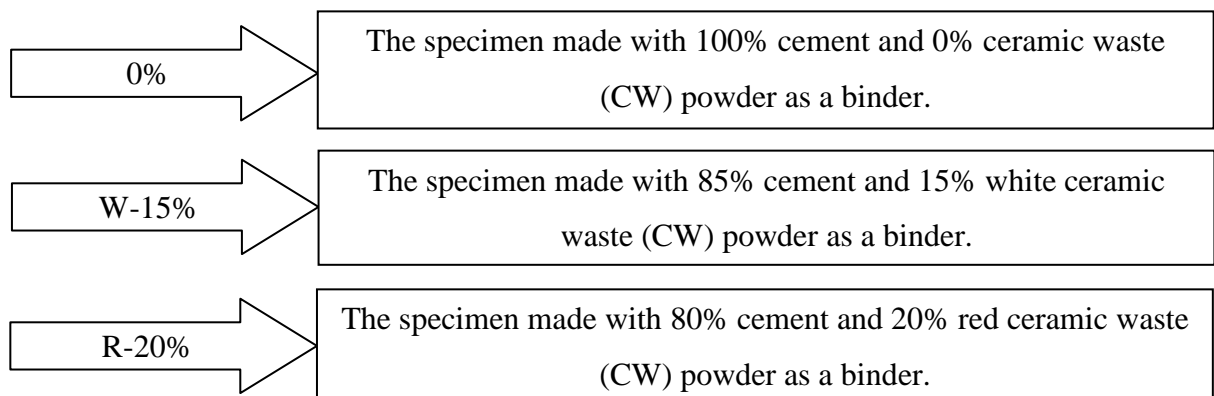
To perform compressive and splitting tensile strength test of cylindrical concrete specimens, investigations were carried out on two groups of concrete samples: group one made with only cement, stone chips and sand; second group made with partial replacements of cement CW powder to perform the test according to ASTM C39. The cement replacements were done by 0%, 5%, 10%, 15%, 20%, 25% and 30% by mass by

white and red CW powder respectively. Tap potable water was utilized to produce concrete mixtures with different dosages as well as in conventional concrete mixtures. The mixing proportions were 1:1.5:3 (cement : sand : coarse aggregate) with constant slum value of all batches of concrete mixes. The w/c ratios were adjusted according to constant slum. The batching for all the proportions is shown in the Table 3.3.

Table 3.3: Mix proportions of cylindrical concrete specimens.

Batch Name	Replacement (%)	Cement (gm)	CW Powder (gm)	Sand (gm)	Stone Chips (gm)	Water (gm)
0%	0%	800	0	1200	2400	356.7
W-5%	5%	760	40	1200	2400	370.0
W-10%	10%	720	80	1200	2400	373.3
W-15%	15%	680	120	1200	2400	376.3
W-20%	20%	640	160	1200	2400	390.0
W-25%	25%	600	200	1200	2400	393.3
W-30%	30%	560	240	1200	2400	400.0
R-5%	5%	760	40	1200	2400	360.0
R-10%	10%	720	80	1200	2400	365.5
R-15%	15%	680	120	1200	2400	371.0
R-20%	20%	640	160	1200	2400	376.3
R-25%	25%	600	200	1200	2400	380.5
R-30%	30%	560	240	1200	2400	386.7

Identification of a particular specimen for mortars test and compressive strength test of cylindrical concrete specimen without referencing table are shown in below:



The steps of preparation of cylindrical concrete specimen for compressive strength tests are described below as shown in Figure 3.6:

- Cylindrical specimens (100mm x 200 mm) were prepared from the desired mix proportions.
- Cement and fine aggregate were mixed on a water tight non-absorbent platform until the mixture was thoroughly blended.
- Percent replacement of cement by CW powder was added according to the specified measurement.
- Mixing was conducted by machine mixing.
- Coarse aggregate was added and mixed with binder and sand until the coarse aggregate was uniformly distributed throughout the batch.
- Water was added and mixed until the concrete appeared to be homogenous and of the desired consistency.



Figure 3.6: Preparation of cylindrical concrete specimens for compressive strength test.

- Workability of the concrete mix was measured.
- The concrete was filled in the molds in 3 layers.
- Each layer was compacted with not less than 25 strokes per layer using a tamping rod.

- The top surface was leveled by trowel.
- After 24 hours of casting, the cylinders were removed from the mold and allowed for curing.

### 3.3.1.1 Capping of Cylindrical Concrete Specimens

Capping is essential to give a flat surface for applying compressive load to concrete cylinders. Capping is performed only for cylindrical concrete test specimens by suitable method. If the surfaces of cylindrical concrete specimens are not flat enough within 0.05 mm, then it is necessary to cap those test samples (Richart et al., 1928). The capped surfaces should be at right angles to the axis of the test specimens. Caps are made as thin as feasible for testing the specimens. Also it should not get scratched when the specimen is tested. This study used gypsum plaster capping method for capping the cylindrical concrete test specimen according to ASTM C617 and presented in Figure 3.7. The necessary steps for capping are mentioned below.

- A stiff plaster was prepared by mixing gypsum and water at a desired ratio. While making the paste, it was mixed well sufficient. This helped gypsum to achieve strength.
- A scoop, placing some quantity of gypsum plaster on top of the cylindrical test specimen was used.



Figure 3.7: Gypsum capping of cylindrical concrete specimens.

- A glass plate was taken having thickness 6.5 mm and diameter 25 mm which was larger than the diameter of the test specimen.
- Using that glass plate, the stiff gypsum plaster was pressed down by giving the plate a rotary motion till it made complete interaction with the rim of the mold.



Before doing that, a thin layer of oil was applied on the glass plate to escape adhesion of the plaster with the glass plate.

- While giving a rotary motion to the plate, the plate remained parallel to the end surface at all times. After preparing the cap, it was left for 20 to 30 minutes to become hard.
- The same process was repeated to cap the other end of the cylindrical test specimen.

### 3.3.2 Testing of Compressive Strength of Cylindrical Concrete Specimens

The compressive strength tests were performed in accordance with ASTM C39. However, the testing procedures are mentioned in briefly as shown in Figure 3.8:

- The specimens were placed in the machine in such a manner so that the load was applied on the center of the specimen.



Figure 3.8: Compressive strength test setup of cylindrical concrete specimens.

- Stands with set of dial gauge were installed to record lateral and vertical deformation of the specimen.
- Loads were applied at uniform rate.
- The deformations were recorded at the rate of 10 kN.
- The maximum load was recorded.

- The tests were performed for 7, 28 and 90 days.

### 3.3.3 Testing of Splitting Tensile Strength of Cylindrical Concrete Specimens

The splitting tensile strength of cylindrical concrete specimens was performed in accordance with ASTM C496. However, some major steps are mentioned below and presented in Figure 3.9:

- A steel strip was placed (formwork for cylinder) along the length of each cylindrical specimen contact area. Ensuring that each end of each strip is aligned with the respective diametric line.
- The sample was placed in the compression-testing machine. At first centered the sample along the length of the upper bearing block and then ensured that the projections of diametric lines were centered on the upper and lower bearing plates.
- It was verified that the top bearing block is parallel with the top surface of the sample and made adjustments as necessary.

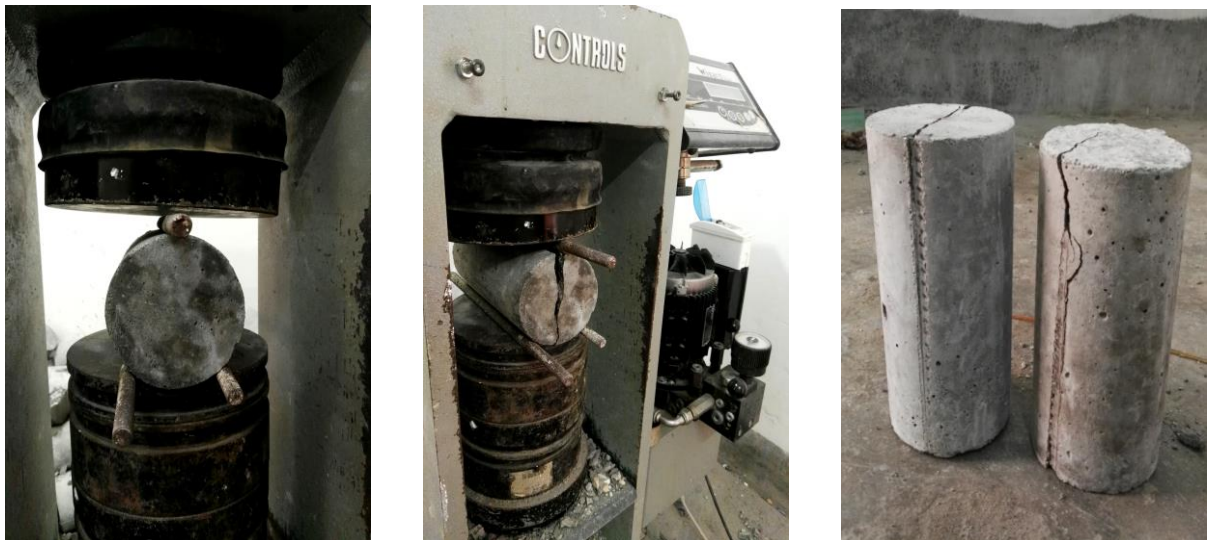


Figure 3.9: Splitting tensile strength test setup of cylindrical concrete specimens.

- Load was applied continuously at a rate of movement corresponding to a splitting tensile stress rate.
- Load was applied continuously until the force indicator shows that the load was decreasing steadily and the sample displayed a well-defined fracture pattern.
- The maximum load carried by the sample during the test was recorded.

- The splitting tensile strength was calculated of each sample using following equation:

$$T = 2P / \pi LD \dots\dots\dots (3.1)$$

Where,  $T$  = splitting tensile strength,

$P$  = maximum applied load indicated by the testing machine,

$L$  = average sample length,

$D$  = sample diameter

- The tests were performed for 7 and 28 days.

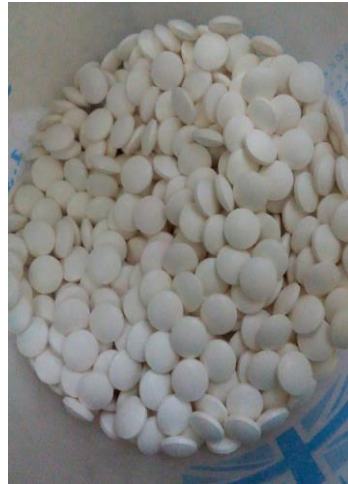
### 3.3.4 X-ray Fluorescence (XRF) Analysis

An X-ray fluorescence (XRF) is an x-ray instrument based popular and comparatively non-destructive chemical analyses of different materials like rocks, minerals, sediments and fluids. Its mechanism based functions on wavelength-dispersive spectroscopic philosophies that are parallel to an electron microprobe (EPMA). Nevertheless, an XRF cannot commonly make analyses at the small spot sizes typical of EPMA work (2 to 5 microns) (Potts et al., 2008). For this reason it is usually conducted for bulk investigation of greater fractions of geological materials. This method of chemical analysis is comparatively eased and cost effective. It has very simple and low cost sample preparation. This is one of the most broadly used means for analysis of major and trace elements in rocks, minerals, and sediment due to the steadiness and comfort of use of X-ray (von Bohlen, 2009). The XRF analysis was conducted in Seven Rings Cement Factory at XRF Analysis Laboratory. The process flow diagram of XRF analysis is described Figure 3.10:





a. Weighted the cement or CW powder ~ 10 gm.



b. Cellulose binder.



c. Cellulose binder was mixed with CW powder (0.80~0.85 gm).



d. Hand grinding was done to produce cement or CW powder and cellulose mixed powder.



e. Five minutes machine grinding was conducted.



f. Placed the grinded powder in a sample holder and weighted.



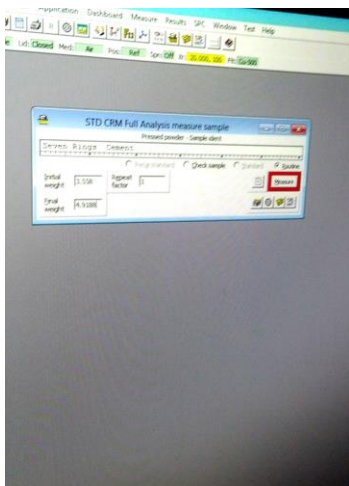
g. Ten ton compressive load was applied by placing the sample with holder in a loading machine.



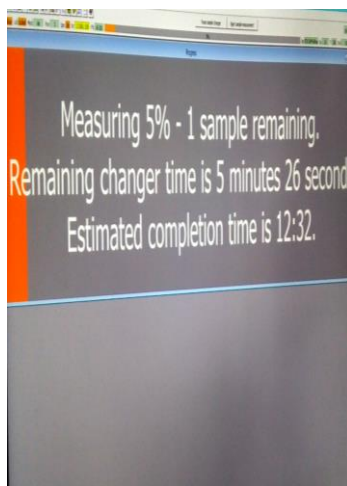
h. Weighted the compressed sample with sample holder.



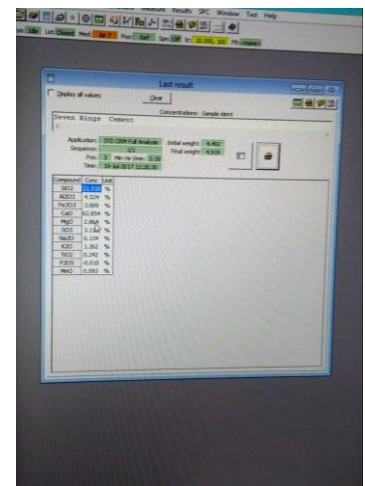
i. Placed the sample in XRF machine and lock the machine cap.



j. Input necessary data (initial and final weight of sample) and run the analysis.



k. Measurement was running.



l. Finally chemical composition was found.

Figure 3.10: Process flow diagram of XRF analysis.

### 3.3.5 X-ray Diffraction (XRD) Analysis

X-ray diffraction (XRD) is a physical investigation process that consists in electromagnetic waves escaping obstacles if the size of the obstacles relates to the

wavelength. This investigation process may be used to the analysis of materials because the atom plans are placed at equivalent distances to X-ray lengths. X-rays are electromagnetic waves comparable to light, however whose wavelength is far shorter ( $= 0.2 - 200 \text{ \AA}$ ) (Elena and Lucia, 2012).

Bale (2010) stated that the XRD is made as a reflection at well-defined angles. Each crystalline phase has its identical diffraction image. The diffraction image comprises a tiny amount of maximal points that is not all the families of crystallographic planes offer maximal diffraction points; all the crystalline phases with the similar type of elementary cell will show the similar succession of Miller indices for the crystalline planes families giving a diffraction maximum point (Bale, (2010)). For the XRD analysis used diffraction devices (diffractometers), mostly according to the Bragg-Brentano system as shown in Figure 3.11. The sample rotates at a diffraction angle " $\theta$ ", while the detector rotates at the angle " $2\theta$ ". In Figure 3.12, the X ray diffractometer (Bruker D8 Advance, Germany) is shown.

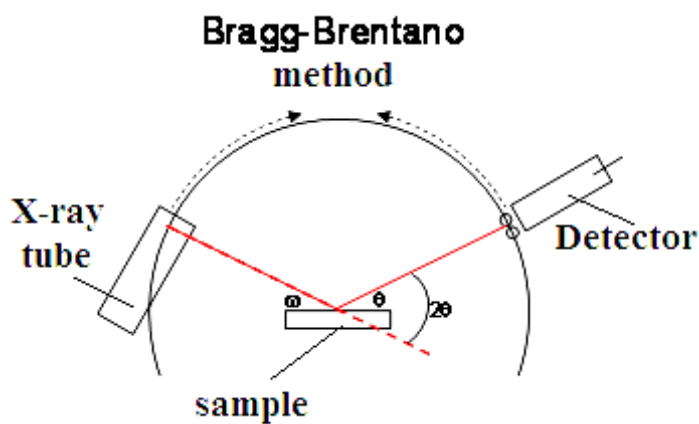


Figure 3.11: The basic layout of an X-ray diffractometer (Jumate and Manea, 2011).



Figure 3.12: X-ray diffractometer (Bruker D8 Advance, Germany) (Photo taken by author).

Several researchers (Elena and Lucia, 2012; Jumate and Manea, 2011) reported that the diffractogram is created from a series of diffraction maximal points, presenting the concentration of the diffracted X radiation on the ordinate observed in pulses/second, and the angle " $2\theta$ ". on the abscissa, where " $\theta$ ", is the Bragg angle, observed in degrees. The

diffraction image is governed by the material structure. The diffraction approaches permit for the presentation of the following studies: the investigation of the crystalline structures, the phase quantitative and qualitative analysis, the study of phase transformations, the study of the crystallographic texture, the scale of the crystallites, the inner stresses within the sample, etc.

The identification of the crystalline phases may be supported with the X-ray diffraction technique if the particular phase signifies more than 3 - 4% mass. The identification may be created by calculation with Bragg's relationship or computer-based, using Match, XpertScore software, in the PDF (Powder Diffraction File) database, where identification files for about 200,000 metal crystalline phases, alloys, oxides, salts, etc. are found (Elena and Lucia, 2012; Jumate and Manea, 2011).

### **3.3.5.1 Sample Collection and Preparation of XRD Analysis**

Determination of an unknown material by XRD analysis involves: the material, an instrument for grinding, and a sample holder. The sample holder with sample is mentioned in Figure 3.13.

- ❖ Took a couple of tenths of a gram (or more) of the material, as clean as probable.
- ❖ Grinded the sample to a fine powder, generally in a fluid to diminish inducing additional strain (surface energy) which will offset peak positions, and to disarrange orientation.
- ❖ Powder less than  $\sim 10\ \mu\text{m}$  (or 200-mesh) in size is desired.
- ❖ Placed into a sample holder or onto the sample surface:
  - Smear uniformly onto a glass slide, assuring a flat upper surface
  - Pack into a sample container
  - Sprinkle on double sticky tape

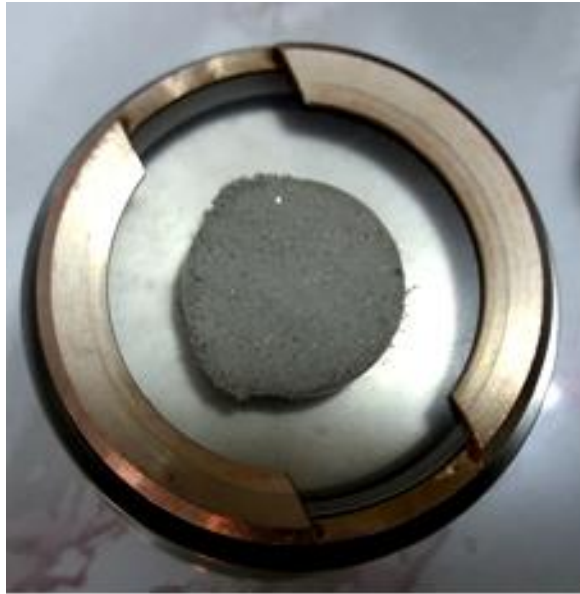


Figure 3.13: Packing of fine powder into a sample holder (Photo by author).

- ❖ Precautionary measures were taken to create a flat upper surface and to attain an arbitrary distribution of lattice angles unless making an oriented smear.
- ❖ For investigation of clays which need a single orientation, specific methods for preparation of clay samples are given by United States Geological Survey (USGS).
- ❖ For unit cell determinations, a little quantity of a standard with known peak positions (that do not interfere with the sample) can be added and used to exact peak positions.

### 3.3.5.2 Test Procedure of XRD Analysis

The BRUKER D8 Advance, Germany XRD machine was used in this study. The minimum requirements of voltage and currents are ~ 40 kV and ~ 40 mA respectively. The detector tube was Cu tube with 1.5418 Å. The step of the XRD test was 0.02°. The XRD analysis was performed in XRD Laboratory, Department of Glass and Ceramic Engineering, RUET, Rajshahi, Bangladesh. The complete test procedures of XRD analysis are described below:

Step No.	Description	Image



- 
01. The cylindrical concrete specimens were casted with prescribed mix proportion. Then the specimens were cured 7 and 28 days.



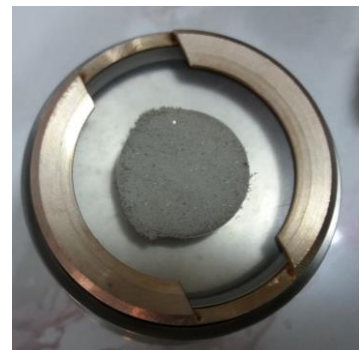
02. After completion of curing, the cylindrical concrete specimen has been broken by applying compressive load.



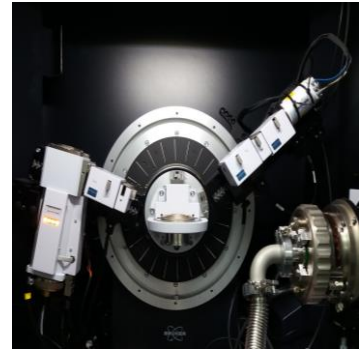
03. The coarse aggregate separated from fine aggregated. Then the fine aggregate especially cement samples is being grinded over and over to make it powder. The powder material was less than  $\sim 10 \mu\text{m}$  (or 200-mesh) in size.



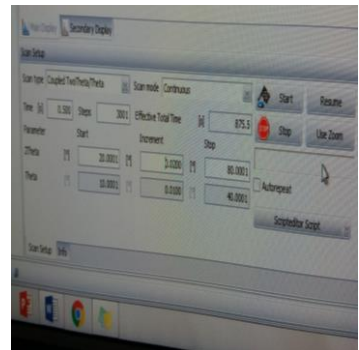
04. The 1.0 ~ 1.5 gm powder placed in a sample holder, The top of sample leveled by glass.



05. The sample holder then placed in sample chamber in the XRD machine. As it is need to be mentioned that left tube was X-ray source, right tube was detector and sample chamber was in the middle of the machine. The machine door was closed.



06. The analysis conducted by the EVA software. The necessary data like starting and ending theta value have been inputted. Then clicked on run button. After analysis the XRD results were found.



### 3.3.5.3 Data Collection and Results Presentation of XRD Analysis

**Data Collection:** The intensity of diffracted X-rays is nonstop documented because the sample and detector rotate over their particular angles. A peak in intensity happen once the mineral contains lattice planes with d-spacings suitable to diffract X-rays at that value of  $\theta$ . While every peak contains of two distinct reflections ( $K_{\alpha 1}$  and  $K_{\alpha 2}$ ), at small values of  $2\theta$  the peak positions overlay with  $K_{\alpha 2}$  appearing as a hump on the side of  $K_{\alpha 1}$ . Larger separation happens at higher values of  $\theta$ . Usually these combined peaks are preserved as one. The  $2\lambda$  position of the diffraction peak is normally taken in consideration because the center of the peak at 80% peak height (Brady and Boardman, 1995; Cullity, 1978; Hovis, 1997; Klug and Alexander, 1974; Moore and Reynolds, 1989).

**Data Reduction:** Outcomes are usually showed as peak positions at  $2\theta$  and X-ray counts (intensity) within the form of a table or an x-y plot as shown in Figure 3.14. Peak locations happen where the X-ray beam has been diffracted by the crystal lattice. The distinctive set of d-spacings resulting from this rhythm can be used to 'fingerprint' the mineral. Intensity (I) is either described as peak height intensity, that intensity greater than background, or as assimilated intensity, the area under the peak. The relative intensity is recorded because

the ratio of the peak intensity to that of the greatest dense peak (relative intensity =  $I/I_1 \times 100$ ) (Brady and Boardman, 1995; Cullity, 1978; Hovis, 1997; Klug and Alexander, 1974; Moore and Reynolds, 1989).

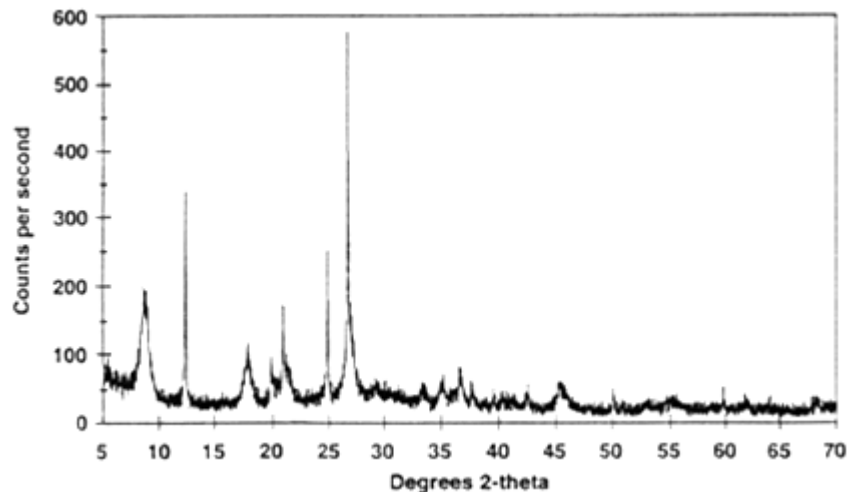


Figure 3.14: Typical X-ray diffractogram (Hovis, 1997).

**Determination of an Unknown:** Several researchers (Brady and Boardman, 1995; Cullity, 1978; Hovis, 1997; Klug and Alexander, 1974; Moore and Reynolds, 1989) mentioned that the d-spacing of every peak is generally achieved by solution of the Bragg equation for the proper value of  $\lambda$ . When all d-spacings are investigated, automated search/match routines compare the *ds* of the unknown to those of known materials. As a result of every mineral has a distinctive set of d-spacings, matching these d-spacings offers an identification of the indefinite sample. A scientific process is employed by ordering the d-spacings in expressions of their intensity starting with the densest peak. Files of d-spacings for hundreds of thousands of inorganic complexes are accessible from the International Centre for Diffraction Data as the Powder Diffraction File (PDF). Several supplementary spots contain d-spacings of minerals such as the American Mineralogist Crystal Structure Database. Usually this data is a fundamental portion of the software that derives with the arrangement (Brady and Boardman, 1995; Cullity, 1978; Hovis, 1997; Klug and Alexander, 1974; Moore and Reynolds, 1989).

**Determination of Unit Cell Dimensions:** For investigation of unit cell parameters, every reflection must be indexed to a definite *hkl* (Brady and Boardman, 1995; Cullity, 1978; Hovis, 1997; Klug and Alexander, 1974; Moore and Reynolds, 1989).



### 3.3.6 Scanning Electron Microscopy (SEM) Analysis

Scanning Electron Microscopy (SEM) exemplifies a best recital technique used to examine the morphological structure of any materials (Beane, 2004; Clarke and Eberhardt, 2002; Egerton, 2005; Reimer, 2013). It is outlined by: acceptance to make samples to be investigated, huge variety of data grasped, good resolution connected with best field depth, great and nonstop range of magnifying, etc. Several researchers (Beane, 2004; Egerton, 2005; Reimer, 2013) stated that the investigation of microstructures with SEM offers two advantages as equaled to optical microscopy (OM): much more resolution and magnification, as well as very giant field depth giving the impression that images achieved are distinctive. The scanning electron microscopy (SEM) of type EVO 18 Research machines used in this research. The following specifications were given by ZEISS EVO SEM 18 Research Manual. ZEISS is an internationally leading technology enterprise operating in the fields of optics and optoelectronics. The specifications of EVO 18 Research machines are described below as presented in Figure 3.15:

- ❖ EVO 18 SEM is the scanning electron microscope from Carl Zeiss, Germany.



Figure 3.15: The scanning electron microscope SEM of type EVO 18 Research (Photo taken by author).

- ❖ System Specification
  - Filament: Tungsten
  - Secondary e-image resolution: 50 nm (Depends on the types of sample)


- BSD Detector: Available
- Tilt: 0 - 60 Degree
- Rotation: 360 Degree
- EHT: 200V - 30KV
- Magnification: Up to 50K ~ 100K (Depends on sample).

❖ Process Capabilities

- Imaging Modes: Surface & Cross-Sectional
- Sample Holder: Maximum 9 stubs (~1 cm Dia.) can be mounted
- Substrates Used: Si, Glass, Sapphire, Ge
- Substrate Size:
  - (2 x 2 x Z) mm to (10 x 10 x Z) mm [For surface imaging]
  - (4 x 4 x Z) mm to (8 x 8 x Z) mm [For cross-sectional imaging]
  - Where Z is the variable substrate thickness (it can vary from 200 microns to 2 mm, depending on the substrate type like: Si / glass substrates).

### 3.3.6.1 Test Procedure of SEM Analysis

The EVO 18 Research SEM machine had a good quality of imaging. The SEM investigation was conducted at SEM Lab, Department of Glass and Ceramic Engineering, RUET, Rajshahi, Bangladesh. The complete SEM analysis procedure described below:

Step No.	Description	Image
01.	The cylindrical concrete specimens were casted with prescribed mix proportion. Then the specimens were cured 7 and 28 days.	

02. After completion of curing, the cylindrical concrete specimen has been broken by applying compressive load.



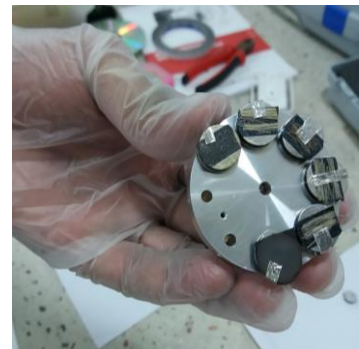
03. The coarse aggregate was separated from fine aggregated. Then the fine aggregate especially cement samples is being chop down to make it 10 mm x 10 mm x 2 mm size.



04. The specified samples placed in each sample holder by carbon tape and connect the sample with sample holder by electric or aluminum tape. The function of carbon tape was to hold the sample with sample holder. And the function of electric or aluminum tape was built an electric conductive connection between sample surface and sample holder.



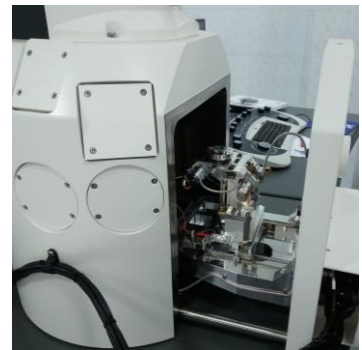
05. The pictorial view of group sample holder.



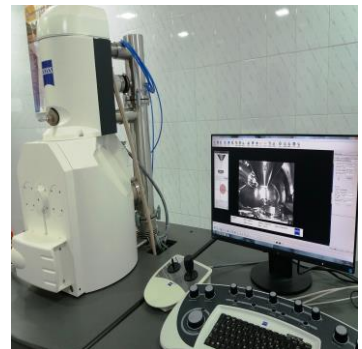
06. The group sample holder then placed in SPUTTER Coater to make the sample conductive. The machine used the gold conductive process.



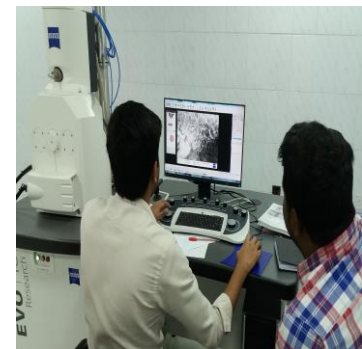
07. The group sample holder placed in SEM machine.



08. Then vacuum the sample holder.



09. Finally switch ON the electric gun and started scanning and imaging at different magnifying range.



## CHAPTER IV

### RESULTS AND DISCUSSION

#### 4.1 General

This chapter discusses the results gathered from compressive strength test, tensile strength of concrete specimens tests, stress-strain diagram, modulus of elasticity, Poisson's ratio and failure pattern of concrete. Also, the microscopic investigations are shown into this chapter. The microscopic investigation includes X-ray fluorescence (XRF) analysis, X-ray diffraction (XRD) analysis and Scanning electron microscopy (SEM) analysis. Finally, this chapter reveals the results and findings of the study including graphs, tables and microscopic image and their interpretations.

#### 4.2 X-ray Fluorescence (XRF) Analysis of Cement and Ceramic Waste Powder

An X-ray fluorescence (XRF) is an x-ray instrument based popular and comparatively non-destructive chemical analyses of different materials like rocks, minerals, sediments and fluids. It functions on wavelength-dispersive spectroscopic philosophies that are very equivalent to an electron microprobe (EPMA). Nevertheless, an XRF cannot commonly make examines at the tiny spot sizes typical of EPMA work (2-5 microns). So it is usually used for bulk examines of bigger fractions of geological constituents. This method of chemical analysis is comparatively eased and cost effective. It has very simple and low cost sample preparation. This is one of the most broadly used means for analysis of major and trace elements in rocks, minerals, and sediment due to the steadiness and comfort of use of X-ray (Wirth and Barth, 2016).

X-Ray fluorescence (XRF) spectrometry analysis is one of the easiest instrumental techniques for analysis in a cement or cement like waste material works because the sample preparation is simple. To find out the chemical composition of cement, red ceramic waste powder and white ceramic waste powder XRF analysis were performed in the laboratory of Seven Rings Cement Company, Khulna, Bangladesh. The chemical composition results of cement and ceramic powder are shown in Table 4.1 and Table 4.2 respectively.

Table 4.1: Chemical composition of cement through XRF analysis.

Chemical Components	Common Name	Chemical Notation	Abbreviated Notation	Cement (%)	
				Author	Marjanovic et al. (2000)
Silicon Dioxide	Silica	SiO <sub>2</sub>	S	23.52	23.07±0.05
Aluminium Oxide	Alumina	Al <sub>2</sub> O <sub>3</sub>	A	4.53	3.28±0.05
Ferric Oxide	Iron	Fe <sub>2</sub> O <sub>3</sub>	F	3.01	1.80±0.01
Calcium Oxide	Lime	CaO	C	61.24	66.04±0.05
Magnesium Oxide	Magnesia	MgO	M	2.87	0.67±0.05
Sulphur Trioxide	Sulphuric Hyrite	SO <sub>3</sub>	St	3.12	2.38±0.05
Alakaline Oxides	Alkalis	Na <sub>2</sub> O	N	0.14	0.15±0.01
		K <sub>2</sub> O	K	1.26	0.25±0.01
Titanium Dioxide	Titania	TiO <sub>2</sub>	T	0.24	0.21±0.01
Manganese Oxide	Manganese (II) Oxide	MnO	Mn	0.09	0.06±0.01

Table 4.2: Chemical composition of ceramic waste powder through XRF analysis.

Chemical Notation	White Ceramic (%)		Red Ceramic (%)		Fly Ash (%)	Slags (%)
	Author	Pacheco-Torgal and Jalali (2010)	Author	Pacheco-Torgal and Jalali (2010)	Swanepoel and Strydom (2002)	Broug and Atkinson (2002)
SiO <sub>2</sub>	41.24	59.8	44.33	51.70	46.28	35.44
Al <sub>2</sub> O <sub>3</sub>	25.77	18.60	18.80	18.20	21.27	13.04
Fe <sub>2</sub> O <sub>3</sub>	1.90	1.70	5.39	6.10	4.29	0.60
CaO	22.65	9.89	23.60	13.81	15.82	40.19
MgO	0.41	3.50	1.86	2.40	2.62	7.94
SO <sub>3</sub>	2.10	1.95	2.44	2.11	1.85	1.25
Na <sub>2</sub> O	1.81	1.60	0.64	0.20	0.72	0.22
K <sub>2</sub> O	3.39	2.50	1.95	4.60	0.95	0.36
TiO <sub>2</sub>	0.748	0.40	0.92	0.80	1.20	0.55
MnO	0.05	0.06	0.07	0.08	0.07	0.35

Table 4.1 depicts the XRF analysis results of cement. Chemical composition of cement found in this study has also been supported by other researchers like as Marjanovic et al. (2000). The XRF analysis result of cement was found quite equivalent to the researcher performed by Marjanovic et al. (2000) as shown in Table 4.1. Table 4.2 presented the XRF analysis results of waste white ceramic powder, waste red ceramic powder and compared them with other pozzolanic materials like as fly ash and slags. The chemical composition of red and white ceramic powder found in the study is followed the linear characteristics investigated by researcher (Pacheco-Torgal and Jalali, 2010). Comparing the chemical composition of waste ceramic powder (white and red) with fly ash and slags, it can be concluded the ceramic powder is a pozzolanic material. The ceramic powder possesses cementitious properties in the presence of water like fly ash and slags. It should be informed that with the presence of chemical composition shown in Table 4.2 researchers Pacheco-Torgal and Jalali (2010) conducted durability performance of ceramic waste concrete and found satisfactory results. Figure 4.1 illustrated that the SiO<sub>2</sub> and Al<sub>2</sub>O<sub>3</sub> present in ceramic powder (both red and white) is almost twice of cement. Red ceramic powder showed higher value of SiO<sub>2</sub> and Fe<sub>2</sub>O<sub>3</sub> compared to cement and white ceramic

powder. Also white ceramic powder figured higher value of  $\text{Al}_2\text{O}_3$  that of cement and red ceramic powder. Analyzed cement showed higher  $\text{CaO}$  than ceramic powder (both red and white). The cement and ceramic powder contained  $\text{MgO}$ ,  $\text{SO}_3$ ,  $\text{Na}_2\text{O}$  and  $\text{K}_2\text{O}$  within a range of 2.00% to 4.00%.  $\text{TiO}_2$  and  $\text{MnO}$  were also present there. ASTM specification of the chemical composition of Portland cement is illustrated in Chapter II. Comparing the XRF analysis results of cement, ASTM specification of Portland cement, fly ash and slags with ceramic waste powders the red and white ceramic powder given satisfactory results.

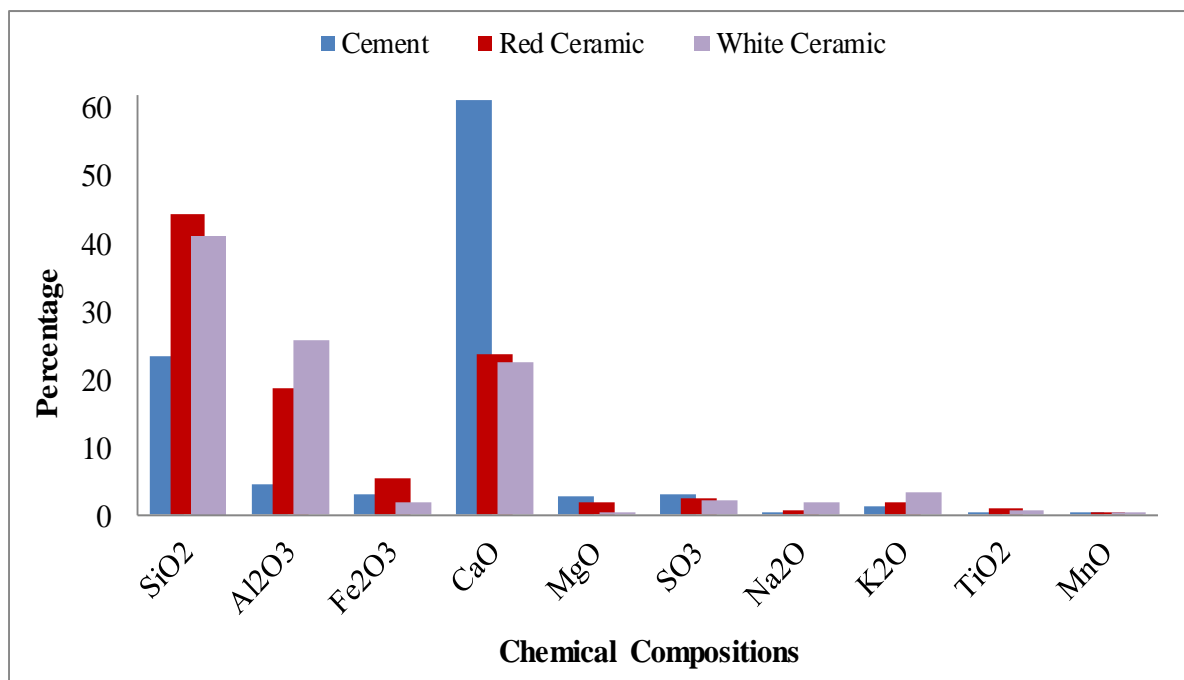


Figure 4.1: XRF analysis results of cement and ceramic waste powder.

### 4.3 Sieve Analysis

The sieve analysis is directed to demonstrate the grain size distribution of material proposed for use as fine and coarse aggregates. Gradation is determined by passing the material through a sets of sieves arranged with gradually smaller openings from top to bottom. Sieve analysis for fine aggregate (Sylhet sand) and coarse aggregate (crushed stone) was determined according to ASTM C136. The data which was got from the sieve analysis process are summarized in the Table 4.3 and Table 4.4 for fine and coarse aggregate respectively.



Table 4.3: Sieve analysis of fine aggregate.

Sieve Size	Sieve Opening (mm)	Weight Retained (gm)	Cumulative Weight Retained (gm)	Cumulative Weight Retained (%)	% Finer	F. M. Value
#4	4.750	0.00	0.00	0.00	100.00	2.55
#8	2.360	25.50	25.500	5.10	94.90	
#16	1.180	85.50	111.00	22.20	77.80	
#30	0.600	162.00	273.00	54.60	45.40	
#50	0.300	121.75	394.75	79.95	20.05	
#100	0.150	71.25	466.00	93.20	6.80	

Table 4.4: Sieve analysis of coarse aggregate.

Sieve Size	Sieve Opening (mm)	Weight Retained (gm)	Cumulative Weight Retained (gm)	Cumulative Weight Retained (%)	% Finer	F. M. Value
3.0"	75.00	0.00	0.00	0.00	100.00	7.06
1.5"	37.50	0.00	0.00	0.00	100.00	
1.0"	25.40	415.00	415.00	8.30	91.70	
3/4"	19.00	572.50	987.50	19.75	80.25	
1/2"	12.50	1232.50	2220.00	44.40	55.60	
3/8"	9.50	990.00	3210.00	64.20	35.80	
#4	4.75	777.50	3987.50	79.75	20.25	
#8	2.38	560.00	4547.50	90.95	9.05	
#16	1.19	377.50	4925.00	98.50	1.50	
#30	0.59	75.00	5000.00	100.00	0.00	
#50	0.30	0.00	5000.00	100.00	0.00	
#100	0.15	0.00	5000.00	100.00	0.00	

Using the data of the sieve analysis, the curve which is got after plotting the sieve size and percent finer in the graph is called a grain size distribution graph. It is also called a gradation curve. It helps to realize about the homogeneity or heterogeneity of particle sizes among an aggregate sample (Bunte and Abt, 2001). Figure 4.3 and Figure 4.4 respectively

shows the graphical analysis of the Sylhet sand and crushed stone which were used as fine aggregate and coarse aggregate in mix designs. Sieve analysis contains of determining the proportional amounts of particles taken on or passing through respectively of a series of sieves stacked in decreasing the sieve opening sizes. Using the percentages of weights retained in each sieve a graph is plotted known as grain size distribution curve. This curve is drawn by plotting the opening size on the X axis in logarithm scale. At the same time, the percentage of particles, by weight, finer than the particular sieve was plotted on the Y axis in regular scale. A uniform shape, like a stairway, shows uniform gradation. When a bulky part of aggregate is prepared the particles of one size, it is redirected in the graph as an adjacent vertical drop.

From gradation curve  $D_{10}$ ,  $D_{30}$  and  $D_{60}$  are found; which are the diameter for 10%, 30% and 60% finer respectively. The diameter in the grain size distribution curve parallel to 10% finer is known as the effective size, or  $D_{10}$ . The uniformity coefficient ( $C_u$ ) and coefficient of curvature or coefficient of gradation ( $C_c$ ) are obtained from equation (4.1) and (4.2) respectively.

Uniformity coefficient,  $C_u = D_{60} / D_{10}$  ..... (4.1).

The coefficient of gradation may be expressed as:

Coefficient of gradation,  $C_c = D_{30}^2 / (D_{60} * D_{10})$  ..... (4.2).

Based on the investigation it is found that the uniformity coefficient ( $C_u$ ) for fine and coarse aggregate as 4.00 and 8.86 respectively. Also, the coefficient of gradation  $C_c$  was found for fine and coarse aggregate as 1.00 and 2.33 respectively. As the value of  $C_u$  is greater than 4 and  $C_c$  in the range of 1 to 3, both the fine and coarse aggregate are said to be a well graded.

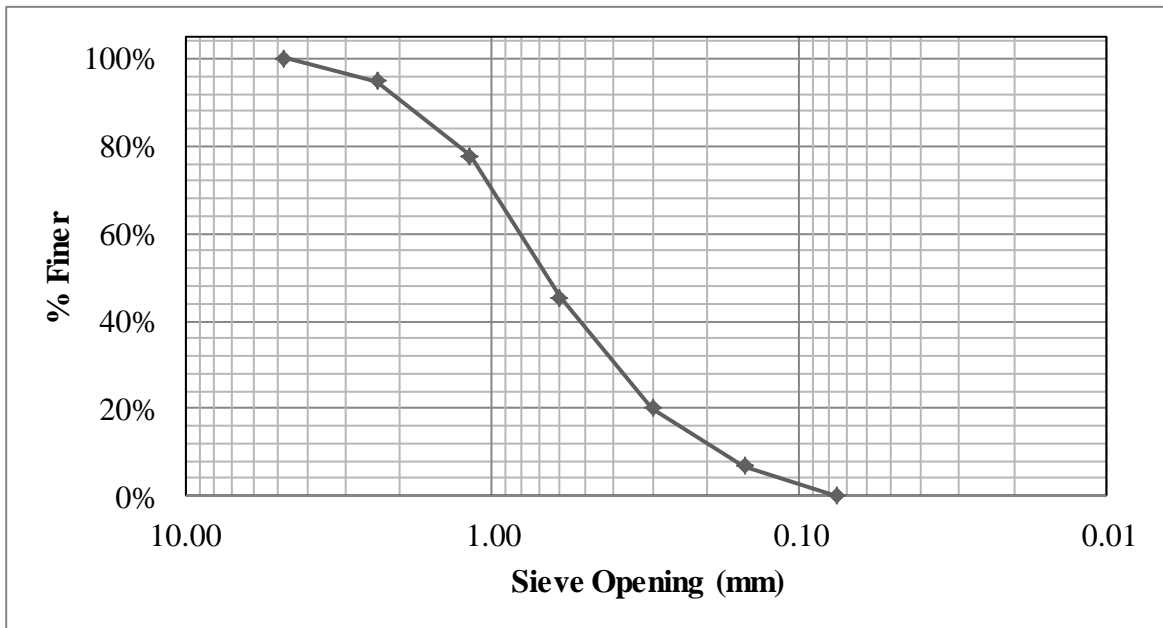


Figure 4.2: Gradation curve of fine aggregate.

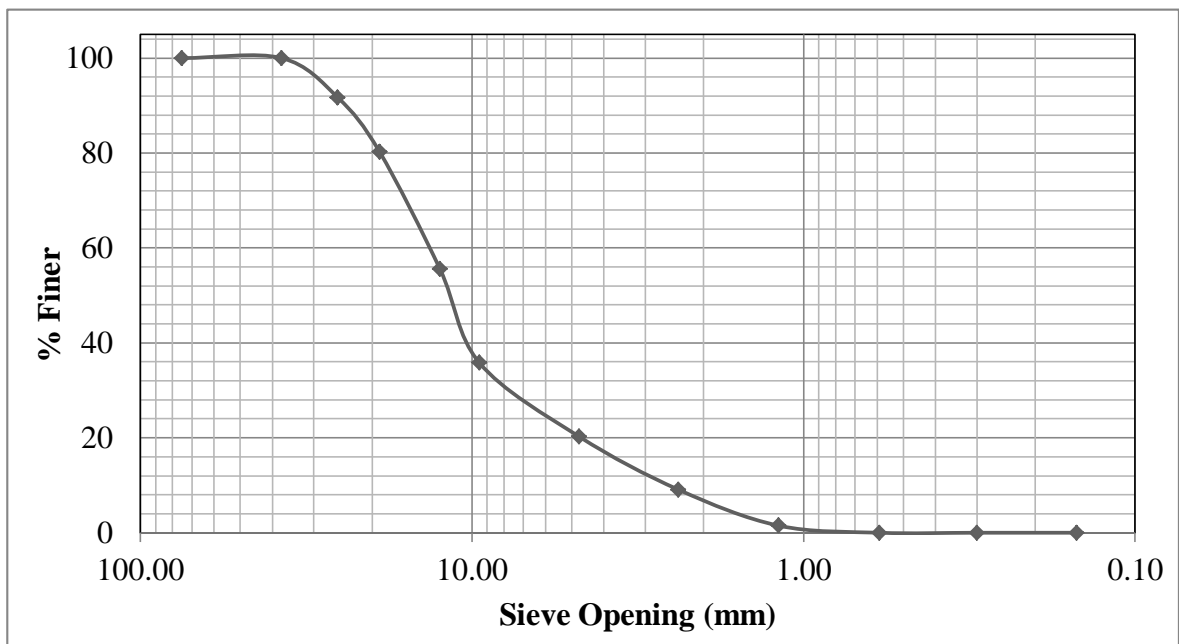


Figure 4.3: Gradation curve of coarse aggregate.

#### 4.4 Test Results for Material Properties

Material properties such as Sylhet sand and crushed stone chips used in this research were determined according to ASTM standard procedures and they are summarized below in Table 4.5.

Table 4.5: Material properties for mix design.

Materials	Properties	Unit	Value
Fine Aggregate	Specific Gravity	-	2.65
	Water Absorption	%	2.12
	Fineness Modulus	-	2.55
	Unit Weight	Kg/m <sup>3</sup>	1452
Coarse Aggregate	Specific Gravity	-	2.84
	Absorption	%	1.1
	Fineness Modulus	-	7.06
	Unit Weight	Kg/m <sup>3</sup>	1570

#### 4.5 Workability of Concrete

Workability of concrete is a comprehensive and subjective term relating however simply freshly mixed concrete are often mixed, placed, consolidated and finished with smallest loss of homogeneity. Concrete workability is a vital property that directly affects concrete strength, durability, surface morphology, setting time and also the cost of labor for casting and finishing operations (Domone and Illston, 2002). Generally, concrete slump test is performed to find out the workability of concrete (Gilson's, 2016). The consistency of fresh concrete is determined by the slump test. It is the way of indirect checking of the specific quantity of water has been added to the mix to obtain best workable concrete. The slump value measurement has been shown in Figure 4.4.



Figure 4.4: Slump value measurement.

The major factors affected the workability of concrete are water/cement (w/c) ratio, aggregate size and admixture. The concrete workability was determined by slump test. It has been observed that the failure pattern of concrete is “true slump”. True slump indicated that the concrete subsides and maintaining its general form. Slump values were kept constant in this study. Based on the investigation it was found that the slump value for all batches of concrete was  $110 \pm 5$  mm. Different experimental results explained that the slump value 100 mm to 175 mm showed high workability of concrete (Ferraris, 1999). So, the concrete in this study was of high workability. This concrete will be applicable for sections with congested reinforcement and it may not react well to vibration.

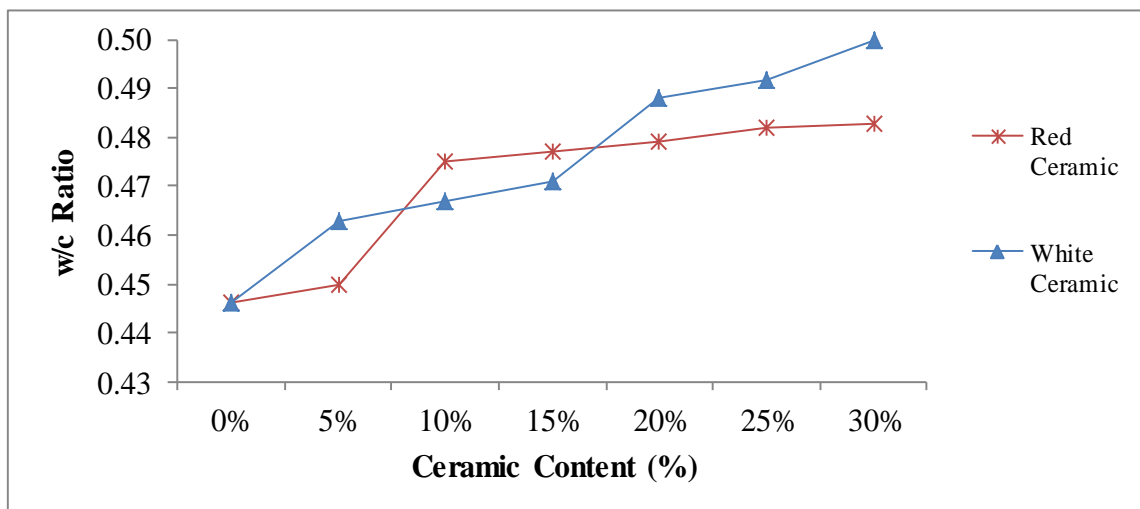


Figure 4.5: Variation of w/c ratio with ceramic content due to constant slump value.

The variations of w/c ratio with ceramic content due to constant slump values have been shown in Figure 4.5. A higher amount of cement or cementitious materials sometimes mean better strength, and with the right quantity of water, additional paste is covering the surface of aggregates at ease consolidation and a much better finishing operation. Proper placement and finishing operation suggests better strength development and a compliant mix. Adding unnecessary water can be said to extend workability as a results it comfortable to place and consolidate. The adverse effects on segregation, finishing processes and final strength could be therefore prejudicial that it ought to be move toward very carefully. The typical water to cement ratio (w/c) of 0.45 to 0.6 is the best spot for making of best workable concrete (Gilson’s, 2016). The concrete was casted w/c ratio within 0.443 to 0.500, which is the sign of good workable concrete. The w/c ratios increased with the increasing of ceramic content i.e. the higher the ceramic content

indicated higher of w/c ratio. It meant that the increasing ceramic content required more water than cement content only due to its chemical compositions. Figure 4.5, also stated that the white ceramic powder required more water than red ceramic powder to obtain sweet workable concrete.

#### **4.6 Strength Tests of Concrete**

All materials have precise intrinsic material properties. For every material, the properties are taken as exceptional when they are autonomous of a specimen size and shape. For design cases, the concrete compressive strength of standard concrete specimen is considered as the most fundamental and vital material property (Yi et al., 2006). Compressive strength of concrete is the main and essential mechanical property, which is usually attained by determining concrete specimen after a standard curing of 28 days (Ni and Wang, 2000). The cylinder and cube strengths achieved from the same batch of concrete might vary because of the variances in the shape, height to diameter ratio, and end restraint happened by the machine platen. Explicitly, it is well-known that cubes have higher strength than cylinders. Since the early 1900s, many studies (Gonnerman, 1925; Gyengo, 1938; Murdock, 1957) on this field have been carried out.

##### **4.6.1 Compressive Strength of Cylindrical Concrete Specimens**

Compressive strength is that the capability of a material or structure to resist loads tending to reduce size, as contrasting to tensile strength, which withstands loads tending to lengthen the specimen. Compressive strength of concrete could be a most important property for design of structures. The most common technique by crushing specimens inside the compressive testing machine determines the compressive strength as the compressive strength test result. Consequently, it is a worldwide standardized direct test method. Along with the modulus of elasticity, the compressive strength is the most significant property of concrete.

According to ASTM C39 the test method covers determination of compressive strength of cylindrical concrete specimens (100 mm diameter and 200 mm height) such as molded cylinders and drilled cores. Three samples were prepared and tested for each batch of concrete mixes. The tests were conducted for 7, 28 and 90 days of cylindrical (100 mm

diameter and 200 mm height) concrete specimens. About 117 cylindrical concrete specimens were prepared and tested to complete the compressive strength test.

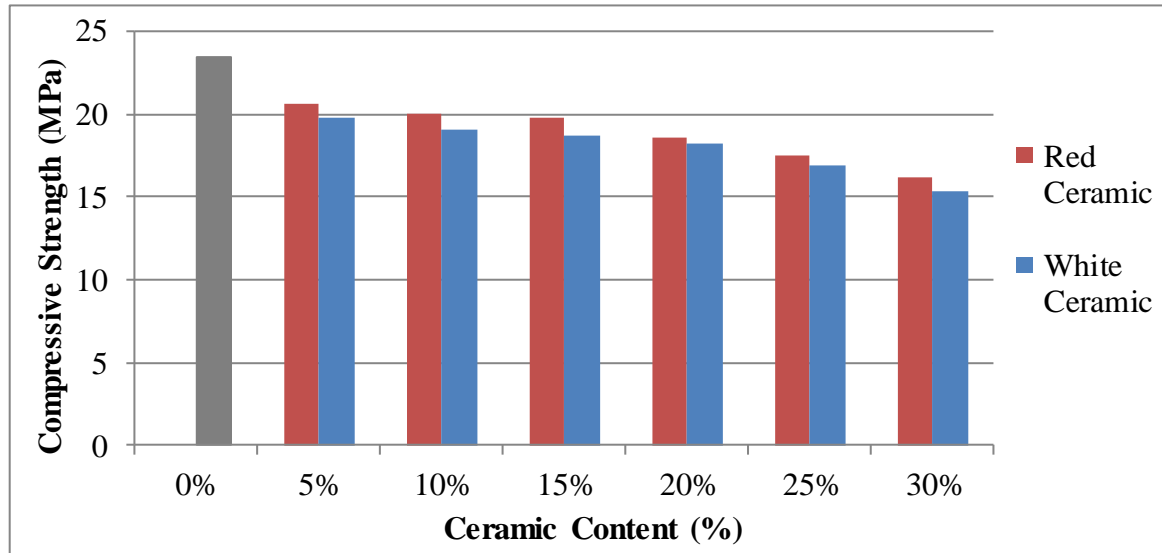


Figure 4.6: Compressive strength of concrete specimens at 7 days.

The compressive strength of cylindrical concrete specimens at 7 days is shown in Figure 4.6. The control (cement) specimen compressive strength was found 23.45 MPa. The minimum and maximum compressive strength of red ceramic concrete was found 16.14 MPa and 20.67 MPa of 30% and 5% concrete mixes respectively. On the other side, the white ceramic concrete illustrated minimum and maximum compressive strength 15.37 MPa and 19.85 MPa of 30% and 5% concrete mixes respectively. The CW powder figured always lower strength than control specimen, but the variations were too little. There was little strength variations up to 15% mix proportions of white ceramic concrete and up to 20% mix proportions of red ceramic concrete compared to the control specimen. Most of the cases the rates of decrement of strength of red ceramic concrete relatively to control specimens were small compared to white ceramic concrete.

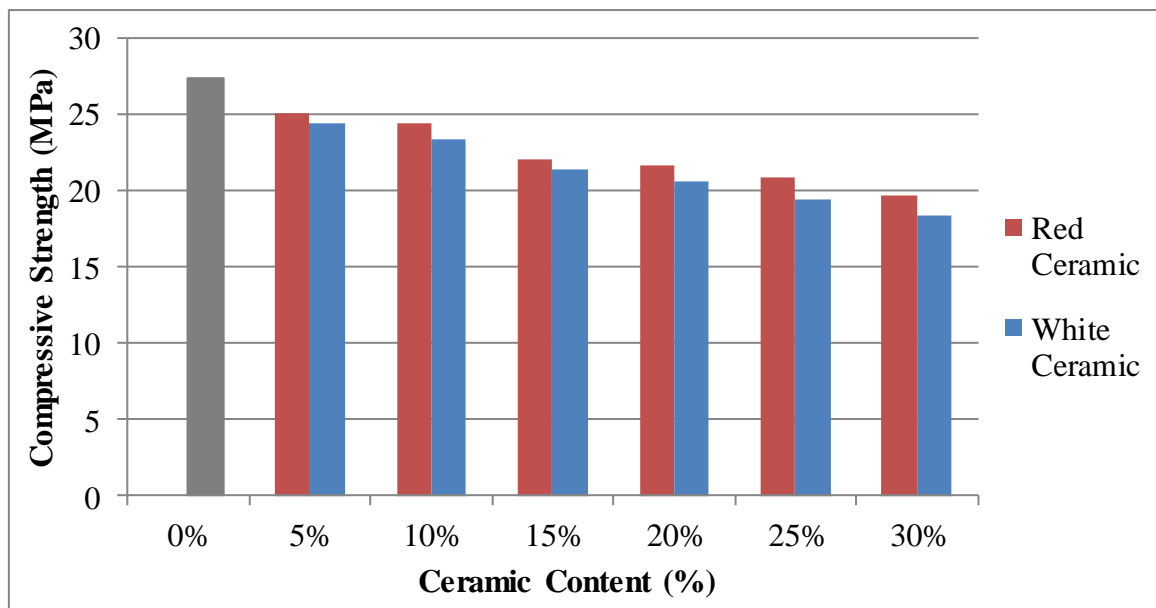


Figure 4.7: Compressive strength of concrete specimens at 28 days.

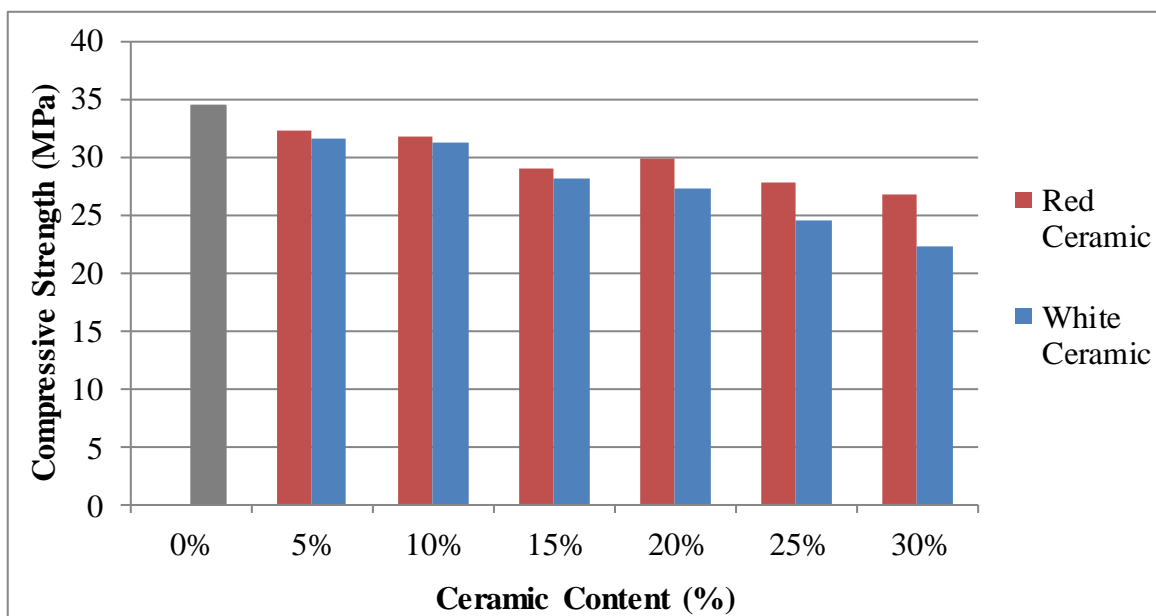


Figure 4.8: Compressive strength of concrete specimens at 90 days.

Figure 4.7 and Figure 4.8 illustrated the compressive strength of cylindrical concrete specimen at 28 days and 90 days respectively. Concrete has lots of beneficial properties like strength, durability, flexibility and effective economy. Consequently, effective and sustainable designing a concrete structure, the compressive strength of concrete is a vital component. The 28 days concrete compressive strength is generally taken as the design



strength of concrete (Kabir et al., 2012). The compressive strength of cylindrical concrete specimens increased with the increase of curing age. The control specimens showed greater strength than white and red ceramic waste powder (CWP) concrete for both 28 and 90 days. The rate of decrease of compressive strength 28 and 90 days white CWP concrete were very small up to 15% replacement. On the other hand, the red CW concretes showed greater compressive strength than white CWP concrete for maximum cases of partial ceramic waste powder replacement for both 28 and 90 days concrete. But the control (cement) specimen showed little bit greater strength than red CWP concrete. The rates of decrease of strength up to 20% partial replacement of red CWP were too small compared to white CWP concrete.

Table 4.6: Variations of compressive strength of concrete specimens at 7, 28 and 90 days.

Batch Name	7 Days		28 Days		90 Days	
	Strength (MPa)	% Variation	Strength (MPa)	% Variation	Strength (MPa)	% Variation
0%	23.45	--	27.36	--	34.48	--
W-5%	19.85	15.35	24.42	10.75	31.54	8.53
W-10%	19.10	18.55	23.37	14.58	31.22	9.45
W-15%	18.77	19.96	21.43	21.67	28.10	18.50
W-20%	18.25	22.17	20.59	24.74	27.24	21.00
W-25%	16.93	27.80	19.41	29.06	24.52	28.89
W-30%	15.37	34.46	18.42	32.68	22.21	35.59
R-5%	20.67	11.86	25.06	8.41	32.20	6.61
R-10%	20.01	14.67	24.39	10.86	31.76	7.89
R-15%	19.83	15.44	22.13	19.12	28.93	16.10
R-20%	18.56	20.85	21.74	20.54	29.79	13.60
R-25%	17.45	25.59	20.91	23.57	27.78	19.43
R-30%	16.14	31.17	19.71	27.96	26.75	22.42

The variations of compressive strength of concrete specimens at 7, 28 and 90 days are shown in Table 4.6. Summarizing the Table 4.6 and Figure 4.6 to 4.8 it can be illustrated that the control specimen showed greater compressive strength than others for all curing

ages. In most of the mix proportions the red CW concrete showed greater compressive strength than white CW concrete at 7, 28 and 90 days. The compressive strength of control specimens was 23.45 MPa, 27.36 MPa and 34.48 MPa at 7, 28 and 90 days. The rate of decrease of cylindrical compressive strength of white and red CW concrete was not significant up to 15% and up to 20% partial replacement respectively. Analyzing the trend of red CW concrete, the compressive strength increased at 20% partial replacement. The analyzing trends has been supported by the study of ceramic aggregate (Pacheco-Torgal and Jalali, 2010; Medina et al., 2012). This is due to chemical composition of red CW concrete i.e. comparative higher percentage  $\text{SiO}_2$  and  $\text{CaO}$ . The strength variations relative to control specimens for 20% red ceramic concrete mixes was found as 20.85%, 20.54% and 13.60% at 7, 28 and 90 days respectively. From 25% to 30% red ceramic concrete mixes the strength varies 20~32%. Other side, the strength variations relative to control specimens for 15% white ceramic concrete mixes was figured out as 19.96%, 21.67% and 18.50% at 7, 28 and 90 days respectively. From 20% to 30% white ceramic concrete mixes the strength varies 20~30%. From compressive strength test results of concrete, it can be concluded that there was minor strength variations up to 20% red ceramic partial replacement and up to 15% white ceramic partial replacement. So, the partial replacement for 20% of red ceramic and for 15% of white ceramic can be concluded as the most favourable mix proportions in terms of strength.

#### **4.6.2 Splitting Tensile Strength of Concrete**

Concretes are strong in compression but weak in tension. Hence, the value of tensile strength of concrete is typically lower than compressive strength. The splitting tensile strength test outcomes for the concretes comprising CWP of varying proportion affording to their ages are very similar to each other, like compressive strength test results. Splitting tensile strength of concrete is generally found by destructive testing of concrete cylinders.

According to ASTM C496, the test method covers determination of splitting tensile strength of cylindrical concrete specimens (100 mm diameter and 200 mm height) such as molded cylinders and drilled cores. Three samples were prepared and tested for each batch of concrete mixes. The tests were conducted for 7 and 28 days of cylindrical (100 mm diameter and 200 mm height) concrete specimens. About 78 cylindrical concrete specimens were prepared and tested to complete splitting tensile strength test. All the

specimens of all proportions were tested for splitting tensile strength using an automated compression testing machine. The data were recorded for all the samples.

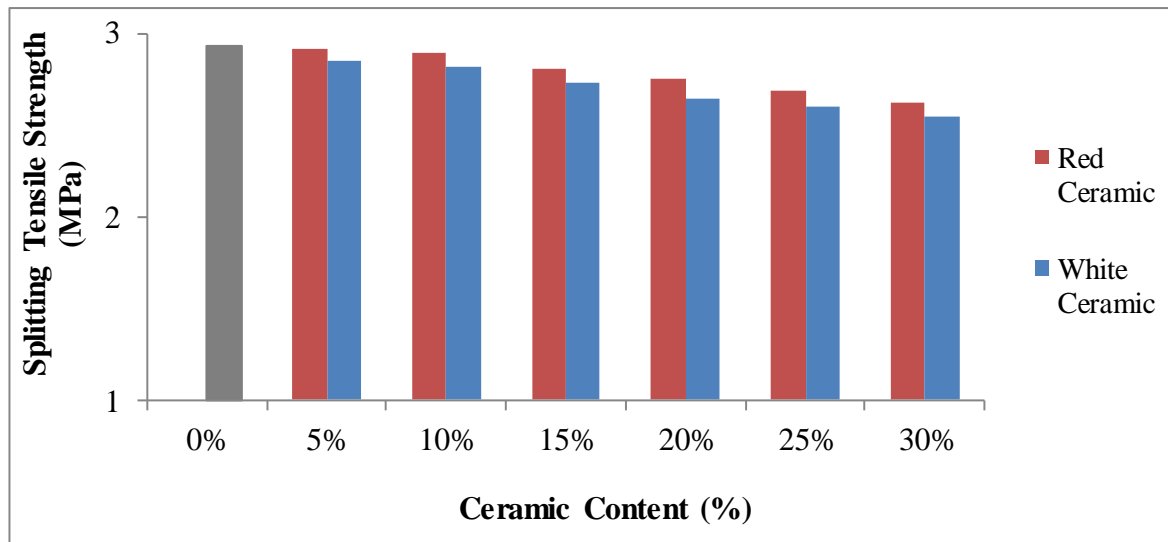


Figure 4.9: Splitting tensile strength of cylindrical concrete specimens at 7 days.

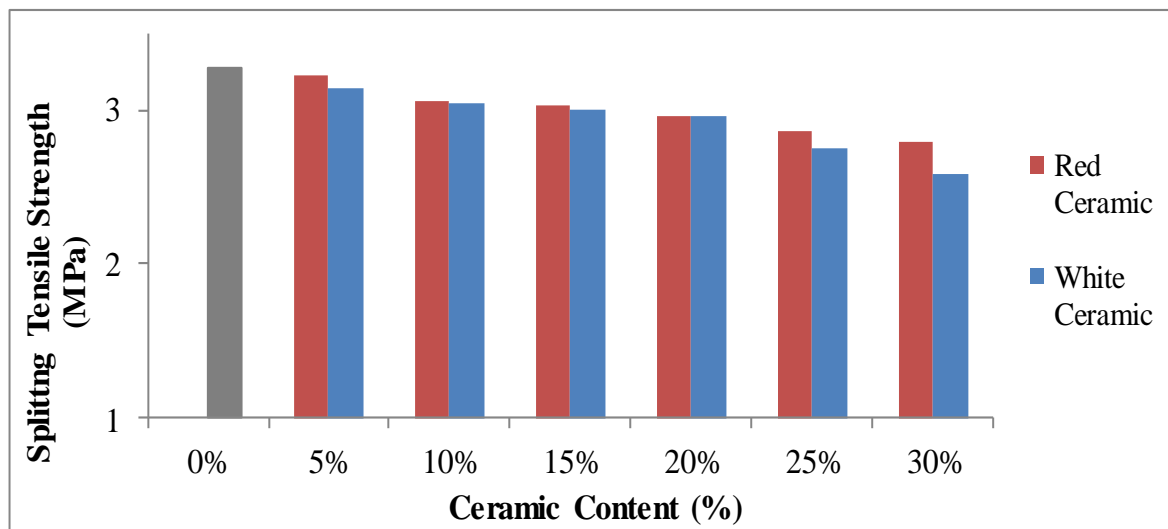


Figure 4.10: Splitting tensile strength of cylindrical concrete specimens at 28 days.

Figure 4.9 and Figure 4.10 illustrated the splitting tensile strength test results of cylindrical concrete specimens at 7 and 28 days respectively. The splitting tensile strength of control (cement) specimen showed always greater value than CWP concrete both at 7 and 28 days. The red CWP concrete gave greater tensile strength than white CWP concrete for all cases of partial replacement. The splitting tensile strength for control specimens were 2.94 MPa and 3.27 MPa at 7 and 28 days respectively. The red CWP concrete showed the strength

ranges from 2.92 MPa to 2.62 MPa and 3.23 MPa to 2.79 MPa at 7 and 28 days respectively; whereas the ranges of strength of white CWP concrete were 2.85 MPa to 2.54 MPa and 3.14 MPa to 2.59 MPa correspondingly.

Table 4.7: Variations of splitting tensile strength of concrete at 7 and 28 days.

Batch Name	7 Days		28 Days	
	Strength (MPa)	% Variation	Strength (MPa)	% Variation
0%	2.94	--	3.27	--
W-5%	2.85	3.06	3.15	3.67
W-10%	2.82	4.08	3.04	7.03
W-15%	2.73	7.14	2.94	10.09
W-20%	2.65	9.86	2.84	13.15
W-25%	2.60	11.56	2.74	16.21
W-30%	2.54	13.61	2.59	20.80
R-5%	2.92	0.68	3.23	1.22
R-10%	2.89	1.70	3.10	5.20
R-15%	2.80	4.76	3.03	7.34
R-20%	2.75	6.46	2.96	9.48
R-25%	2.68	8.84	2.86	12.54
R-30%	2.62	10.88	2.79	14.68

The variations of splitting tensile strength of concrete at 7 and 28 days are shown in Table 4.7. The rate of variations of tensile strength of red and white CW concrete with control specimen was too not significant for 20% and 15% partial replacement respectively. The splitting tensile strength variations relative to control specimens for 20% red ceramic concrete mixes was found as 6.46% and 9.48% at 7 and 28 days respectively. On the other hand, the splitting tensile strength variations relative to control specimens for 15% white ceramic concrete mixes was figured out as 7.14% and 10.09% at 7 and 28 days respectively. However, after the 20% and 15% partial replacement of red and white CWP concrete, tensile strength decreased with higher rate. Hence here as well, likewise compressive strength test, 20% of red CWP and 15% of white CWP can be considered the most favourable partial replacement of cement.

#### 4.7 Failure Types of Control and Ceramic Waste Powder Concrete

The most common failure pattern of cylindrical concrete specimens is cone. There are other types of concrete cylinders specimens fracture as shown in Figure 4.11 stated in ASTM C 39 (2015).

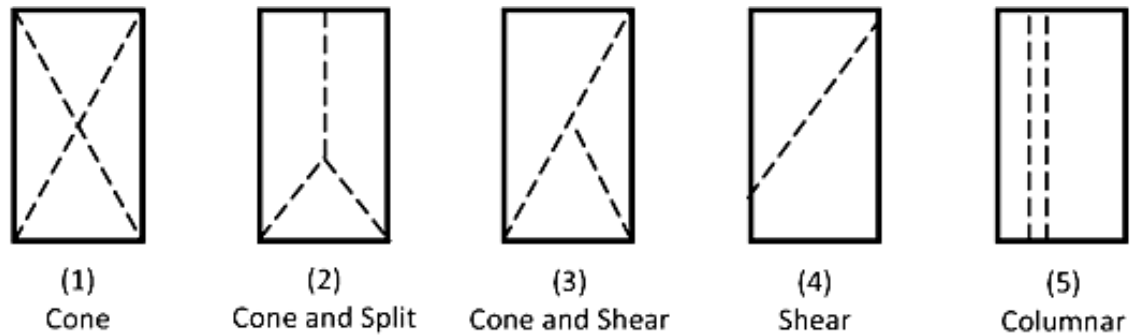


Figure 4.11: Sketches of types of cylinders fracture (ASTM C 39, 2015).

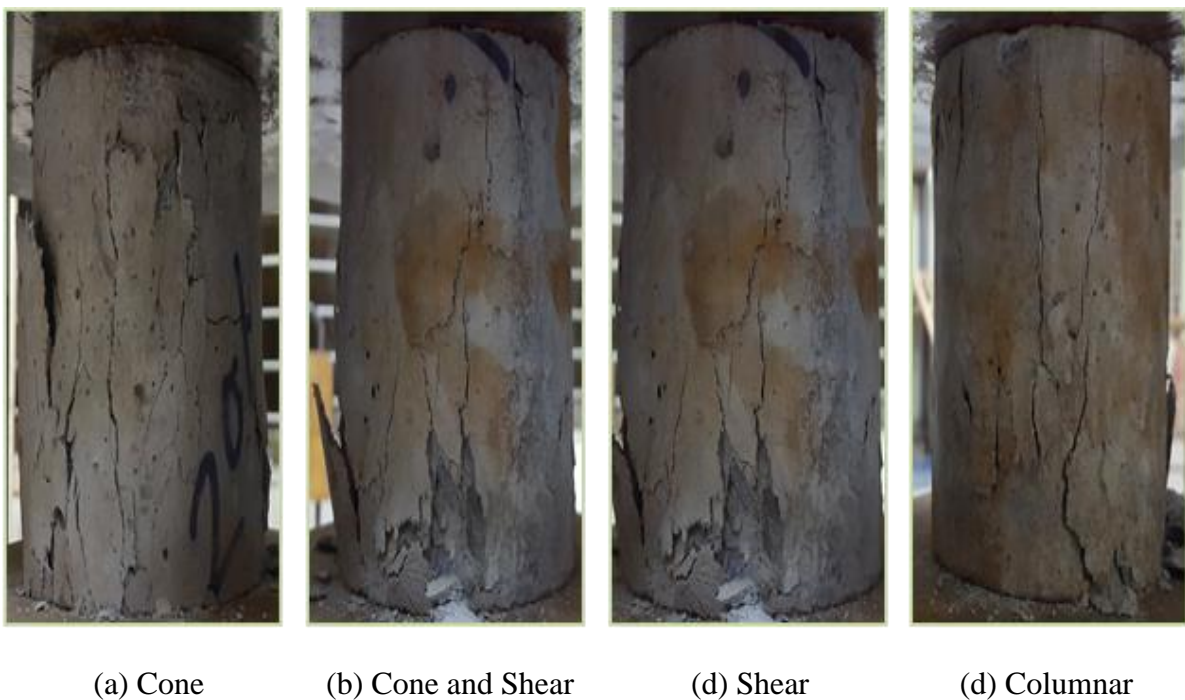


Figure 4.12: Different failure patterns of cylindrical concrete specimens.

Four failure types were observed in the experimental program. The failure types are shown in Figure 4.12. The most common type of failure was found as the conical type. Conical failures indicated the good quality concrete. Other types of failure were found rare in the study are cone and shear, cone and split, shear and columnar. These are the commonly

fracture types for normal concretes. Concretes may fail in the shear mode due to huge amount of sand. Generally columnar splitting failure sometimes denotes a testing problem in normal-strength concretes. The splitting failure occurred due to the existence of an oil or lubricant on the cylinder cap, which decreases friction between the specimen end sides and the testing machine platen (Hamad, 2017). This approach decreases the lateral confining pressure that's usually present, and thus decreases the apparent strength. Columnar splitting failure happened due to the convex capping rather than plane (Hamad, 2017).

#### 4.8 Stress-Strain Diagram of Concrete

A representative relationship between stress and strain for normal strength concrete aforementioned that once an initial linear portion lasting up to about 30 - 40% of the ultimate load, the curve becomes non-linear, with high strains being considered for slight increases of stress. Generally, it is recognized that the 28 days concrete is usually used as mix design as well as the modulus of elasticity. So the modulus of elasticity of concrete is always reliable to the curing ages.

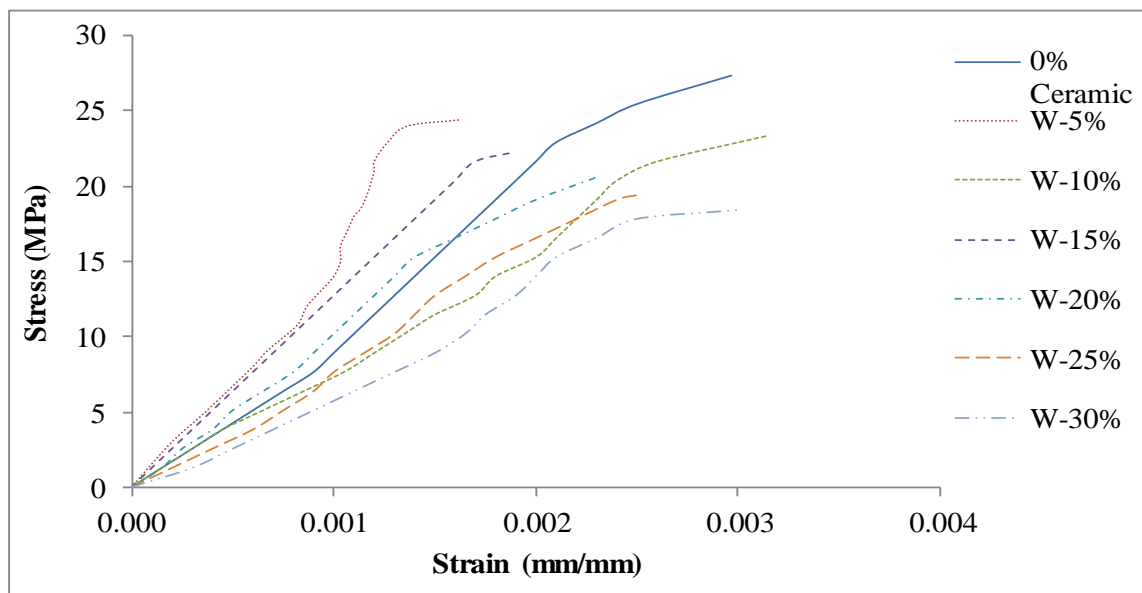


Figure 4.13: Stress-strain diagram of control and white CWP concrete at 28 days.

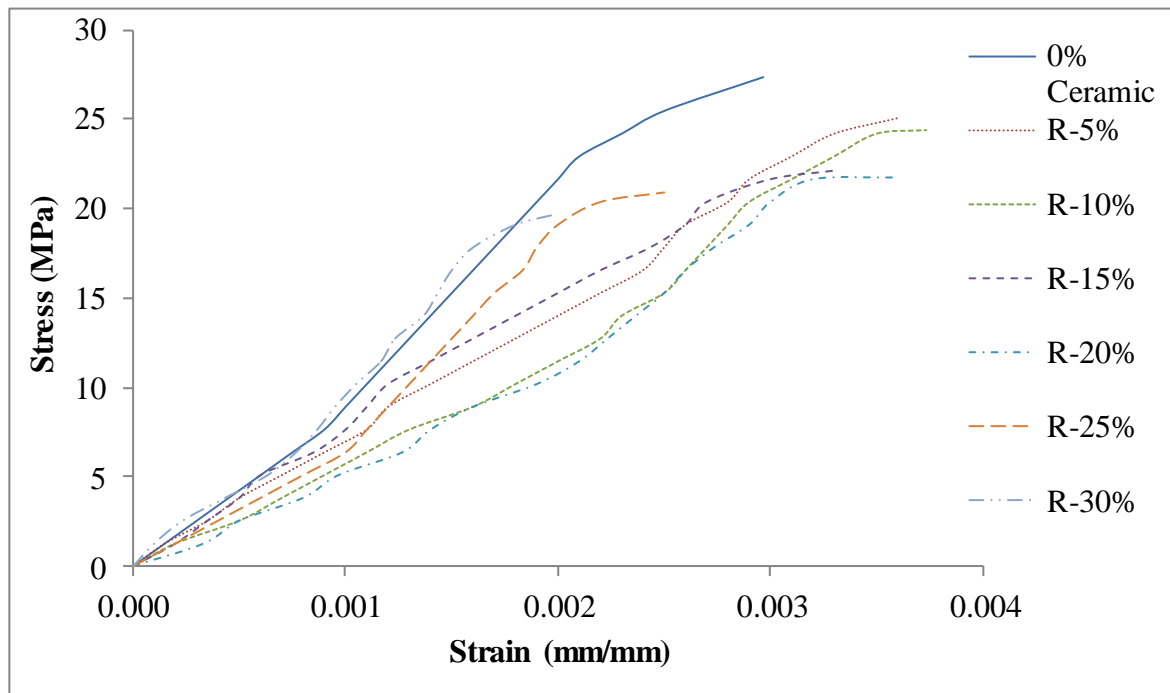


Figure 4.14: Stress-strain diagram of control and red CWP concrete at 28 days.

The stress versus strain diagram of control and CWP concrete (both red and white) at 28 days were described in Figure 4.13 and Figure 4.14. It is also shown for 7 and 90 days of control and ceramic waste powder (CWP) concrete from Figure 4.15 to Figure 4.18 respectively. The stress-strain curve for red and white CWP concrete was almost linear up to 20% and up to 15% partial replacement respectively. The initial partial white ceramic replacement concrete was more rigid than the cement paste and thus deformed less (i.e. have a lower strain) beneath the equivalent applied stress. But the initial partial red ceramic replacement to optimum marked concrete followed normal concrete stress-strain curve. The stress-strain curve of concrete lied between those of the initial and the final partial replacement of white CWP concrete. Nevertheless, this relationship is found as non-linear at the maximal cases. The explanation for this non-linear performance is due to micro-cracks are induced at the edge between aggregate particles and cement or CWP paste as a consequence of the discrepancy drive between the two segments, and in the cement or CWP paste itself. These cracks are induced because of the changes in temperature and moisture and the loading pattern.

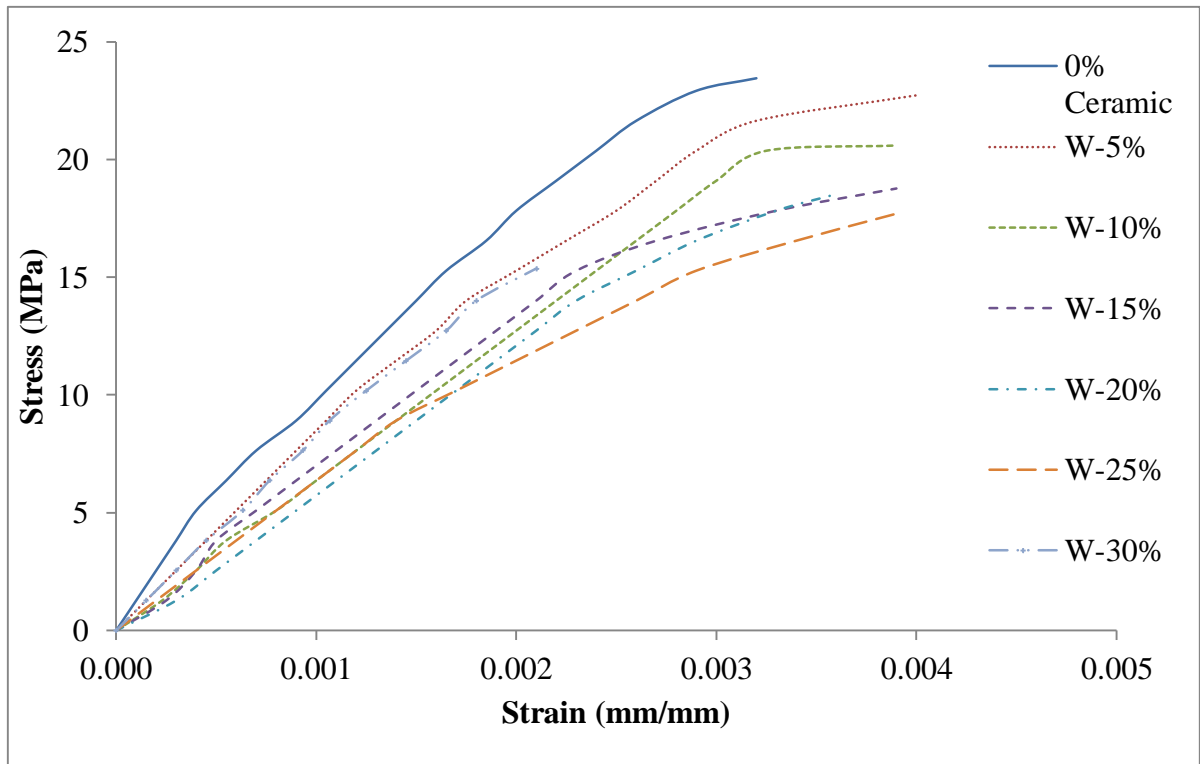


Figure 4.15: Stress-strain diagram of control and white CWP concrete at 7 days.

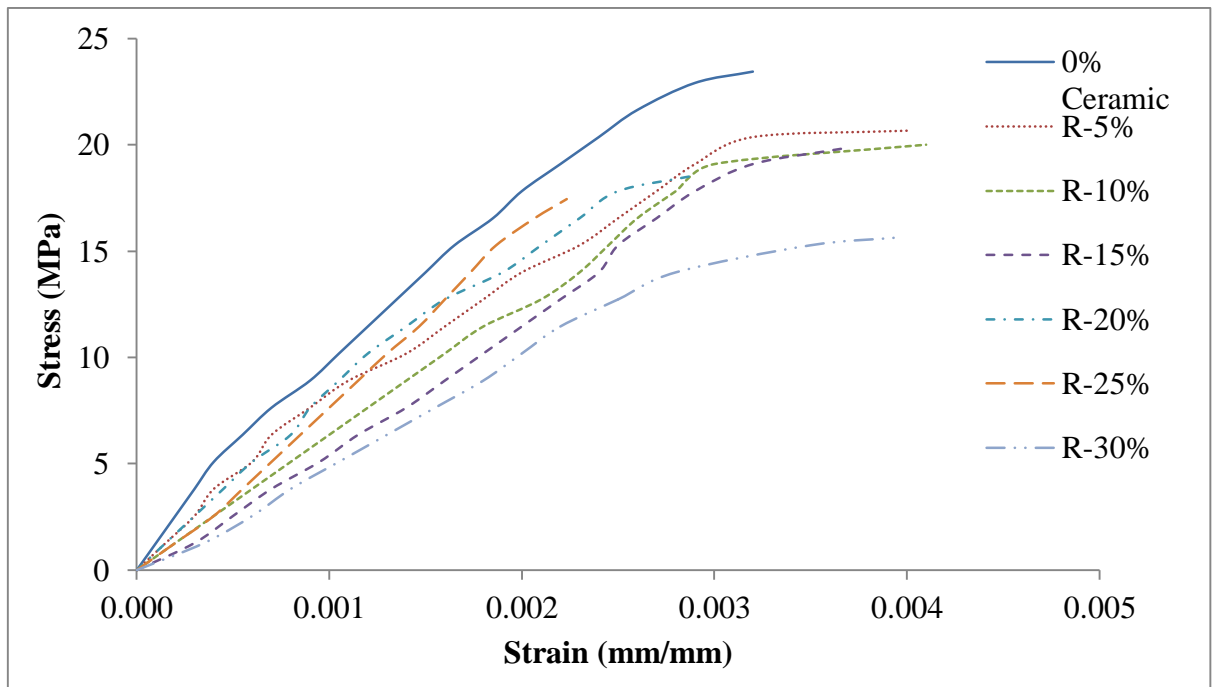


Figure 4.16: Stress-strain diagram of control and red CWP concrete at 7 days.



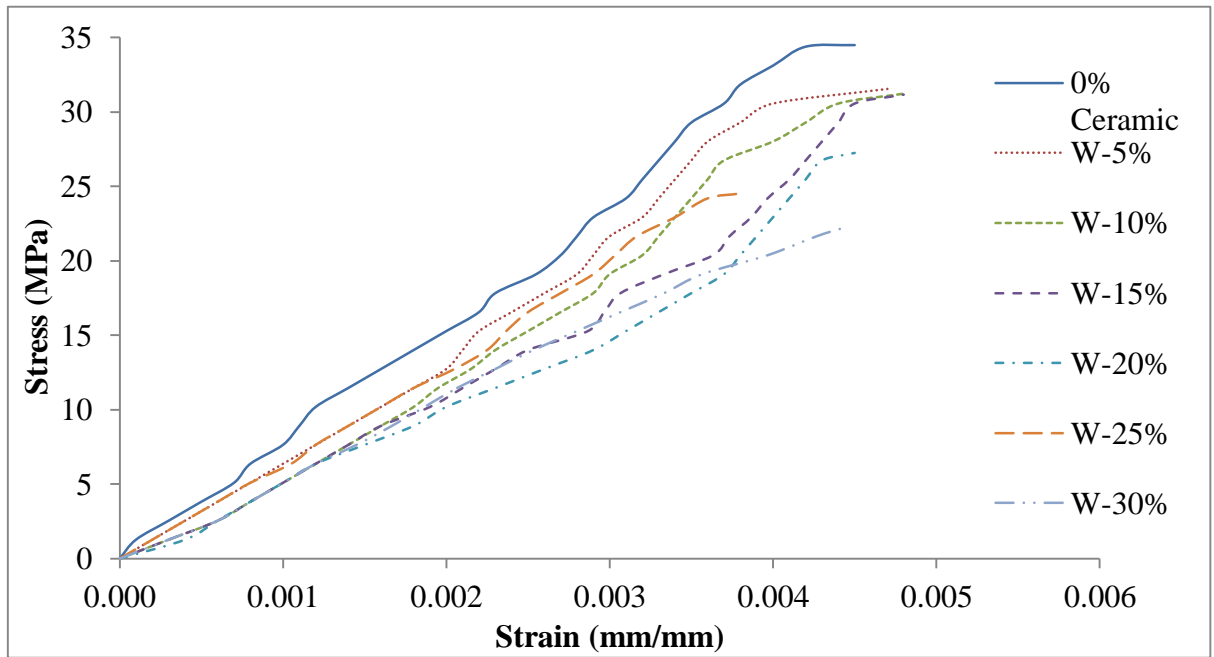


Figure 4.17: Stress-strain diagram of control and white CWP concrete at 90 days.

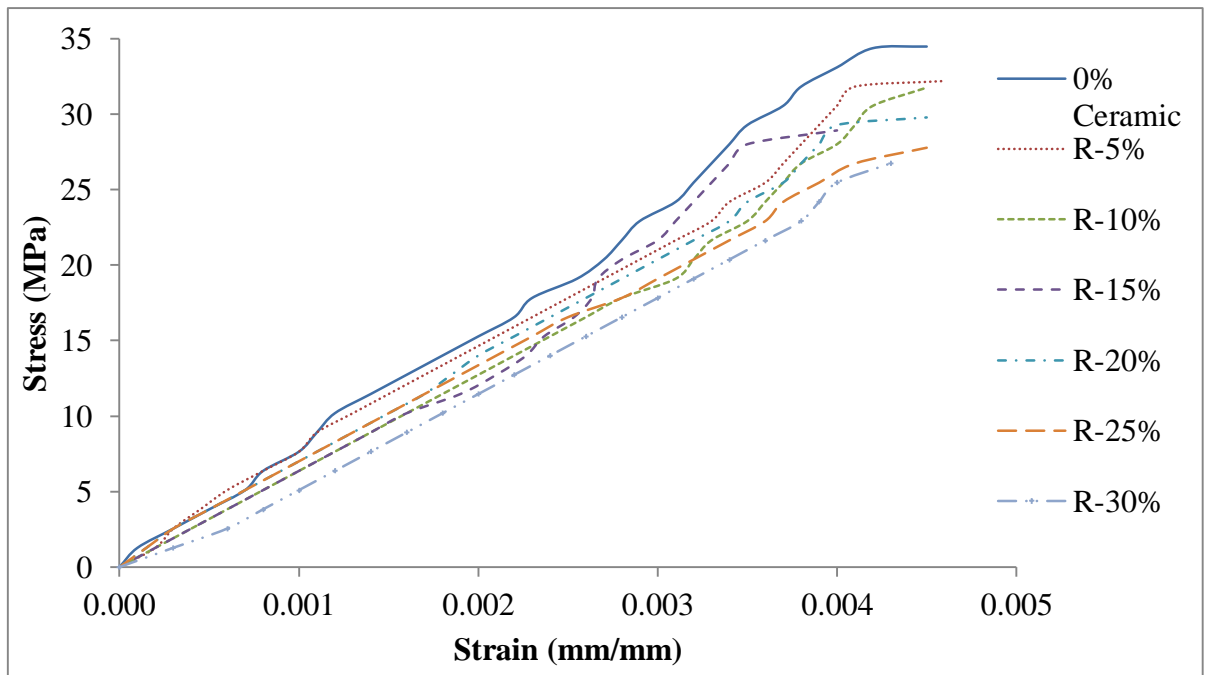


Figure 4.18: Stress-strain diagram of control and red CWP concrete at 90 days.

#### 4.9 Modulus of Elasticity of Concrete

The modulus of elasticity of concrete  $E_c$  adopted in modified form by the ACI Code can be calculated by the formula given below:

$$E_c = 33w_c^{1.5} \sqrt{f'_c} \text{ lb/in}^2 \text{ in USCS units} \dots\dots\dots (4.3)$$

$$E_c = 0.043w_c^{1.5} \sqrt{f'_c} \text{ MPa in SI units} \dots\dots\dots (4.4)$$

With normal-weight, normal density concrete these two relations can be simplified to:

$$E_c = 57000 \sqrt{f'_c} \text{ lb/in}^2 \text{ in USCS units} \dots\dots\dots (4.5)$$

$$E_c = 4700 \sqrt{f'_c} \text{ MPa in SI units} \dots\dots\dots (4.6)$$

where,  $f'_c$  = Specified 28 days compressive strength of concrete (lb/in<sup>2</sup> or MPa).

In this study the modulus of elasticity calculated by the equation (4.6) of  $E_c = 4700 \sqrt{f'_c}$  MPa in SI units.

According to ASTM C469 the modulus of elasticity has been calculated in this study, to the nearest 50000 psi (344.74 MPa) as follows:

$$E_c = \frac{(S_2 - S_1)}{(\varepsilon_2 - 0.00005)} \dots\dots\dots (4.7)$$

Where,

$E_c$  = Chord modulus of elasticity, psi,

$S_2$  = Stress corresponding to 40% of ultimate load,

$S_1$  = Stress corresponding to a longitudinal strain,  $\varepsilon_1$ , of 50 millionths, psi, and

$\varepsilon_2$  = Longitudinal strain produced by stress  $S_2$ .

Table 4.8: Comparison of modulus of elasticity of cement and CWP concrete.

Batch Name	7 Days	28 Days		90 Days
	ASTM (GPa)	ACI (GPa)	ASTM (GPa)	ASTM (GPa)
0%	22.23	24.58	26.58	28.99
W-5%	23.17	23.22	24.06	26.77
W-10%	22.26	22.72	23.20	25.08
W-15%	21.17	22.19	22.45	24.03
W-20%	19.81	21.33	20.46	23.18
W-25%	17.95	20.71	19.91	22.74
W-30%	16.47	20.17	18.71	22.53
R-5%	22.88	23.53	24.93	27.33
R-10%	21.59	23.21	23.02	27.03
R-15%	20.63	22.10	21.01	26.78
R-20%	20.51	21.91	20.67	25.47
R-25%	18.66	21.49	19.62	24.26
R-30%	17.62	20.87	19.12	23.82

The comparison modulus of elasticity according to ACI and ASTM of cement and CWP concrete at 7, 28 and 90 days has been demonstrated in Table 4.8. From investigation it is concluded that the modulus of elasticity value increased with the curing ages. Although, the modulus of elasticity calculated by ACI and ASTM methods have slight variations at 28 days. The red CWP concrete gave greater value of modulus of elasticity than white CWP concrete for approximately all partial replacement. The study revealed that CWP concrete has almost identical outcomes compared to that of control (cement) concrete of the modulus of elasticity for 20% and 15% partial replacement of red and white CWP respectively. The 28 days modulus of elasticity according to ACI and ASTM methods of red and white CWP concrete for 20% and 15% concrete mix were 21.91 GPa & 20.67 GPa and 22.19 GPa & 22.45 GPa respectively. Table 4.8 also illustrated the incorporation after 20% and 15% partial replacement of red and white CWP respectively, this study revealed that the modulus of elasticity decreased with the incorporation of CW in concrete. Because of the inappropriate spreading of CWP in concrete, the weaker zones became induced and

caused in the reduction in the modulus of elasticity of concrete. The another reason may be the quantity of CWP was greater than that of requisite to react with the liberated  $\text{Ca(OH)}_2$ . So there is a surplus quantity of unreacted silica, which produced a reduction in strength, caused in a decrease of the modulus of elasticity.

#### 4.10 Poisson's Ratio of Concrete

Poisson's ratio is defined as the ratio of lateral strain to longitudinal strain in a material subjected to loading. It is typically considered as 0.15 for strength design and 0.2 for serviceability principles (Kou et al., 2009).

Table 4.9: Poisson's ratio of concrete mixes at 7, 28 and 90 days.

Batch Name	7 Days	28 Days	90 Days
0%	0.15	0.18	0.20
W-5%	0.16	0.20	0.23
W-10%	0.15	0.19	0.22
W-15%	0.15	0.18	0.21
W-20%	0.14	0.17	0.20
W-25%	0.13	0.17	0.19
W-30%	0.12	0.15	0.18
R-5%	0.17	0.22	0.25
R-10%	0.16	0.21	0.24
R-15%	0.15	0.21	0.23
R-20%	0.15	0.19	0.21
R-25%	0.13	0.17	0.20
R-30%	0.13	0.16	0.20

The Poisson's ratio values of the concrete mixes are shown in Table 4.9. Every showed value is the average of three consecutive measurements. The main problem in Poisson's ratio tests is to record precisely the lateral strain which is rather minor compared with the axial strain. From investigation it is illustrated the Poisson's ratio range of control, red CWP and white CWP concrete were 0.15 to 0.20, 0.16 to 0.25 and 0.15 to 0.23 respectively. The 28 day Poisson's ratios of these concrete samples were supposed to be

0.20 which is similar to that reported by others (Kou et al., 2009). The values of Poisson's ratio enlarged with curing ages. Also, it increased with the increase of CWP content up to 20% of red ceramic and up to 15% of white CWP mix proportions of concrete. It is familiar that greater value of Poisson's ratios means upper value of ductility. The upgrading of the ductility of the concrete can be endorsed due to the increment of CW content up to optimum marked. As red CW concrete gave higher value of Poisson's values than white CW concrete. So, it is concluded that the red CW concrete were more design friendly and fulfill serviceability criteria.

#### 4.11 Test Results of X-ray Diffraction (XRD) Analysis

The development of the Ordinary Portland Cement (OPC) in the hydration process was examined by several investigators as well, with the assistance of the materials definition methods that use X-ray diffraction (XRD) and scanning electron microscopy (SEM) (Roy and Misra, 2018). They recognized the changes that happen in the mineral compounds (alite, belite, celite I and brownmillerite) during the hydration processes, wherever from calcium silicate hydrates and calcium aluminate hydrates appear (tobermorite, portlandite and ettringite) (Elena and Lucia, 2012).

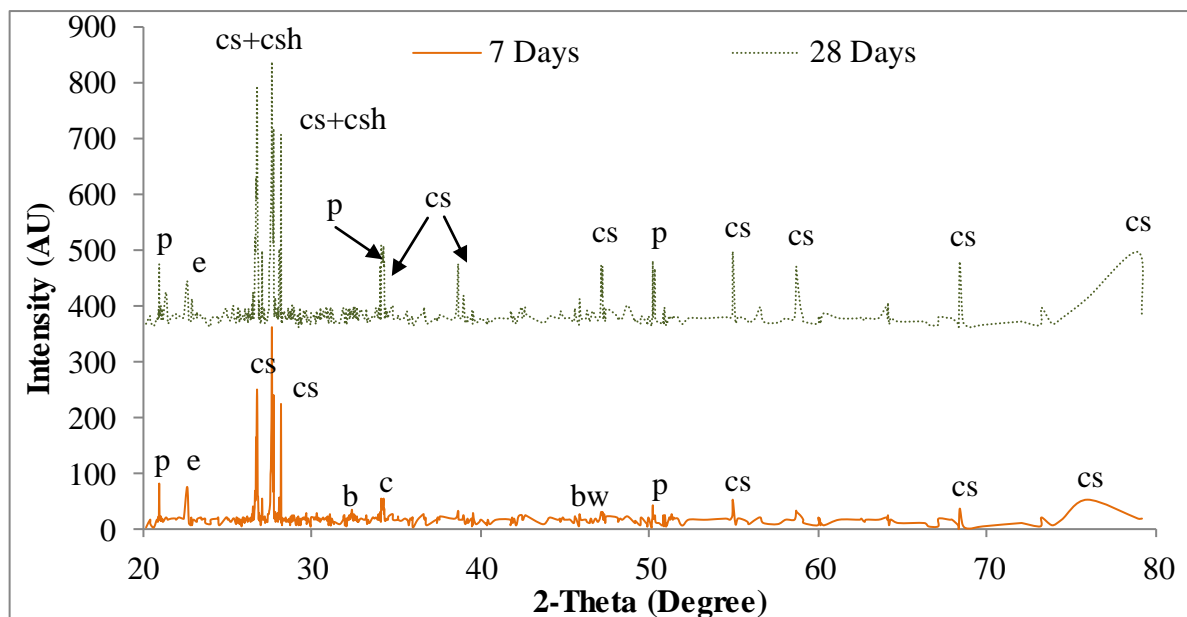


Figure 4.19: XRD results of control (cement) concrete specimens (cs-alite; csh- hydrated calcium silicate (tobermorite); p-portlandite; e-ettringite, b-belite; c-celite; bw-brownmillerite).

This study performed on Ordinary Portland Cement (OPC) and ceramic waste powder (CWP) with respect to the cement hydration processes performed at 7 and 28 days. The techniques used concerning X-ray diffraction (XRD) and scanning electronic microscopy (SEM) analysis conducted to explain materials and to comprehend the variations happening in mineral compounds (alite, belite, celite and brownmillerite) during their changes into mineral compounds (tobermorite, portlandite and ettringite).

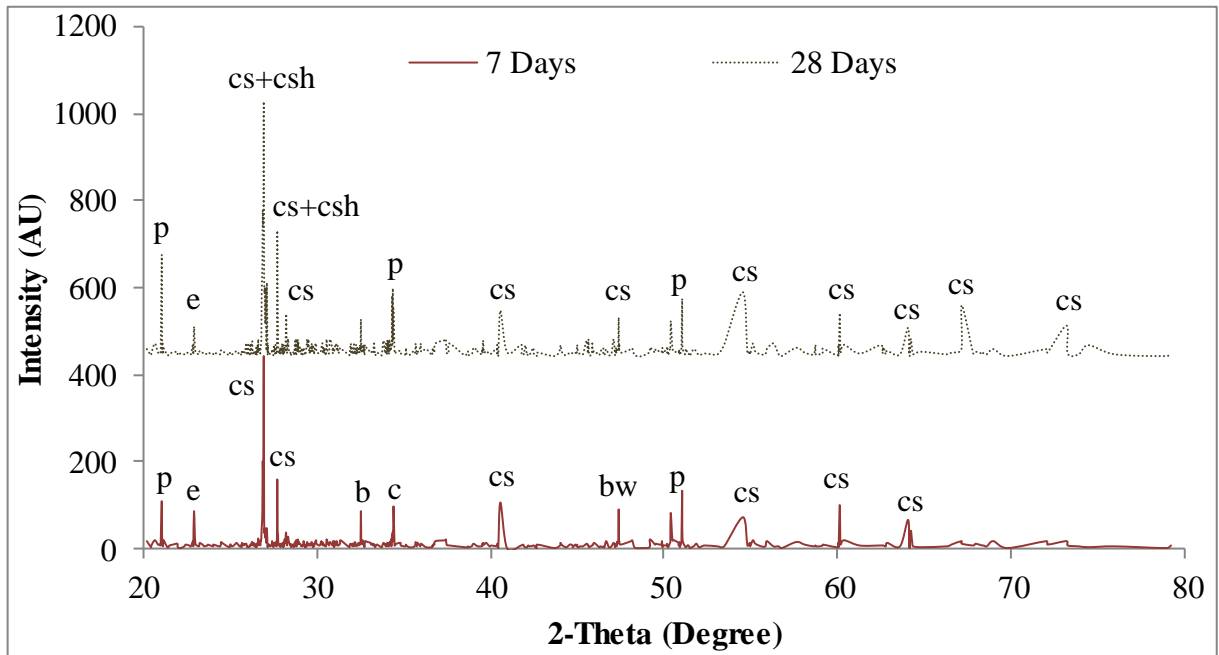


Figure 4.20: XRD results of white CWP concrete specimens.

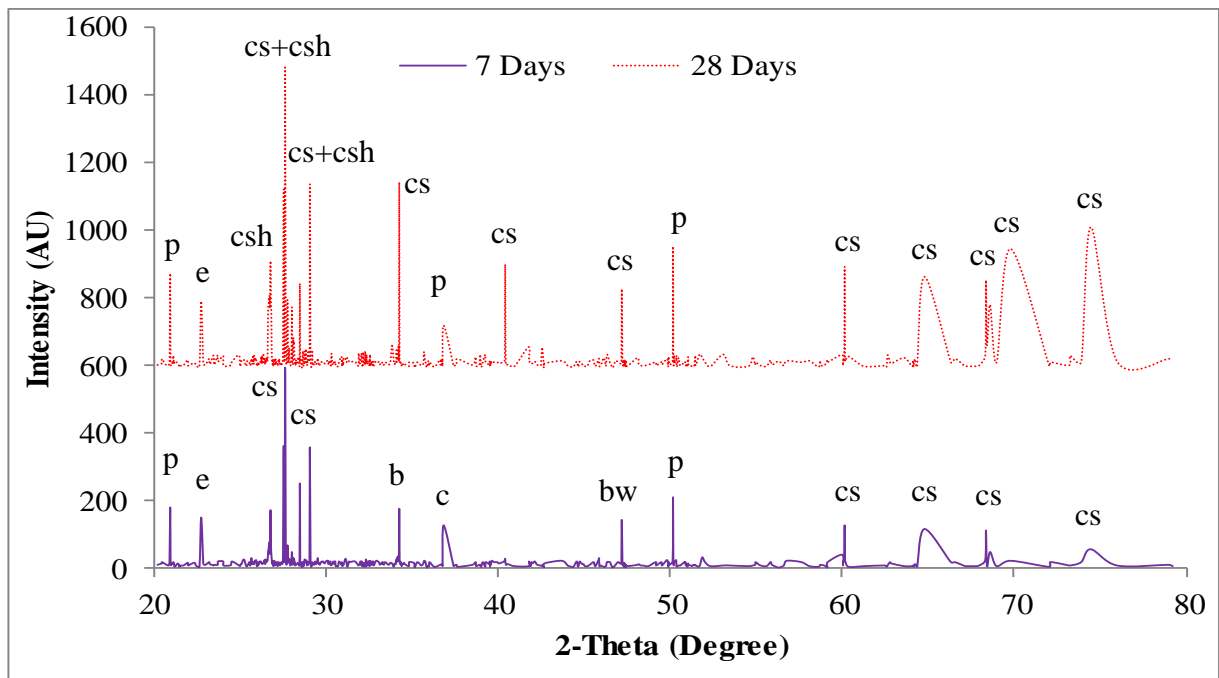


Figure 4.21: XRD results of red CWP concrete specimens.

The XRD analysis results of control (cement), white and red CWP concrete specimens are presented in Figure 4.19, Figure 4.20 and Figure 4.21 respectively. The diffraction angle (2-Theta Degree) and intensity (AU-Arbitrary Unit) has been plotted in the horizontal and

vertical axis respectively. As from the mechanical and chemical analysis the optimum partial replacement proportions found up to 20% of red ceramic and up to 15% of white ceramic concrete. So the XRD analysis conducted only on control (cement), 15% of white CW and 20% of red CWP concrete specimens. From all the XRD analysis it can be concluded that the diffraction spectra showed the alite was obtained mainly in all the samples, that part of it was hydrated and the calcium silicate hydrate was produced. The presence of calcium silicate hydrate has been supported by the similar XRD study on ordinary Portland cement (Elena and Lucia, 2012; Roy and Misra, 2018). Ettringite and portlandite were found in every hydration phases. Variations of the mineral components at time of hydration were emphasized where from silicate hydrates and aluminate hydrates are found (tobermorite, portlandite and ettringite).

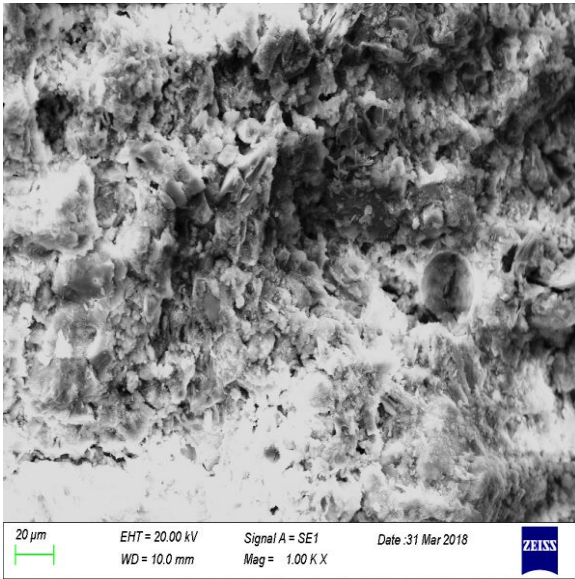
After 7 days, the greatest peaks were found in the diffractograms with respect to alite and tobermorite. After 28 days, the spectrum was quite higher to the spectrum after seven days. At the time of hydration process, values between tobermorite and portlandite stages are found to increase for 7 and 28 days. The phenomenon can be described in such a way that in the 7 days of hydration process tobermorites initiating from alite are major, that alite exist in greater amount than belite that is the source of portlandite that, in turn, is induced more gently. Supplementary portlandite is formed in time, so that at 7 days, the changing in between tobermorite and portlandite decreases. At 28 days, the change between the two compounds rises as tobermorite grows plentiful. The intensity of all the mineral compound of red CWP concrete specimens during hydration process was found greater than white CWP and cement concrete specimens. The alite and tobermorite was the most dominating compound found in the XRD analysis. The intensity of alite and tobermorite of ceramic waste (red and white) concrete was greater than control specimen.



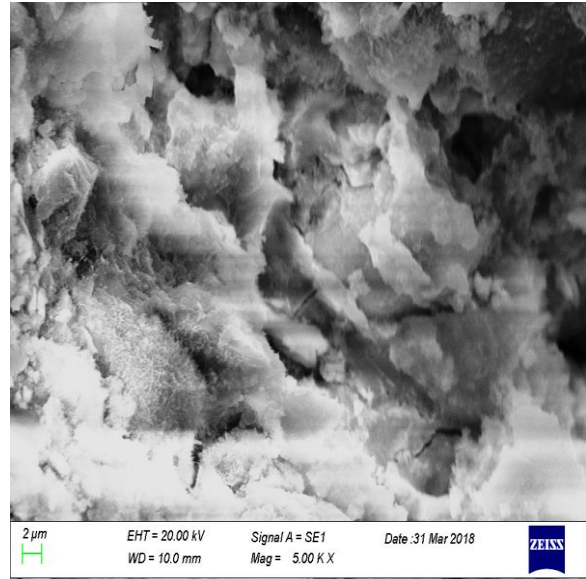
#### 4.12 Test Results of Scanning Electron Microscopy (SEM) Analysis

The technique scanning electronic microscopy (SEM) executed to define materials and to comprehend the changes happening in mineral compounds (alite, belite, celite and brownmillerite) throughout their modification into hydrated mineral compounds (tobermorite, portlandite and ettringite). To analyze the morphological development of the Ordinary Portland cement (OPC) and CW samples at 7 and 28 days, the scanning electron microscope SEM of type EVO 18 Research machine was used in the study. As the microscopic analysis needs the samples that are electrically conductive, the samples are placed in SPUTTER Coater to make the sample conductive. The machine used the gold conductive process. The samples were then fragmented and the analysis conducted on the breaking surface. The SEM analyses conducted on cement and most favourable partial replacement of ceramic waste powder (20% of red CWP and 15% of white CWP) specimens at 7 and 28 days. The presence of mineral compounds and zooming range to identify those compounds have been also supported by the similar SEM study on ordinary Portland cement (Vida-Simiti et al., 2004; Elena and Lucia, 2012).

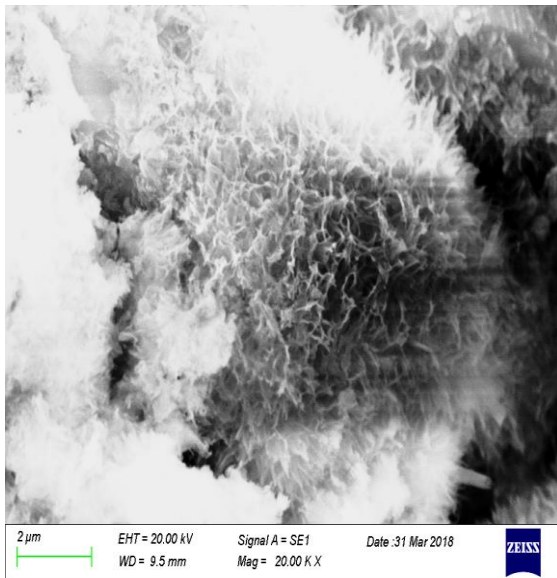
The Scanning Electron Microscopy (SEM) analyses results are presented sequentially of cement at 7 days in Figure 4.22. A sequential magnified image show the clear surface morphology of the samples as illustrated in Figure 4.22(a) to (l). After 7 days SEM analyses of cement samples, while alite was hydrated; tobermorite formed more and more, developing a continuous matrix in the form of coatings joined together. Portlandite is also recognized, in a hexagonal shape as presented in Figure 4.22(i). Alite and belite grains are little bit hydrated and yet they are still present. The most common elements found in these samples are ettringite as depicted in Figure 4.22(d) to (h), which is a prismatic crystals are typically colorless, turning white on partial dehydration and plate like structure was visible almost everywhere. The tobermorite (compact mass) with ettringite (plate) from alite and belite have been observed in Figure 4.22(g) and Figure 4.22(h). A little micro-crack as celite and brownmillerite found in the samples and, thus diverged to dense morphology as illustrated in Figure 4.22(j) to (l).



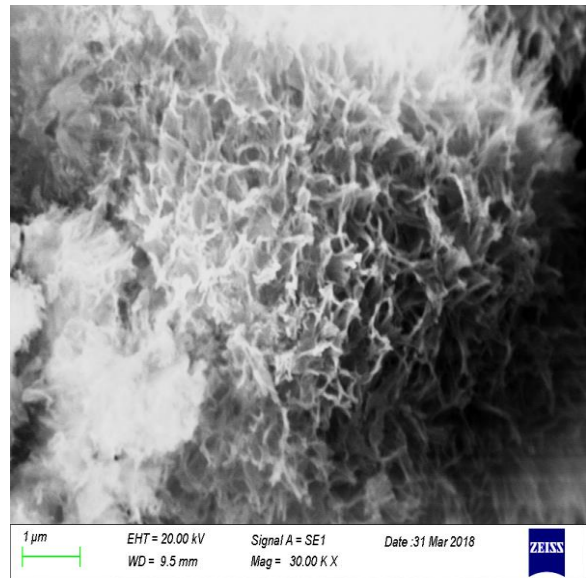
(a) Mag = 1 KX (20 μm)



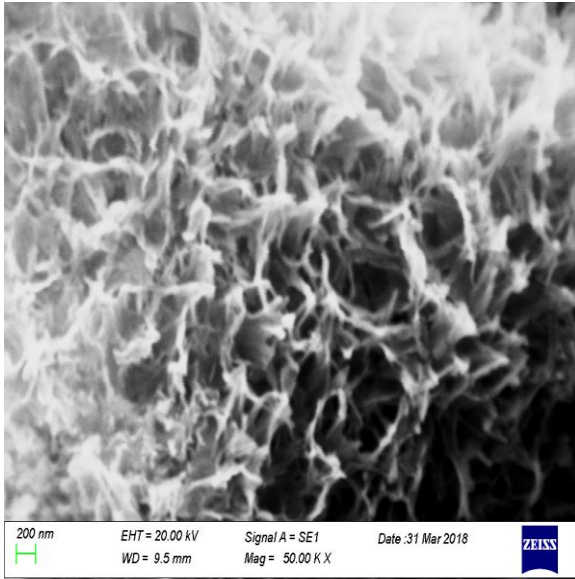
(b) Mag = 5 KX (2 μm)



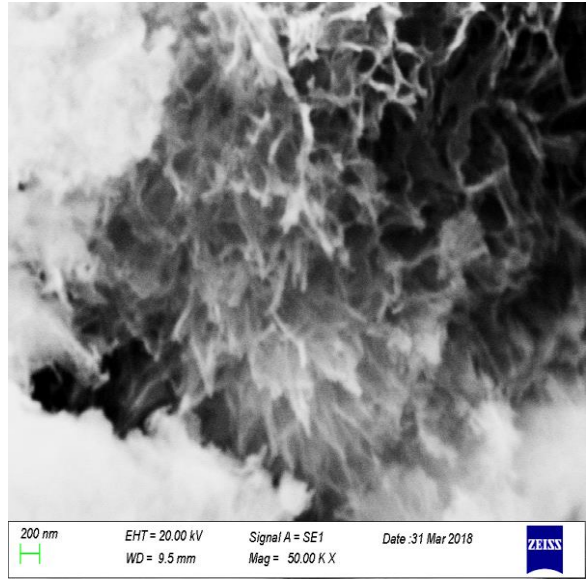
(c) Mag = 20 KX (2 μm)



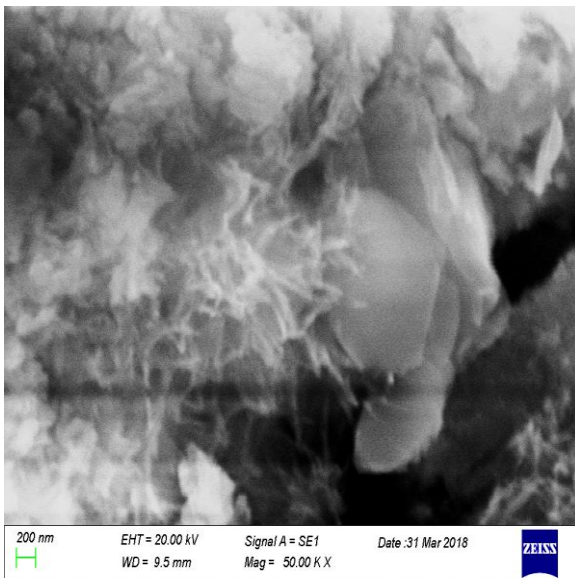
(d) Mag = 30 KX (1 μm)



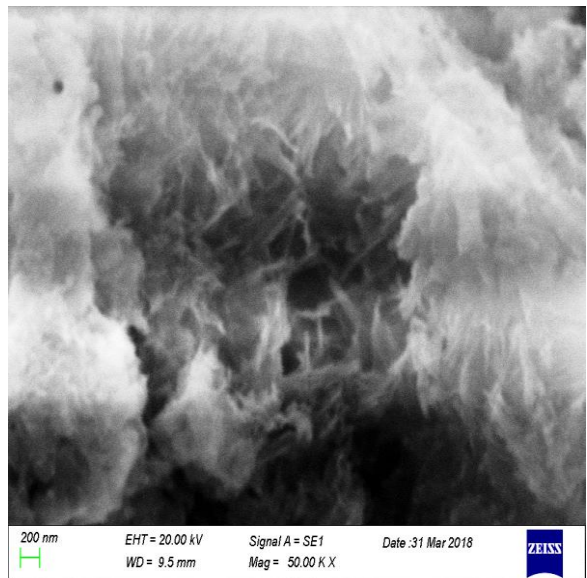
(e) Mag = 50 KX (200 nm)



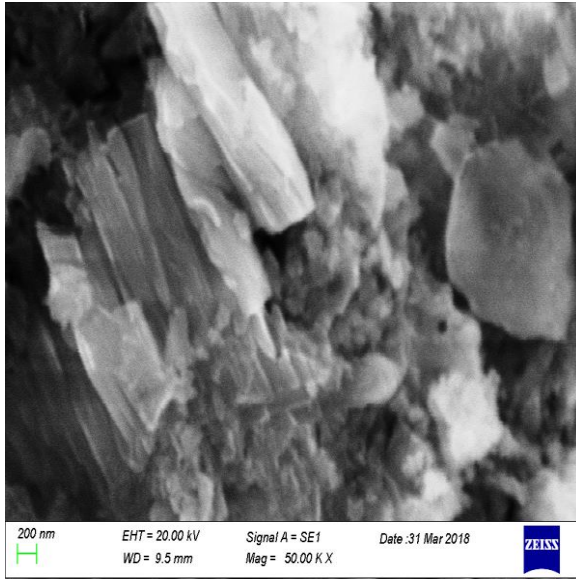
(f) Mag = 50 KX (200 nm)



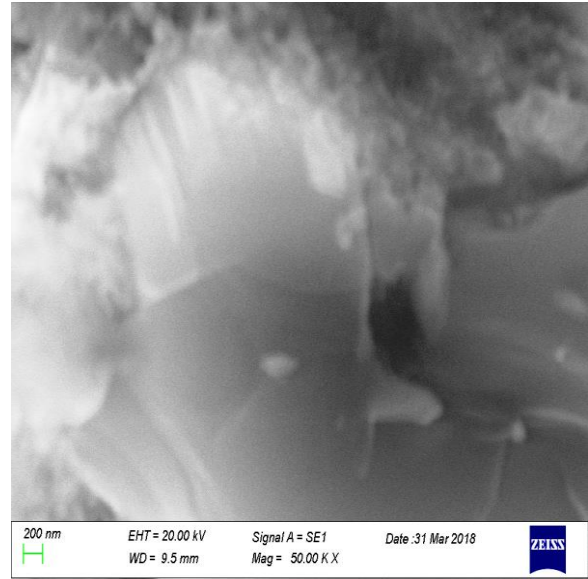
(g) Mag = 50 KX (200 nm)



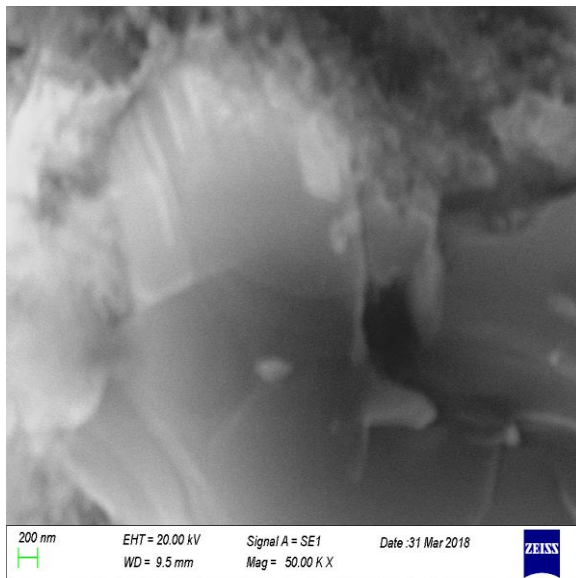
(h) Mag = 50 KX (200 nm)



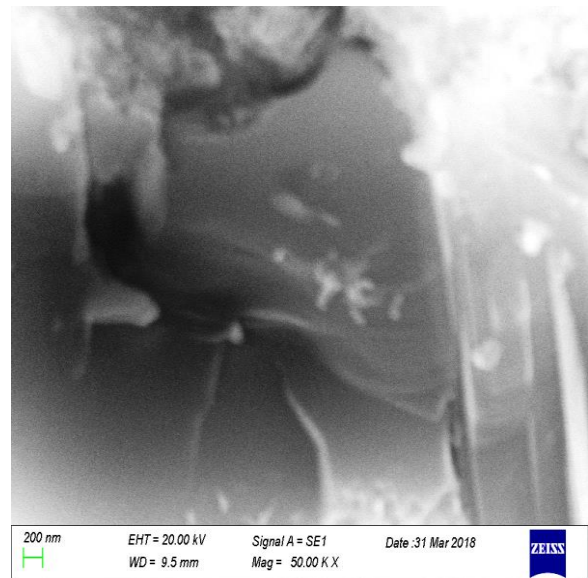
(i) Mag = 50 KX (200 nm)



(j) Mag = 50 KX (200 nm)



(k) Mag = 50 KX (200 nm)



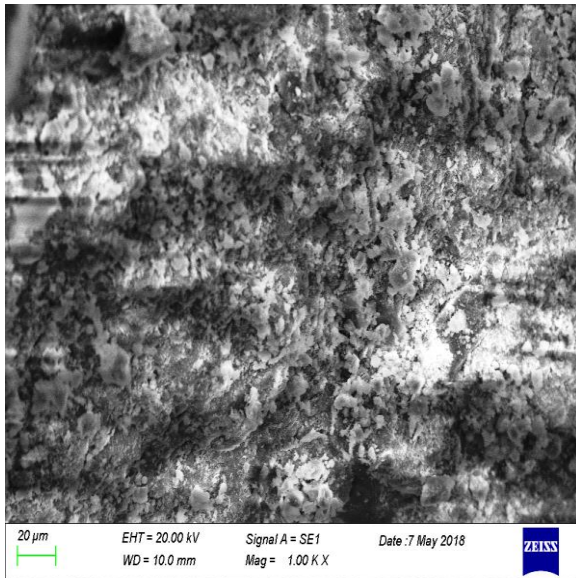
(l) Mag = 50 KX (200 nm)

Figure 4.22: SEM analysis results of cement concrete samples at 7 days.

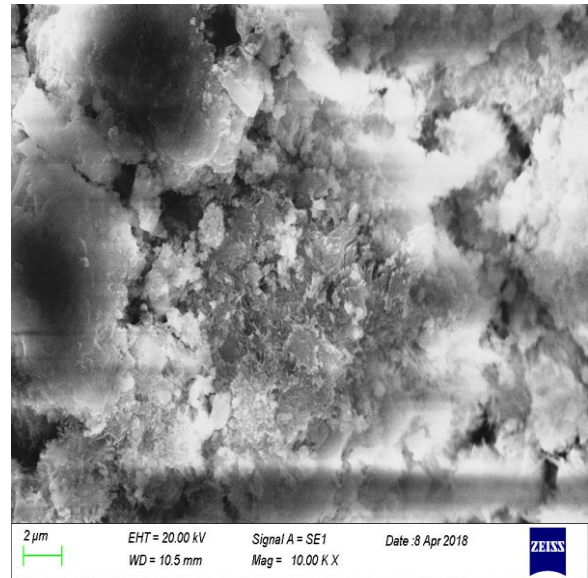
Figure 4.23 illustrated the Scanning Electron Microscopy (SEM) analyses results at 7 days of white CWP samples. A chronological expanded image illustrated the clear surface morphology of the samples as presented in Figure 4.23(a) to (i). The initial surface morphology has been shown in Figure 4.23(a) and Figure 2.23(b) respectively. After 7 days SEM analyses of white CWP samples, alite was hydrated; tobermorite developed more and more, jointly forming a continuous matrix as like as cement samples as



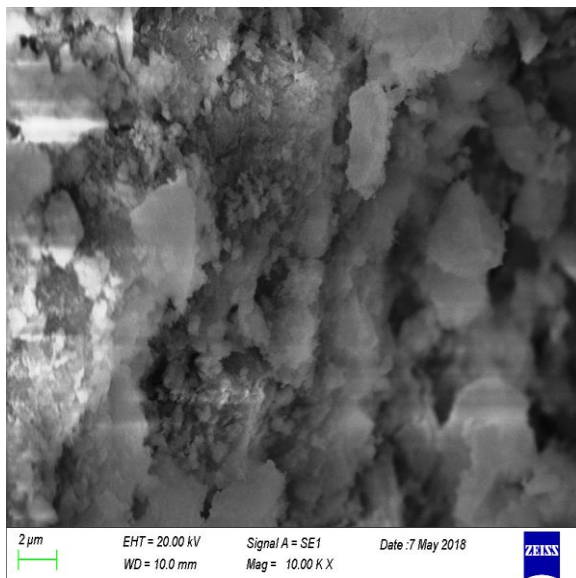
illustrated in Figure 4.23(c) to (i). Portlandite is also found in these specimens. A few ettringite, plate like structure found here as presented in Figure 4.23(e). The surface morphology of the white CWP specimens showed denser morphology than of cement containing specimens.



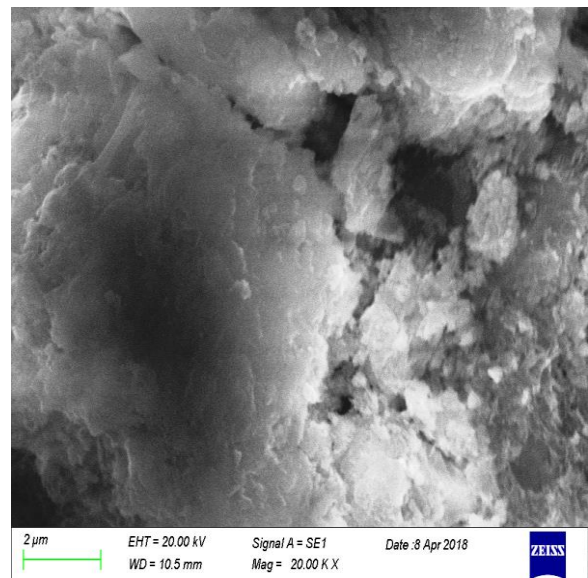
(a) Mag = 1 KX (20 µm)



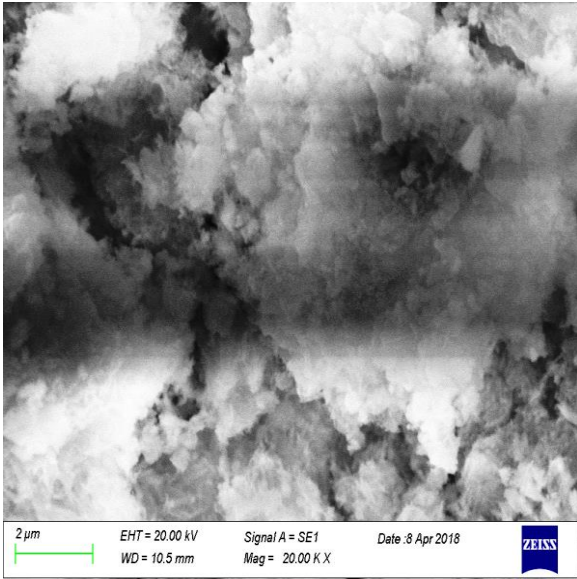
(b) Mag = 10 KX (2 µm)



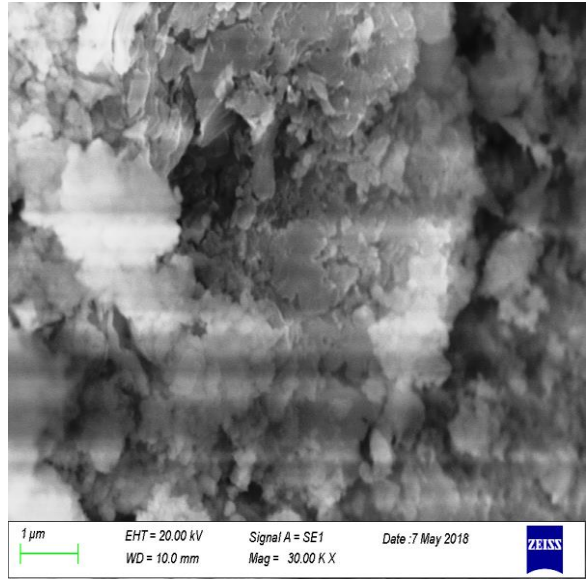
(c) Mag = 10 KX (2 µm)



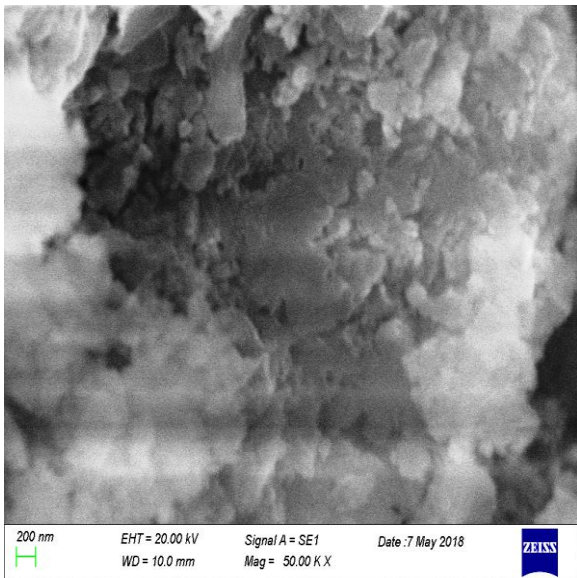
(d) Mag = 20 KX (2 µm)



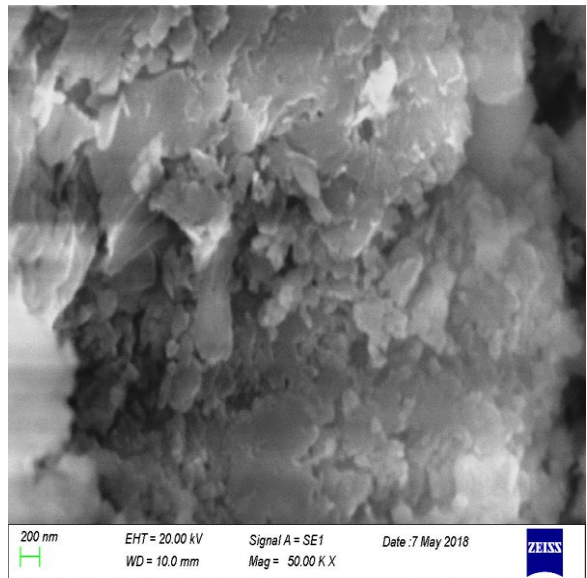
(e) Mag = 20 KX (2 μm)



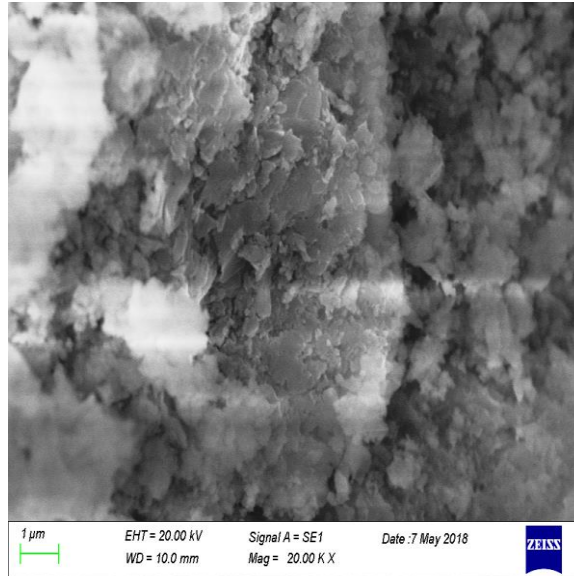
(f) Mag = 30 KX (1 μm)



(g) Mag = 50 KX (200 nm)



(h) Mag = 50 KX (200 nm)

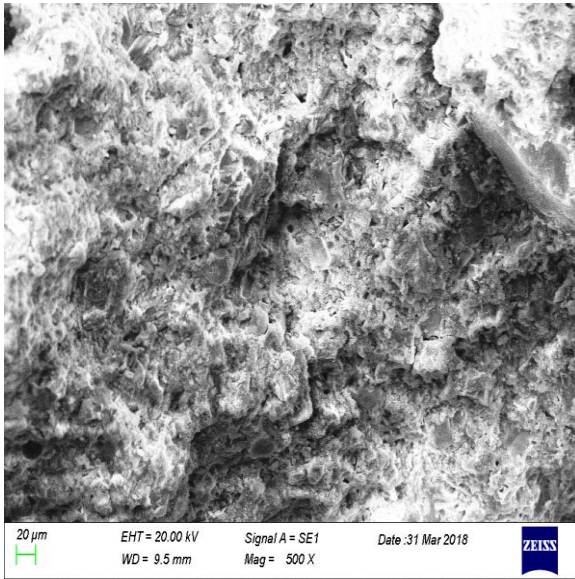


(i) Mag = 20 KX (1 μm)

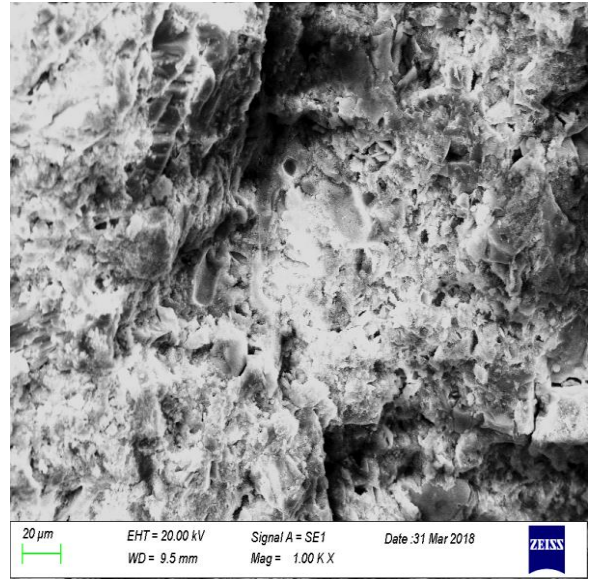
Figure 4.23: SEM analysis results of white CWP concrete samples at 7 days.

Figure 4.24(a) to (i) exemplified the Scanning Electron Microscopy (SEM) analyses results at 7 days of red CWP samples. The surface morphology of the samples explained chronologically with SEM analysis image. The simple morphological surface has been shown in Figure 4.24(a) and Figure 4.24(b). After 7 days SEM analyses of red CWP samples, alite was hydrated; more tobermorite developed and jointly forming a continuous matrix as like as cement and white CWP specimens as illustrated in Figure 4.24(e) to (i). A more hexagonal shape mineral that is portlandite has been found in red CWP concrete than cement and white CWP specimens. A few ettringite, plate like structure has also observed in red CWP concrete shown in Figure 4.24(c) and Figure 4.24(d). The surface morphology of the red CWP specimens showed very denser and well-structured than that of cement and white CWP specimens.

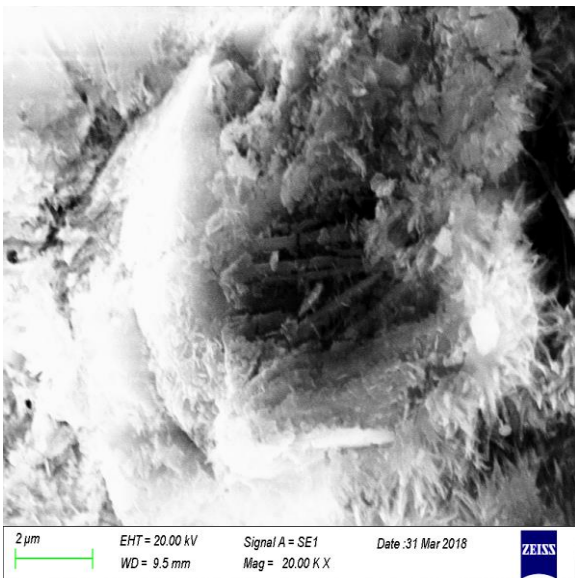




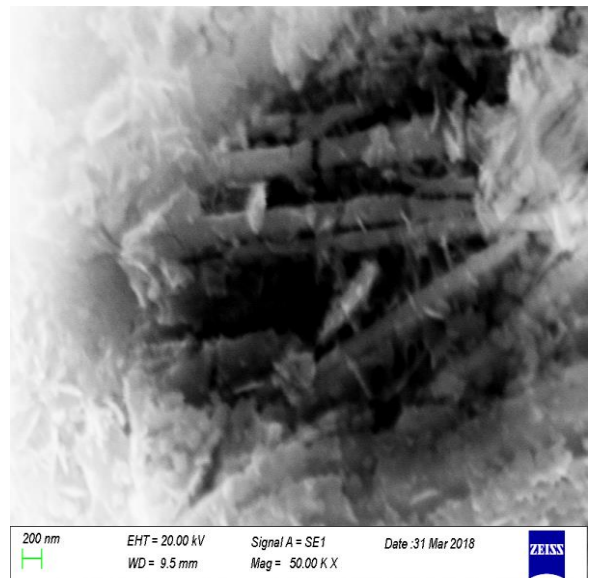
(a) Mag = 500 X (20 μm)



(b) Mag = 1 KX (20 μm)

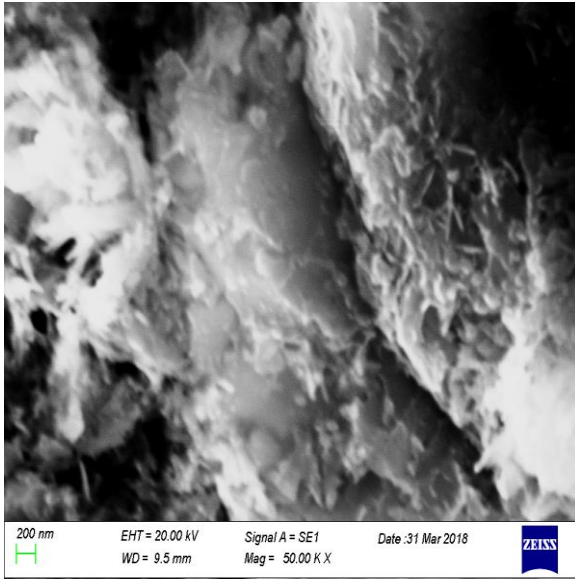


(c) Mag = 20 KX (2 μm)

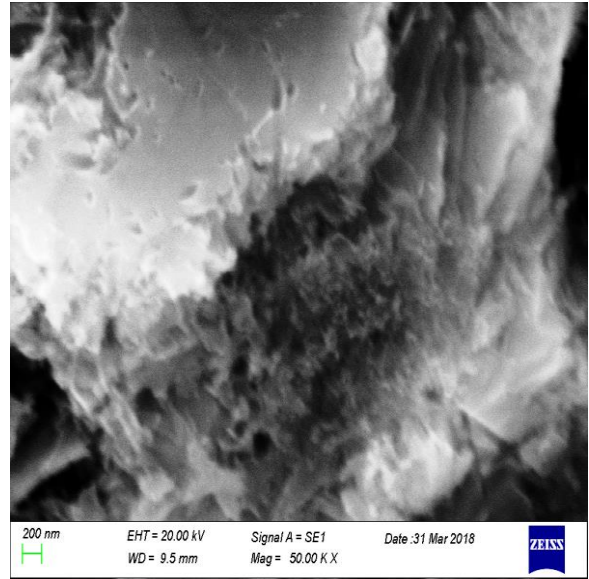


(d) Mag = 50 KX (200 nm)

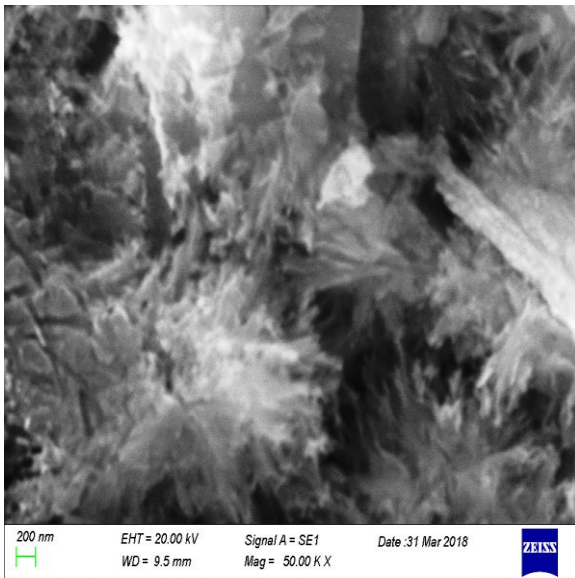




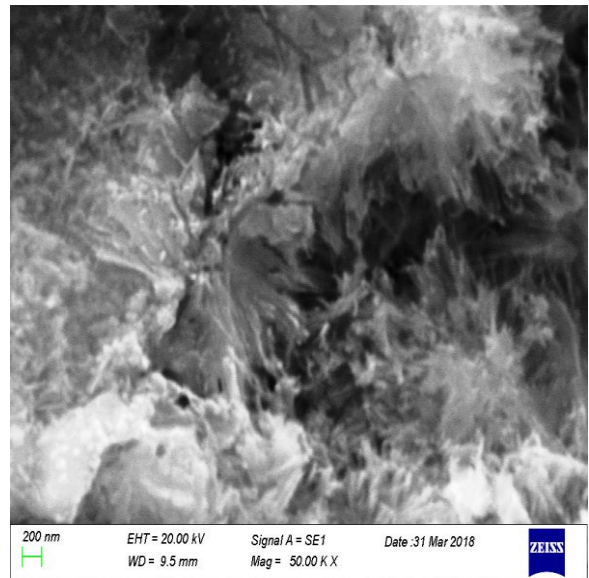
(e) Mag = 50 KX (200 nm)



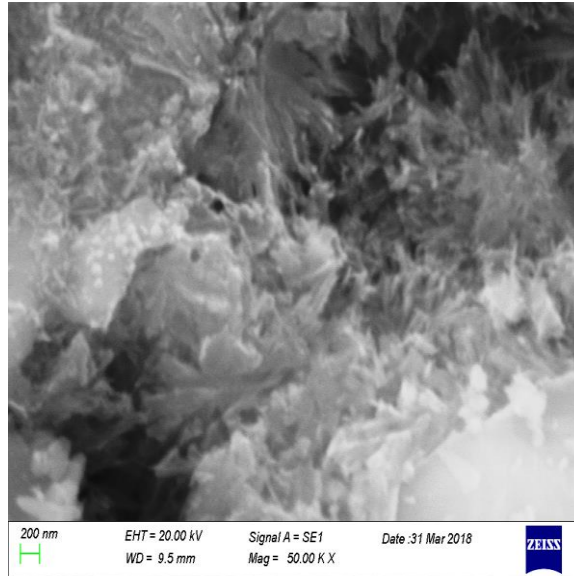
(f) Mag = 50 KX (200 nm)



(g) Mag = 50 KX (200 nm)



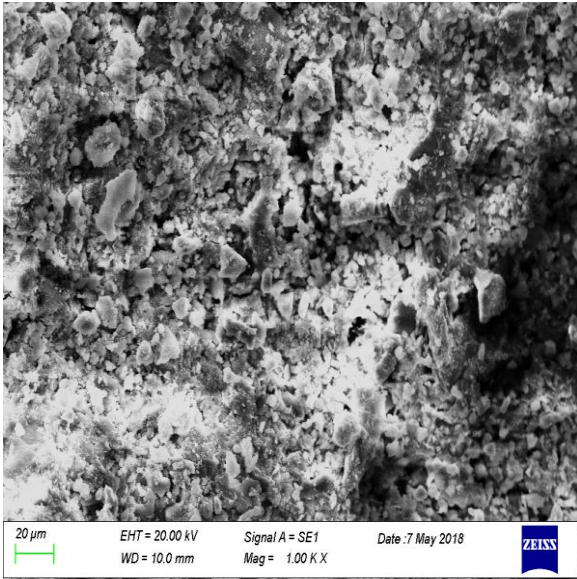
(h) Mag = 50 KX (200 nm)



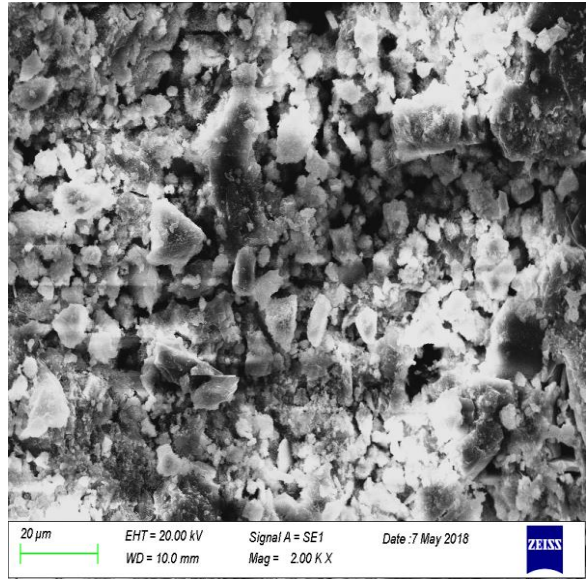
(i) Mag = 50 KX (200 nm)

Figure 4.24: SEM analysis results of red CWP concrete samples at 7 days.

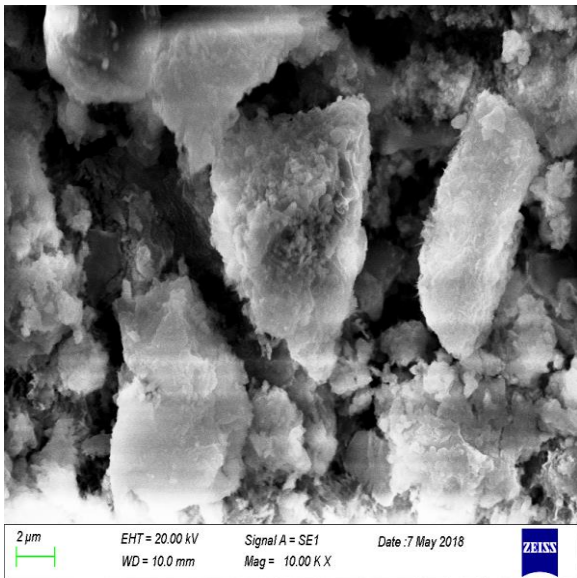
Comparing the SEM analyses results of cement, white and red CWP concrete samples, it can be concluded that after 7 days, while alite is hydrated, tobermorite grows to a greater amount and develops a continuous matrix of coatings joined together. Portlandite is also found in hexagonal shape. Also, elements of stagnant non-hydrated alite and belite have been found. Ettringite begins seeming in minor quantities. Because of hydration heat, cracks are noticed at the scanning electron microscope investigation. The micro-cracks in red CWP concrete were lesser than that of cement and white CWP samples.



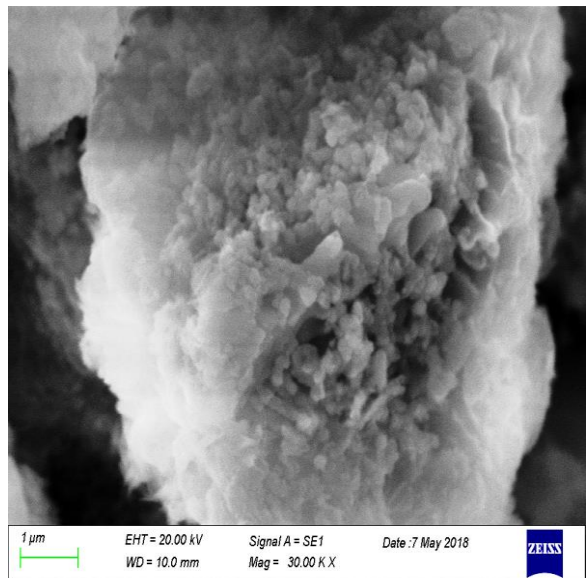
(a) Mag = 1 KX (20 μm)



(b) Mag = 2 KX (20 μm)

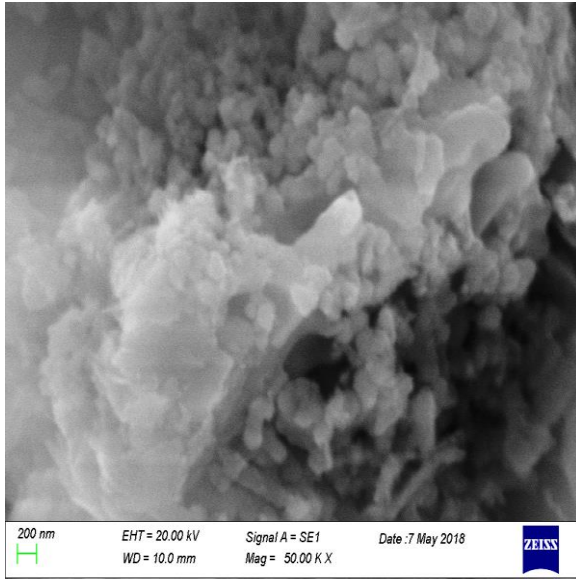


(c) Mag = 10 KX (2 μm)

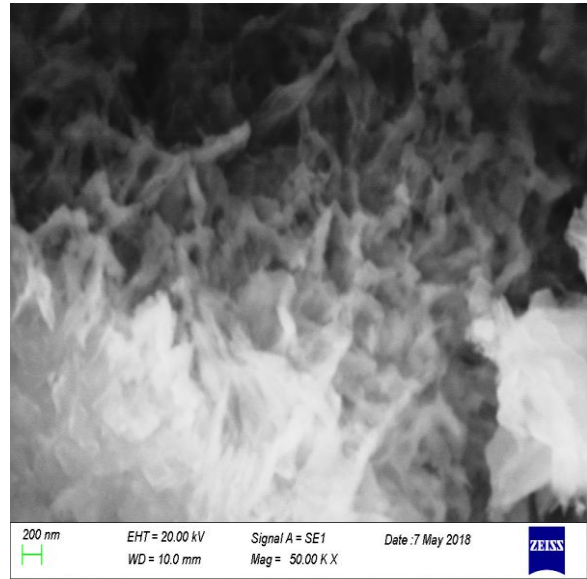


(d) Mag = 30 KX (1 μm)

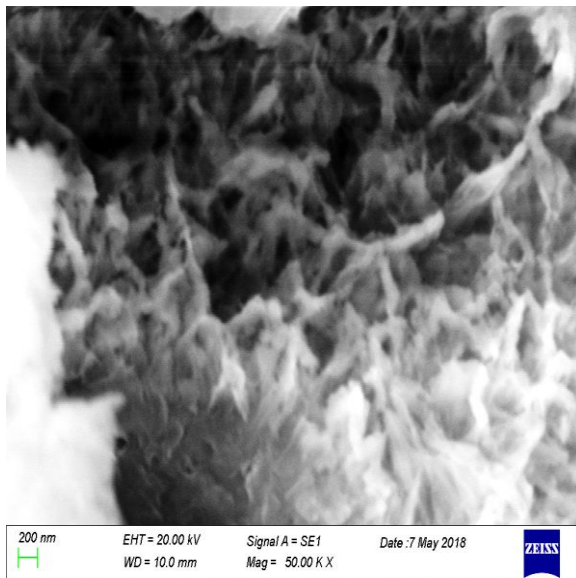




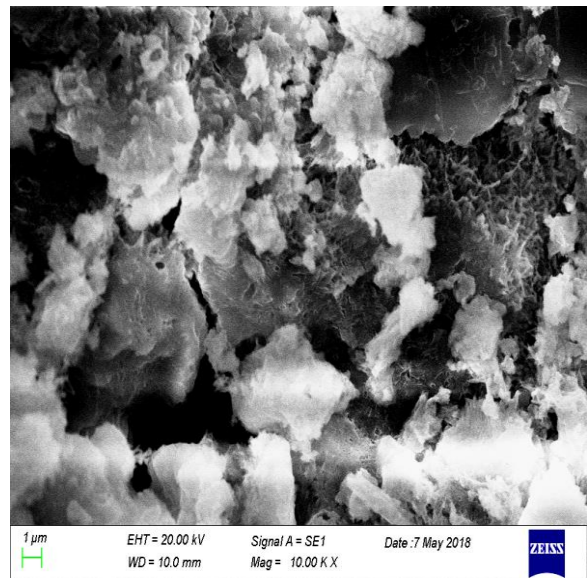
(e) Mag = 50 KX (200 nm)



(f) Mag = 50 KX (200 nm)

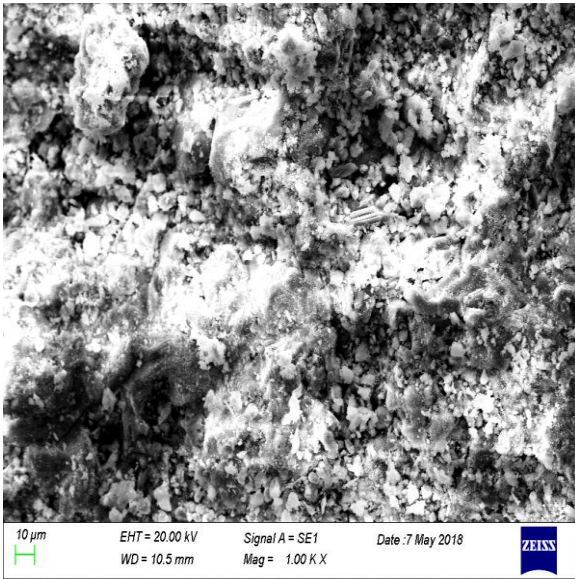


(g) Mag = 50 KX (200 nm)

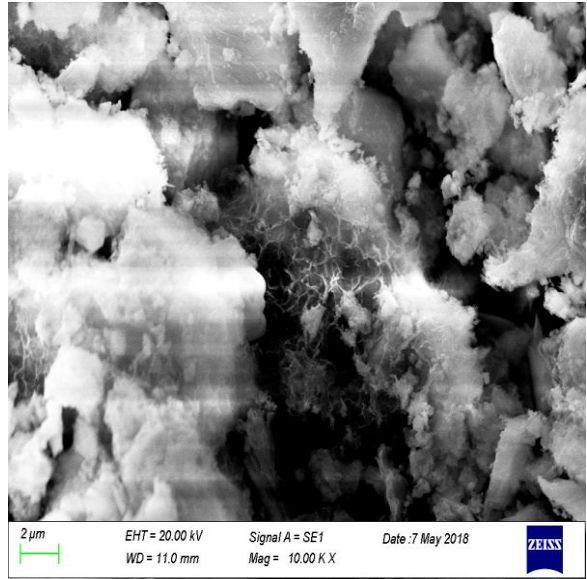


(h) Mag = 10 KX (1 μm)

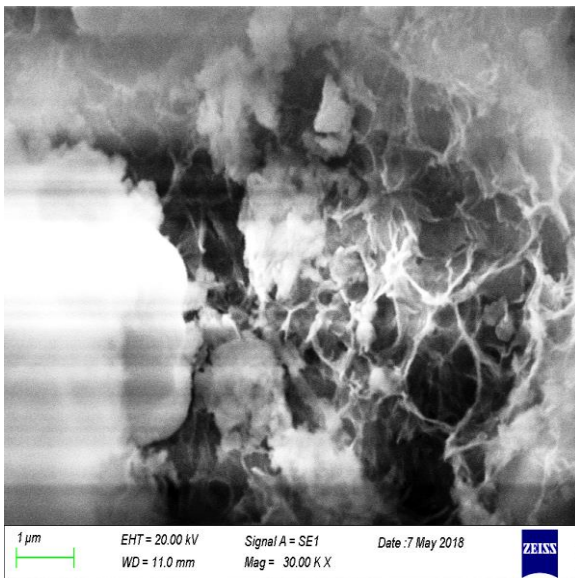
Figure 4.25: SEM analysis results of cement concrete samples at 28 days.



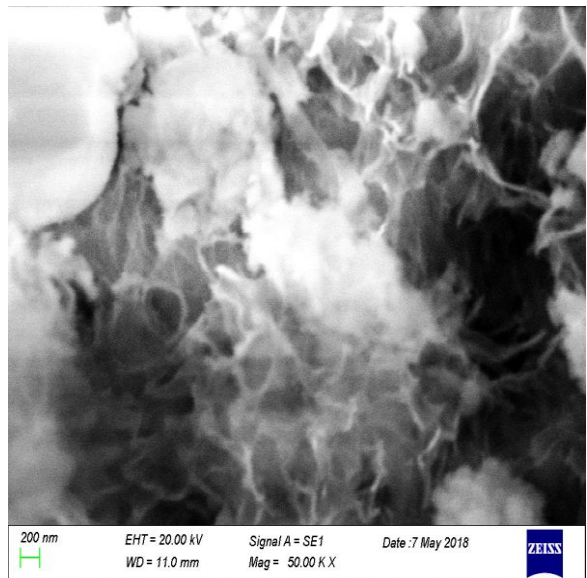
(a) Mag = 1 KX (10 μm)



(b) Mag = 10 KX (2 μm)

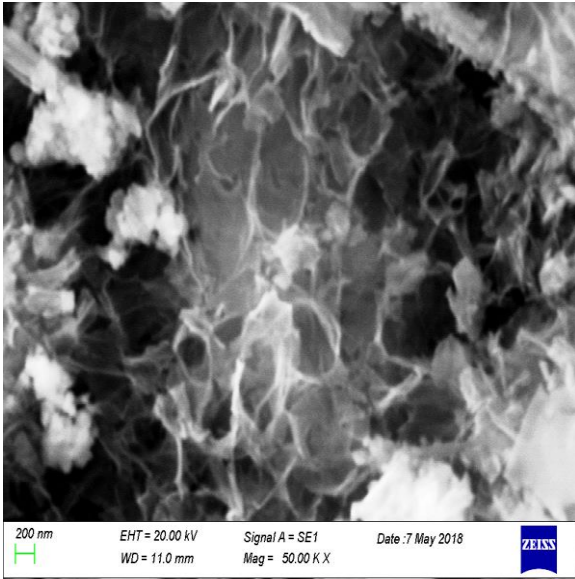


(c) Mag = 30 KX (1 μm)

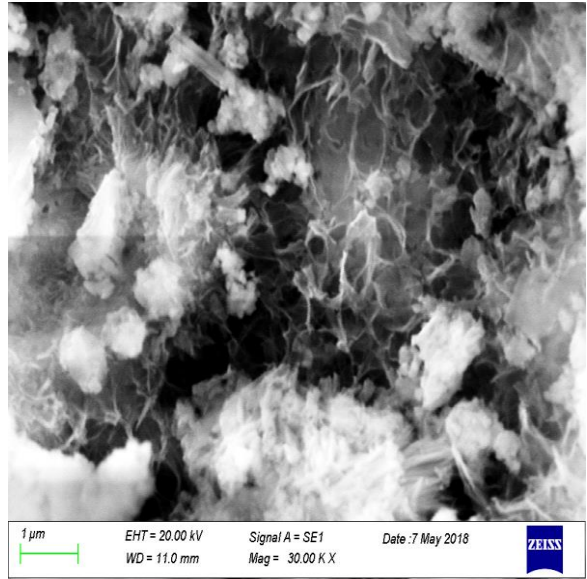


(d) Mag = 50 KX (200 nm)

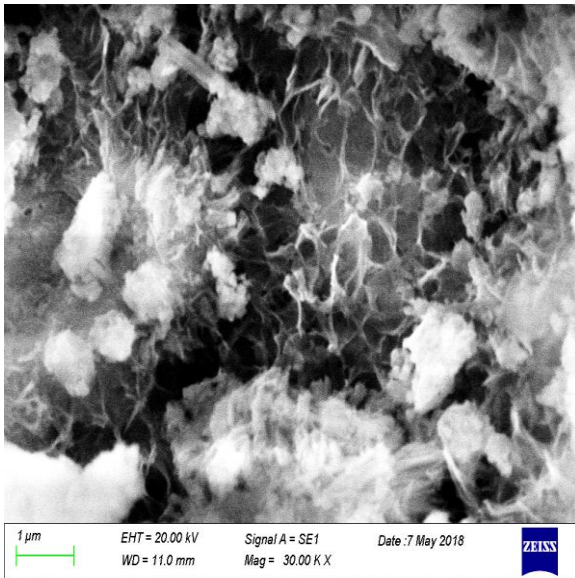




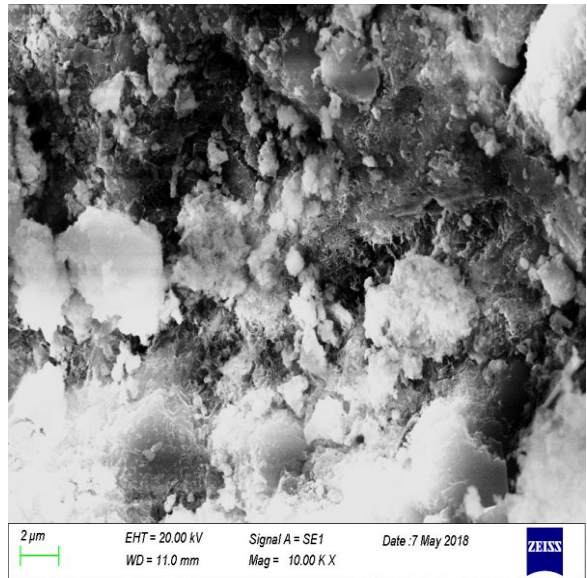
(e) Mag = 50 KX (200 nm)



(f) Mag = 30 KX (1 μm)

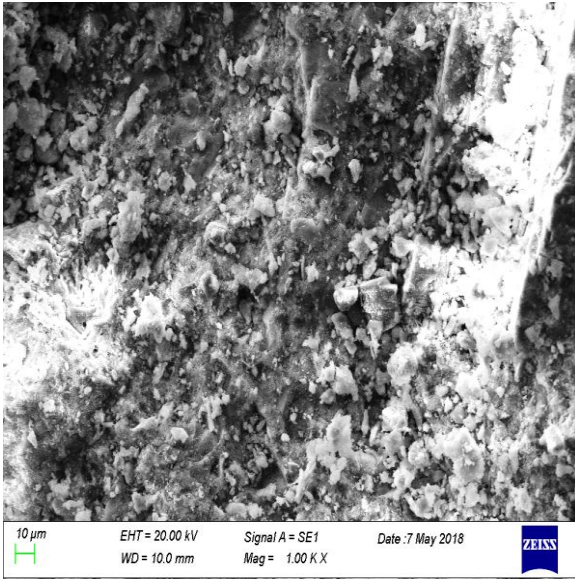


(g) Mag = 30 KX (1 μm)

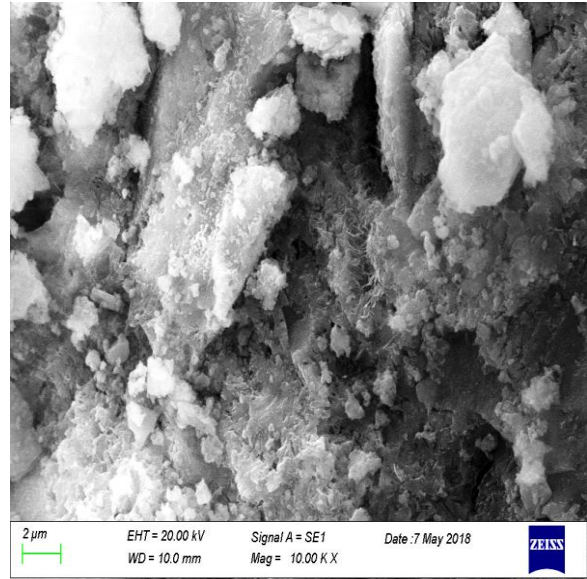


(h) Mag = 10 KX (2 μm)

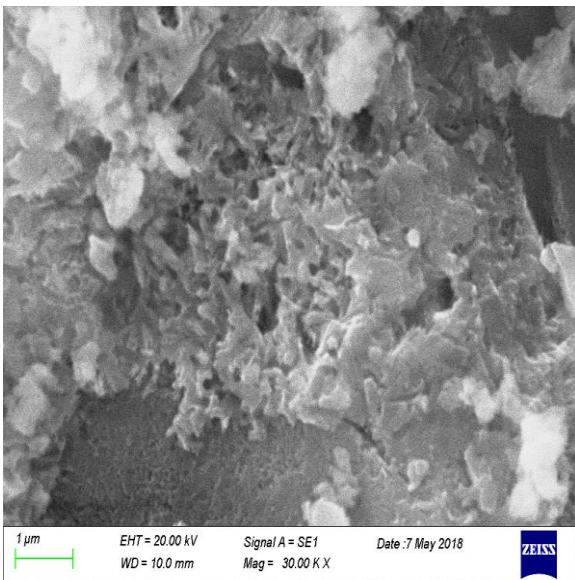
Figure 4.26: SEM analysis results of white CWP concrete samples at 28 days.



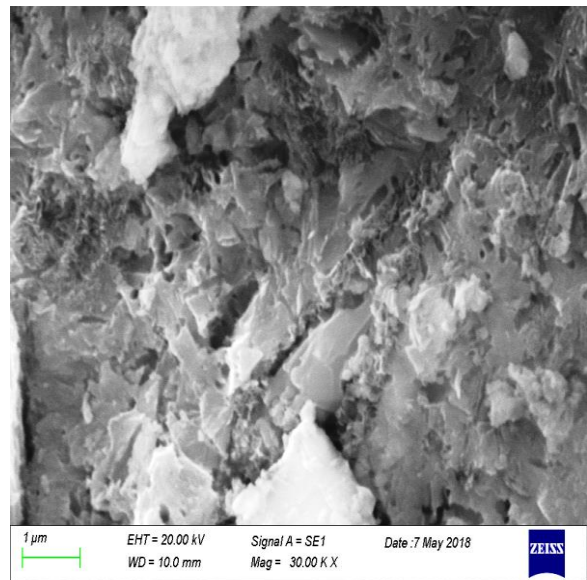
(a) Mag = 1 KX (10  $\mu$ m)



(b) Mag = 10 KX (2  $\mu$ m)

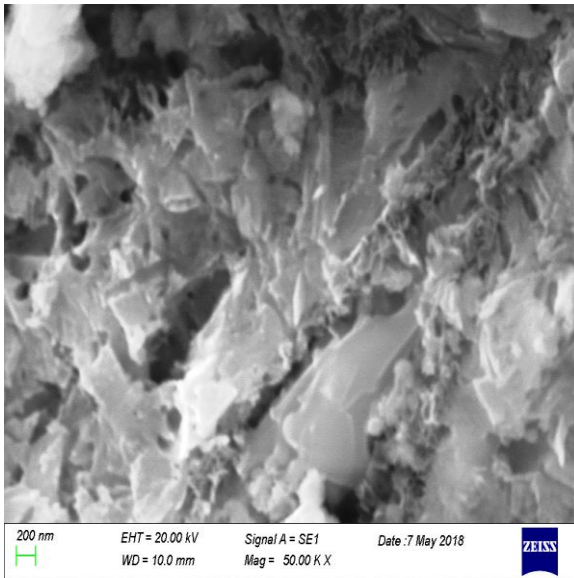


(c) Mag = 30 KX (1  $\mu$ m)

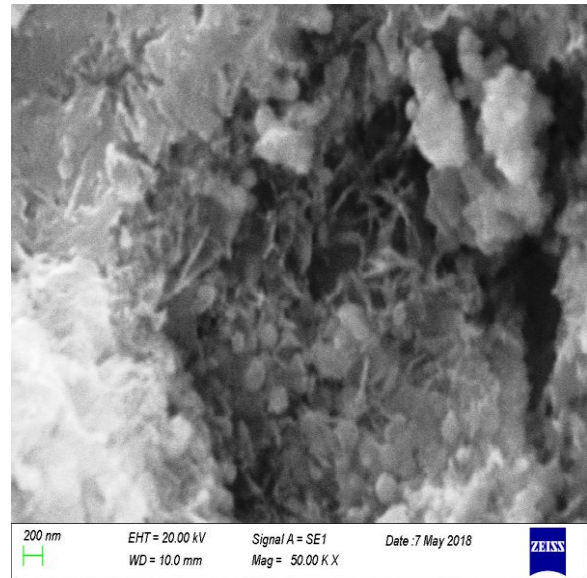


(d) Mag = 30 KX (1  $\mu$ m)

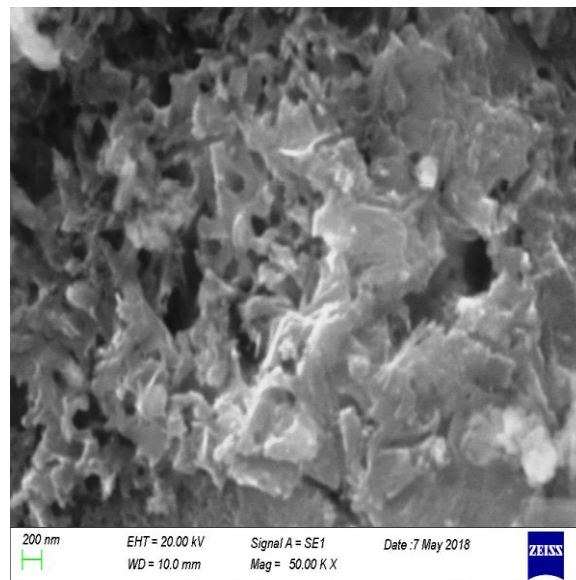




(e) Mag = 50 KX (200 nm)



(f) Mag = 50 KX (200 nm)



(g) Mag = 50 KX (200 nm)

Figure 4.27: SEM analysis results of red CWP concrete samples at 28 days.

The SEM analyses results at 28 days have been figured out in Figure 4.25, Figure 4.26 and Figure 4.27 for cement, white CWP and red CWP specimens respectively. The magnified images are shown sequentially to describe morphology of those samples. If the samples kept up to 28 days, their structures have been changed, so that its surface, under a minor zooming condition, showed more dense in Figure 4.25(e), Figure 4.26(c) and Figure 4.27(c) of the cement, white CWP and red CWP samples respectively. The SEM results of



cement concrete samples at 28 days showed huge amount tobermorite and compact mass as illustrated in Figure 4.25(a) to (e). From Figure 4.25(f) to (h) it has been observed that there is a very tiny amount of portlandite. In case of white CWP at 28 days SEM analysis results showed more compact mass than cement concrete as illustrated in Figure 4.26(b) to (h). The 28 days SEM analysis results of red CWP concrete showed better performance than cement and white CWP concrete. All the minerals are converted into very compact mass at 28 days red ceramic concrete as shown in Figure 4.27(b) to (g). On the other hand, slight cracks were observed because of the hydration heat, developed by the exothermal hydration reactions. The cement and CWP concrete samples showed more degree of hydration, tobermorite formulates and grows its continuous matrix obvious after the 28 days. Moreover, portlandite was recognizable in its distinctive hexagonal form and ettringite in the forms of needles have been found at this age concrete as depicted in Figure 4.25(e) and Figure 4.26(e). After 28 days, tobermorite forms a mass that showed much compact and steadiness and where very little amount of belite found that have not yet hydrated. The surface morphology of red and white CWP concrete was more denser than that of cement concrete specimens. From SEM analysis, it can be revealed that the red CWP concrete are denser, compact and lesser micro-cracks than that of cement and white CWP concrete.

## CHAPTER V

### CONCLUSIONS AND RECOMMENDATIONS

#### 5.1 Conclusions

In construction industry concrete is the most vital construction materials. The ceramic industry generates huge amounts of pozzolanic clay wastes every year in Bangladesh and worldwide. Most of these wastes are directly dumped into the landfill, increasing the burden on landfill loading. Reusing the ceramic wastes in concrete would be the sustainable solutions considering the costs of cement productions and environmental issues. This study investigates the mechanical properties and microscopy of concrete incorporating the ceramic waste as partial replacement of cement. In this research work, chemical composition by XRF, compressive strength test, splitting tensile strength test, XRD and SEM analysis were conducted on cement and partially replaced ceramic waste powder (CWP) concrete. The partial replacement proportions of cement by CWP (both red and white) were 0%, 5%, 10%, 15%, 20%, 25% and 30%. Therefore, reusing these wastes as a binder in concrete production could be an effective measure in maintaining the environment as well as the properties of concrete.

Based on the results of experimental test program, the following conclusions can be drawn with respect to XRF analysis, mechanical properties, SEM and XRD analysis:

- The XRF analysis illustrated that the existence of  $\text{SiO}_2$  and  $\text{Al}_2\text{O}_3$  in CWP (both red and white) is almost twice of cement. Red ceramic waste powder (CWP) showed higher value of  $\text{SiO}_2$  and  $\text{Fe}_2\text{O}_3$  compared to cement and white CWP. Besides, white CWP figured out higher value of  $\text{Al}_2\text{O}_3$  than that of cement and red ceramic waste powder. The XRF analysis results of red and white ceramic waste powder showed satisfactory results compared to ASTM specification of Portland cement, fly ash, slags and control cement.
- From the slump test of concrete, it can be stated that the increasing ceramic content require more water than cement content. It can also be stated that the white ceramic

powder require more water than red ceramic powder to obtain suitable workable concrete.

- Analyzing and discussing the compressive strength test and splitting tensile strength test results with cement (control) specimens, it can be concluded that the partial replacement of cement for 20% of red CWP and for 15% of white CWP is the most favourable mix proportions. The partial replacement for 20% of red CWP concrete provide more satisfactory results than that of cement and white CWP concrete.
- The CWP concrete showed satisfactory results up to optimum partial replacement in terms of strength, modulus of elasticity, stress-strain diagram and Poisson's ratio of cement concrete. From investigation it can be concluded that the modulus of elasticity values increased with the curing ages. Although, the modulus of elasticity calculated by ACI and ASTM methods have slight variations. The modulus of elasticity at 28 days according to ACI and ASTM methods of red and white CW concrete for 20% and 15% concrete mix were were 21.91 GPa & 20.67 GPa and 22.19 GPa & 22.45 GPa respectively.
- The alite and tobermorite is the most dominating compound found in the XRD analysis of ceramic waste specimens. The intensity of alite and tobermorite of CWP concrete was greater than control specimens.
- From the SEM analysis, it can be concluded that with the increase of curing ages the alite is hydrated, tobermorite developed and jointly formed a continuous matrix. Portlandite and ettringite found in small amounts. After 28 days, tobermorite developed a mass that exhibits denser, more compactness and steadiness and where belite found which have not yet hydrated. The density of the surface morphology was very solid of red and white CWP concrete than cement concrete. The red CWP concrete were denser, compact and lesser micro-cracks than cement and white ceramic concrete.

Finally, it can be revealed through the mechanical and microscopic investigation that the ceramic waste powder (CWP) can be used as partial replacement of binder (cement) in concrete up to certain proportion.

## **5.2 Recommendations for Future Study**

For future studies about the same concept, this study suggested some recommendations.

- It is suggested to perform the thermal behavior, shrinkage behavior and fire resistance of partially replaced ceramic waste powder (CWP) concrete.
- To get better morphology of the samples, it is recommended to use scanning electron microscopy (SEM) with energy dispersive X-ray (EDX) analysis.

## REFERENCES

- Abdunnabi, A. (2012). XRF analysis of portland cement for major and trace elements. Arab Conference on the Peaceful use of Atomic Energy; Khartoum (Sudan); 23-27 Dec 2012, pp 11.
- Ahmaruzzaman, M. (2010). A review on the utilization of fly ash. *Progress in energy and combustion science*, 36(3), 327-363.
- Akinpelu, M. A., Odeyemi, S. O., Olafusi, O. S., and Muhammed, F. Z. (2017). Evaluation of splitting tensile and compressive strength relationship of self-compacting concrete. *Journal of King Saud University-Engineering Sciences*.
- Al-Sahawneh, E. (2013). Size effect and strength correction factors for normal weight concrete specimens under uniaxial compression stress. *Contemporary Engineering Sciences*, 6(2), 57-68.
- Asensio, E., Medina, C., Frías, M., and Rojas, M. I. S. (2016). Characterization of Ceramic-Based Construction and Demolition Waste: Use as Pozzolan in Cements. *Journal of the American Ceramic Society*, 99(12), 4121-4127.
- ASTM C150, (2015). Standard Specification for Portland cement (ASTM c 150-86), annual book of ASTM standards 4.02:89-93.
- ASTM C29, (2017). Standard Test Method for Bulk Density (“Unit Weight”) and Voids in Aggregate, ASTM International, West Conshohocken, PA.
- ASTM C39, (2018). Standard Test Method for Compressive Strength of Cylindrical Concrete Specimens, ASTM International, West Conshohocken, PA.
- ASTM C109, (2016). Standard Test Method for Compressive Strength of Hydraulic Cement Mortars (Using 2-in. or [50-mm] Cube Specimens), ASTM International, West Conshohocken, PA.
- ASTM C127, (2015). Standard Test Method for Relative Density (Specific Gravity) and Absorption of Coarse Aggregate, ASTM International, West Conshohocken, PA.

- ASTM C128, (2015). Standard Test Method for Relative Density (Specific Gravity) and Absorption of Fine Aggregate, ASTM International, West Conshohocken, PA.
- ASTM C136, (2014). Standard Test Method for Sieve Analysis of Fine and Coarse Aggregates, ASTM International, West Conshohocken, PA.
- ASTM C150, (2018). Standard Specification for Portland Cement, ASTM International, West Conshohocken, PA.
- ASTM C469, (2014). Standard Test Method for Static Modulus of Elasticity and Poisson's Ratio of Concrete in Compression, ASTM International, West Conshohocken, PA.
- ASTM C496, (2017). Standard Test Method for Splitting Tensile Strength of Cylindrical Concrete Specimens, ASTM International, West Conshohocken, PA.
- ASTM C617, (2015). Standard Practice for Capping Cylindrical Concrete Specimens, ASTM International, West Conshohocken, PA.
- Ay, N., & Ünal, M. (2000). The use of waste ceramic tile in cement production. *Cement and Concrete research*, 30(3), 497-499.
- Bahoria, B., Parbat, D., Naganaik, P., and Waghe, U. (2013). Comprehensive literature review on use of waste product in concrete. *International journal of Application or Innovation in Engineering & Management*, 2(4), 387-394.
- Baldi, G., Bellotti, R., Ghionna, V., Jamiolkowski, M., and Pasqualini, E. (1985). Penetration resistance and liquefaction of sands. Proc. 11<sup>th</sup> ICSMFE, San Francisco, 4, 1891-1896.
- Batayneh, M., Marie, I., and Asi, I. (2007). Use of selected waste materials in concrete mixes. *Waste management*, 27(12), 1870-1876.
- Batchelor, B. (2006). Overview of waste stabilization with cement. *Waste management*, 26(7), 689-698.
- Beane, R. J. (2004). Using the scanning electron microscope for discovery based learning in undergraduate courses. *Journal of Geoscience Education*, 52(3), 250-253.

- Benezet, J., and Benhassaine, A. (1999). The influence of particle size on the pozzolanic reactivity of quartz powder. *Powder Technology*, 103(1), 26-29.
- Bhattacharjee, B. (2015). Concrete Mix Design, Quality Control and Specification: Thomas Telford Ltd.
- Bale, H. (2010). Measurement and analysis of residual stresses in zirconia dental composites using micro X-ray diffraction. Oklahoma State University. Thesis Book of Doctor of Philosophy in Mechanical Engineering, ProQuest Dissertations Publishing, 3499704.
- Boakye, K. A. (2012). Improvement of setting time and early strength development of pozzolana cement through chemical activation, Kwame Nkrumah University of Science and Technology (Doctoral dissertation).
- Botta, D., Dotelli, G., Biancardi, R., Pelosato, R., and Sora, I. N. (2004). Cement–clay pastes for stabilization/solidification of 2-chloroaniline. *Waste management*, 24(2), 207-216.
- Boyle, M. (1997). Civic Boosterism in the Politics of Local Economic Development—‘Institutional Positions’; and ‘Strategic Orientations’ in the Consumption of Hallmark Events. *Environment and planning A*, 29(11), 1975-1997.
- Brady, J. B., and Boardman, S. J. (1995). Introducing mineralogy students to X-ray diffraction through optical diffraction experiments using lasers. *Journal of Geological Education*, 43(5), 471-476.
- Brough, A. R., and Atkinson, A. (2002). Sodium silicate-based, alkali-activated slag mortars: Part I. Strength, hydration and microstructure. *Cement and concrete research*, 32(6), 865-879.
- Bunte, K., and Abt, S. R. (2001). Sampling surface and subsurface particle-size distributions in wadable gravel-and cobble-bed streams for analyses in sediment transport, hydraulics, and streambed monitoring. Gen. Tech. Rep. RMRS-GTR-74. Fort Collins, CO: US Department of Agriculture, Forest Service, Rocky Mountain Research Station. 428 p., 74.

- Cabrera, J., Cusens, A., and Lynsdale, C. (1989). Porosity and permeability as indicators of concrete performance. Paper presented at the Durability of Structures. IABSE Symposium, September 6-8 1989, Lisbon (Iabse Report Volume 57/1).
- Clarke, A. R., and Eberhardt, C. N. (2002). A book on *microscopy techniques for materials science*: Woodhead Publishing, Boca Raton New York Washington, DC.
- Cullity, B. D. (1978). *Answers to Problems: Elements of X-Ray Diffraction*: Addison-Wesley Publishing Company.
- De Brito, J., Pereira, A., and Correia, J. (2005). Mechanical behaviour of non-structural concrete made with recycled ceramic aggregates. *Cement and concrete composites*, 27(4), 429-433.
- Devanathan, R., Gao, F., and Sun, X. (2011). Challenges in Modeling the Degradations of Ceramic Waste Forms: Pacific Northwest National Laboratory (PNNL), Richland, WA (US).
- Domone, P., and Illston, J. (2002). *Construction materials: their nature and behaviour*. CRC Press.
- Dutrow, B. L., and Clark, C. M. (2017). X-ray Powder Diffraction (XRD) Geochemical Instrumentation and Analysis. *Louisiana State University Eastern Michigan University*.
- ECA. (1995). *The Bangladesh Environment Conservation Act, 1995*. Dhaka, Bangladesh: The People's Republic of Bangladesh, Bangladesh Gazette Extra-ordinary issue of 16-2-1995 and Amended by Act Nos 12 of 2000 and 9 of 2002, pp. 153-166.
- Egerton, R. F. (2005). *Physical principles of electron microscopy*: Springer, University of Alberta, Edmonton, Canada, Published by Department of Material Science .
- Elena, J., and Lucia, M. D. (2012). Application of X ray diffraction (XRD) and scanning electron microscopy (SEM) methods to the Portland cement hydration processes. *Journal of applied engineering sciences*, 2(15), 35-42.



- Feng, D., Yi, J., and Wang, D. (2013). Performance and thermal evaluation of incorporating waste ceramic aggregates in wearing layer of asphalt pavement. *Journal of Materials in Civil Engineering*, 25(7), 857-863.
- Ferraris, C. F. (1999). Measurement of the rheological properties of high performance concrete: state of the art report. *Journal of research of the national institute of standards and technology*, 104(5), 461.
- Gartner, E. (2004). Industrially interesting approaches to “low-CO<sub>2</sub>” cements. *Cement and Concrete Research*, 34(9), 1489-1498.
- Gartner, E. M., Young, J. F., Damidot, D. A., and Jawed, I. (2002). Hydration of Portland cement. *Structure and performance of cements*, 2, 57-108.
- Gaucher, E. C., and Blanc, P. (2006). Cement/clay interactions—a review: experiments, natural analogues, and modeling. *Waste management*, 26(7), 776-788.
- Gilson's. (2016). What is Workability of Concrete, Gilson Company Inc., Materials Testing Equipment Retrieved 01 June, 2018, from <https://www.globalgilson.com/what-is-workability-of-concrete>.
- Gjørsv, O. (1996). Performance and serviceability of concrete structures in the marine environment. Paper presented at the Proceedings, Odd E. Gjørsv Symposium on Concrete for Marine Structures.
- Glasser, F. P., Marchand, J., & Samson, E. (2008). Durability of concrete - degradation phenomena involving detrimental chemical reactions. *Cement and Concrete research*, 38(2), 226-246.
- Gomes, M., and de Brito, J. (2009). Structural concrete with incorporation of coarse recycled concrete and ceramic aggregates: durability performance. *Materials and Structures*, 42(5), 663-675.
- Gonnerman, H. F. (1925). Effect of size and shape of test specimen on compressive strength of concrete: *Structural materials research laboratory*.

- Gyengo, T. (1938). Effect of type of test specimen and gradation of aggregate on compressive strength of concrete. *Paper presented at the Journal Proceedings*.
- Hamad, A. J. (2017). Size and shape effect of specimen on the compressive strength of HPLWFC reinforced with glass fibres. *Journal of King Saud University-Engineering Sciences*, 29(4), 373-380.
- Hammond, S. F. (2016). Department of Building Technology, In brief analysis of ceramic waste concrete: A chemical composition analysis, Department of Building Technology, Kwame Nkrumah University of Science and Technology.
- Hatsopoulos, G. N. (2006). Thermo Fisher Scientific is an American multinational biotechnology product development company, created in 2006 by the merger of Thermo Electron and Fisher Scientific. Access on 13 May, 2018.
- Higashiyama, H., Yagishita, F., Sano, M., and Takahashi, O. (2012). Compressive strength and resistance to chloride penetration of mortars using ceramic waste as fine aggregate. *Construction and Building Materials*, 26(1), 96-101.
- Hovis, G. L. (1997). Determination of Chemical Composition, State of Order, Molar Volume, and Density of a Monoclinic Alkali Feldspar using X-ray Diffraction In Teaching Mineralogy. *JB Brady, DW Mogk, y DI Perkins, Eds*, 107-118.
- Ibáñez-Forés, V., Bovea, M., and Azapagic, A. (2013). Assessing the sustainability of Best Available Techniques (BAT): methodology and application in the ceramic tiles industry. *Journal of Cleaner Production*, 51, 162-176.
- Imaggeo. (2012). The European Geosciences Union is a non-profit international union in the fields of Earth, planetary, and space sciences. The organization has headquarters in Munich, Germany, Retrieved 19.05.2018.
- Islam, M. T., and Rashid, M. H. (2015). Municipal solid waste (MSW) management in Dhaka, Bangladesh: Pergamon-Elsevier Science Ltd The Boulevard, Langford Lane, Kidlington, Oxford Ox5 1GB, England.
- Jennings, H. (2014). *Basic of Ceramic Engineering*. In (01, Ed.), Vol. 2017. Evanston, Illinois: Northwestern University.

- Jiménez, J., Ayuso, J., López, M., Fernández, J., and De Brito, J. (2013). Use of fine recycled aggregates from ceramic waste in masonry mortar manufacturing. *Construction and Building Materials*, 40, 679-690.
- Johnson, R. L. (2009). *Ceramics in the Classroom, Definition of Ceramic, Its History, Processing and Properties* Retrieved July 26, 2018.
- Juan, A., Medina, C., Morán, J. M., Guerra, M. I., Aguado, P. J., De Rojas, M. I. S., and Rodríguez, O. (2010). Re-use of ceramic wastes in construction, *Ceramic Materials: InTech*, Instituto de Ciencias de la Construcción Eduardo Torroja. Consejo Superior de Investigaciones Científicas (CSIC ) Madrid, Spain.
- Jumate, E., and Manea, D. (2011). X-ray Diffraction (XRD) study of hydration processes in the Portland Cement. *J. of Appl. Eng. Sci*, 1(1), 79-86.
- Kabir, A., Hasan, M., and Miah, M. K. (2012). Predicting 28 days compressive strength of concrete from 7 days test result. In *Proceedings of the International Conference on Advances in Design and Construction of Structures* (pp. 18-22).
- Khajuria, C., Kumar, M. G., and Siddique, R. G. (2013). *Effect of Partial Replacement of Sand by Iron Slag on Strength Characteristics of Concrete*.
- Kim, J.-K., and Yi, S.-T. (2002). Application of size effect to compressive strength of concrete members. *Sadhana*, 27(4), 467.
- Klug, H. P., and Alexander, L. E. (1974). X-ray diffraction procedures: for polycrystalline and amorphous materials. *X-Ray Diffraction Procedures: For Polycrystalline and Amorphous Materials, 2nd Edition*, by Harold P. Klug, Leroy E. Alexander, pp. 992. ISBN 0-471-49369-4. Wiley-VCH, May 1974., 992.
- Kou, S., Lee, G., Poon, C., and Lai, W. (2009). Properties of lightweight aggregate concrete prepared with PVC granules derived from scraped PVC pipes. *Waste Management*, 29(2), 621-628.
- Koyuncu, H., Guney, Y., Yilmaz, G., Koyuncu, S., and Bakis, R. (2004). Utilization of ceramic wastes in the construction sector. *Paper presented at the Key Engineering Materials*.

- Lavat, A. E., Trezza, M. A., and Poggi, M. (2009). Characterization of ceramic roof tile wastes as pozzolanic admixture. *Waste Management*, 29(5), 1666-1674.
- Li, Z. (2011). *Advanced concrete technology*. John Wiley and Sons.
- Lilkov, V., Dimitrova, E., and Petrov, O. E. (1997). Hydration process of cement containing fly ash and silica fume: the first 24 hours. *Cement and concrete research*, 27(4), 577-588.
- Lindquist, W. D. (2008). *Development and Construction of Low-Cracking High-Performance Concrete (LC-HPC) Bridge Decks: Free Shrinkage, Mixture Optimization, and Concrete Production* (Doctoral dissertation, University of Kansas).
- Lopez, V., Llamas, B., Juan, A., Moran, J., and Guerra, I. (2007). Eco-efficient concretes: impact of the use of white ceramic powder on the mechanical properties of concrete. *Biosystems Engineering*, 96(4), 559-564.
- Malhotra, V. (1987). *Supplementary cementing materials for concrete*: Canada Centre for Mineral and Energy Technology.
- Marjanovic, L., McCrindle, R. I., Botha, B. M., and Potgieter, J. H. (2000). Analysis of cement by inductively coupled plasma optical emission spectrometry using slurry nebulization. *Journal of Analytical Atomic Spectrometry*, 15(8), 983-985.
- Mayfield, L. L. (1988). Limestone additions to Portland cement-an old controversy revisited. *Cement, concrete and aggregates*, 10(1), 3-8.
- Medina, C., De Rojas, M. S., and Frías, M. (2012). Reuse of sanitary ceramic wastes as coarse aggregate in eco-efficient concretes. *cement and concrete composites*, 34(1), 48-54.
- Mehta, K. P. (2001). Reducing the environmental impact of concrete. *Concrete international*, 23(10), 61-66.
- Meyer, C. (2009). The greening of the concrete industry. *Cement and Concrete Composites*, 31(8), 601-605.

- Monteny, J., De Belie, N., Vincke, E., Beeldens, A., and Taerwe, L. (2001). Simulation of corrosion in sewer systems by laboratory testing. Paper presented at the Proceedings of the FIB-Symposium Concrete and Environment, Berlijn, 3-5 October 2001, 99.91-82, paper a5-2 on CD-ROM.
- Moore, D. M., & Reynolds, R. C. (1989). *X-ray Diffraction and the Identification and Analysis of Clay Minerals* (Vol. 332): Oxford university press New York.
- Mora, E. P. (2007). Life cycle, sustainability and the transcendent quality of building materials. *Building and Environment*, 42(3), 1329-1334.
- Murdock, J. (1957). Effect of length to diameter ratio of specimen on the apparent compressive strength of concrete. *ASTM bulletin*(221), 68-73.
- Naceri, A., & Hamina, M. C. (2009). Use of waste brick as a partial replacement of cement in mortar. *Waste management*, 29(8), 2378-2384.
- Nehdi, M., and Khan, A. (2001). Cementitious composites containing recycled tire rubber: an overview of engineering properties and potential applications. *Cement, concrete and aggregates*, 23(1), 3-10.
- Neville, A. M. (1995). *Properties of concrete*, Vol. 4. London: Longman.
- Ni, H.-G., and Wang, J.-Z. (2000). Prediction of compressive strength of concrete by neural networks. *Cement and Concrete Research*, 30(8), 1245-1250.
- Oh, B. H., Cha, S. W., Jang, B. S., and Jang, S. Y. (2002). Development of high-performance concrete having high resistance to chloride penetration. *Nuclear Engineering and Design*, 212(1), 221-231.
- Pacheco-Torgal, F., and Jalali, S. (2010). Reusing ceramic wastes in concrete. *Construction and Building Materials*, 24(5), 832-838.
- Portella, K., Joukoski, A., Franck, R., and Derksen, R. (2006). Secondary recycling of electrical insulator porcelain waste in Portland concrete structures: determination of the performance under accelerated aging. *Cerâmica*, 52(323), 155-167.

- Popovics, S. (1992). Concrete materials: Properties, specifications, and testing. William Andrew.
- Puertas, F., García-Díaz, I., Barba, A., Gazulla, M., Palacios, M., Gómez, M., and Martínez-Ramírez, S. (2008). Ceramic wastes as alternative raw materials for Portland cement clinker production. *Cement and Concrete Composites*, 30(9), 798-805.
- Potts, P. J., and West, M. (Eds.). (2008). Portable X-ray fluorescence spectrometry: Capabilities for in situ analysis. Royal Society of Chemistry.
- Roy, D., and Misra, A. K. (2018). Quantification of phase changes and hydration behavior studies of OPC-43 grade cement through powder X-RAY diffraction. *Int. J. Sustain. Build. Technol. Urban Dev.*, 9(2), 74-86.
- Reimer, L. (2013). Scanning electron microscopy: physics of image formation and microanalysis (Vol. 45): Springer.
- Richart, F. E., Brandtzaeg, A., and Brown, R. L. (1928). A study of the failure of concrete under combined compressive stresses. University of Illinois at Urbana Champaign, College of Engineering. Engineering Experiment Station..
- Sabir, B., Wild, S., and Bai, J. (2001). Metakaolin and calcined clays as pozzolans for concrete: a review. *Cement and concrete composites*, 23(6), 441-454.
- Sadek, D. M., El-Attar, M. M., and Ali, H. A. (2016). Reusing of marble and granite powders in self-compacting concrete for sustainable development. *Journal of Cleaner Production*, 121, 19-32.
- Sánchez de Rojas, M. I., Marin, F., Rivera, J., and Frías, M. (2006). Morphology and properties in blended cements with ceramic wastes as a pozzolanic material. *Journal of the American Ceramic Society*, 89(12), 3701-3705.
- Scrivener, K. L., and Kirkpatrick, R. J. (2008). Innovation in use and research on cementitious material. *Cement and concrete research*, 38(2), 128-136.

- Senthamarai, R., and Manoharan, P. D. (2005). Concrete with ceramic waste aggregate. *cement and concrete composites*, 27(9-10), 910-913.
- Shetty, M. (2009). Concrete Technology Theory and Practice—S. Chand & Company Ltd. *New Delhi*.
- Suzuki, M., Meddah, M. S., and Sato, R. (2009). Use of porous ceramic waste aggregates for internal curing of high-performance concrete. *Cement and Concrete research*, 39(5), 373-381.
- Swanepoel, J. C., and Strydom, C. A. (2002). Utilisation of fly ash in a geopolymeric material. *Applied geochemistry*, 17(8), 1143-1148.
- Swapp, S. (2017). Scanning Electron Microscopy (SEM), Geochemical Instrumentation and Analysis, University of Wyoming.
- Tay, D., & Tam, C. (1996). In situ investigation of the strength of deteriorated concrete. *Construction and Building Materials*, 10(1), 17-26.
- Torgal, F. P., and Castro-Gomes, J. P. (2006). Influence of physical and geometrical properties of granite and limestone aggregates on the durability of a C20/25 strength class concrete. *Construction and Building Materials*, 20(10), 1079-1088.
- Vida-Simiti, I., Jumate, N., Chicinas, I., and Batin, G. (2004). Applications of scanning electron microscopy (SEM) in nanotechnology and nanoscience. *Rom. J. Phys*, 49(9-10), 955-965.
- von Bohlen, A. (2009). Total reflection X-ray fluorescence and grazing incidence X-ray spectrometry - tools for micro-and surface analysis. *A review. Spectrochimica Acta Part B: Atomic Spectroscopy*, 64(9), 821-832.
- Wirth, K., and Barth, A. (2016). X-Ray Fluorescence (XRF), Geochemical Instrumentation and Analysis Retrieved 03 June, 2018.
- Yan, K., Xu, H., Shen, G., and Liu, P. (2013). Prediction of splitting tensile strength from cylinder compressive strength of concrete by support vector machine. *Advances in Materials Science and Engineering*, 2013.

Yi, S.-T., Yang, E.-I., and Choi, J.-C. (2006). Effect of specimen sizes, specimen shapes, and placement directions on compressive strength of concrete. *Nuclear Engineering and Design*, 236(2), 115-127.

Zimbili, O., Salim, W., and Ndambuki, M. (2014). A review on the usage of ceramic wastes in concrete production. *International Journal of Civil, Environmental, Structural, Construction and Architectural Engineering*, 8(1), 91-95.